STRUCTURAL STUDIES OF ACTINIDE COMPOUNDS

by

David John Flanders

A thesis submitted to the University of Warwick in partial fulfilment of the requirements for the degree of Doctor of Philosophy

Department of Chemistry
and Molecular Sciences,
University of Warwick,
Coventry CV4 7AL

March 1985

DECLARATION

The work described in this thesis is entirely original and my own, except where otherwise indicated.

Parts of the work contained in this thesis have been published, accepted, or submitted for publication in the Scientific literature with the following references:

N.W. Alcock, D.J. Flanders and D. Brown, *J. Chem. Soc., Dalton Trans.*, 1984, 679

N.W. Alcock, D.J. Flanders and D. Brown, *Inorg. Chim. Acta*, 1984, **94**, 279.

N.W. Alcock, D.J. Flanders, T.J. Kemp and M.A. Shand, *J. Chem. Soc., Dalton Trans.*, In Press, Paper No. 4/810

N.W. Alcock, D.J. Flanders and D. Brown, *J. Chem. Soc., Dalton Trans.*, In Press, Paper No. 4/1278

Acknowledgements

I would like to thank my supervisor, Dr. N.W. Alcock, for his guidance in crystallography throughout the course of my work. For their supervision and assistance in preparative neptunium chemistry at the Chemistry Division of A.E.R.E. Harwell I thank Dr. D. Brown, members of his staff and past research students. I am indebted to Mr. G.S. Topping for the preparation of crystals of $Cs_7(NpO_2)_3Cl_{12}$, Mr. M.A. Shand and Mr. R.V. Astley for the synthesis and crystal preparation of $UO_2(gly)_4(NO_3)_2$, Mr. G.F. Payne for the preparation of $(\eta^5\text{-}C_5H_5)Np(IV)Cl_3.2mdppo$ and Professor K.W. Bagnall for supplying the crystals of $UO_2(CCl_3COO)Cl.2tppo$. I would also like to thank everyone in the Chemistry department for help and encouragement throughout the period of my research.

This thesis has been written using the *troff* word processing program with the preprocessors *refer*, *tbl* and *eqn* running under the UNIX† operating system and printed on a Xerox 2700 laserprinter. I would like to thank Dr. R. Countryman and Mr. R. McMahon for their help with the system and the staff of the computer unit for assistance and support during my project.

In particular I thank my wife Jane whose support in every way has enabled me to complete this work.

I gratefully acknowledge the support of a CASE award from the Science and Engineering Research Council and the Chemistry Division of A.E.R.E. Harwell.

† UNIX is a trademark of A.T.&T. Bell Laboratories.

ABSTRACT

The work described in this thesis was an investigation into the coordination chemistry of uranium(VI) and neptunium(VI). Structural determinations of comparable uranium and neptunium compounds were used to examine the actinide contraction between uranium and neptunium, the changes in metal-ligand bond length on substituting nitrogen for oxygen as the donor atom and to establish the mode of coordination of certain ligands around the actinyl(VI) ion. These areas have been explored through the determination of the crystal structures of the following compounds:-

a) The 2,2'-dipyridyl complexes $[UO_2(NO_3)_2C_{10}H_8N_2]$, $[NpO_2(NO_3)_2C_{10}H_8N_2]$, $[UO_2(CH_3COO)_2C_{10}H_8N_2]$ and $[NpO_2(CH_3COO)_2C_{10}H_8N_2]$.

b) The 1,10-phenanthroline complex $[UO_2(NO_3)_2C_{12}H_8N_2]$.

c) The pentan-2,4-dionate complexes $[UO_2(CH_3COCHCOCH_3)_2C_5H_5N]$, $[NpO_2(CH_3COCHCOCH_3)_2C_5H_5N]$, $[UO_2(CH_3COCHCOCH_3)_2.H_2O]$ and $[UO_2CH_3COCHCOCH_3(NO_3)_2]^-[(CH_3)_3C_5H_3N]^+$.

d) The 4,4'-dipyridyl compound $[(UO_2(NO_3)_2OH)_2]^{2-}[C_{10}H_{10}N_2]^{2+}$.

In addition the structure determination of the compound bis(nitrato)dioxo tetrakis(glycinato)uranium(VI) showed that the glycine ligands are coordinated *via* the oxygen atoms with two bidentate and two monodentate glycines. Other structures which have been determined are the mixed oxidation state neptunium alkali metal salt $[Cs_7Np^{(V)}O_2(Np^{(VI)}O_2)_2Cl_{12}]$, the organoneptunium(IV) compound $[(C_5H_5)Cl_3Np(OPPh_3)_2]$ and the photo-oxidation product $[UO_2(CCl_3COO)Cl.(OPPh_3)_2]$

There is also an uncompleted structure of a 1,10-phenanthroline complex with uranyl(VI)acetate which is described as far as possible.

Table of Contents

List of Tables

List of Figures

CHAPTER 1

Introduction

1.1. The Elements

The actinide elements, which are referred to as the 5*f* transition series, are the fourteen elements following actinium (Z=89) in the periodic table. The series arises from the successive addition of electrons to the 5*f* orbitals and is analogous in this respect to the lanthanide or 4*f* transition series. The majority of chemical investigations of the actinide elements have been carried out on thorium and uranium for the reason that both these elements are readily available in large quantities. Of the other actinides protactinium, neptunium, plutonium and americium are available in quantities ranging from a few hundred grams in the case of protactinium to hundreds of kilograms in the case of plutonium. The transamericium elements are available in much smaller quantities ranging down to a few atoms for the heaviest element, lawrencium (Z=103).

All the known isotopes of the actinides are radioactive, but the half-lives of ^{232}Th, ^{235}U and ^{238}U are sufficiently long for them to be found in nature as primordial material. Protactinium is found in nature, despite the short half-life of ^{231}Pa (3.28×10^4 years), since it is a member of the ^{235}U decay chain. Actinium and the transuranium elements are produced synthetically since their half-lives are so short that any primordial deposits of these elements have decayed completely.

The chemical investigations described in this thesis involve the elements uranium and neptunium, preparative work on the latter being carried out at A.E.R.E. Harwell. Neptunium was first discovered in 1940 by McMillan and Abelson[1] as ^{239}Np, but the most stable isotope is ^{237}Np with a half-life of 2.14×10^6 years which is the isotope used for the preparative chemistry described here. Neptunium is produced by neutron irradiation of uranium:[2]

$$30\%: \quad {}^{235}\mathrm{U}(n,\gamma)\ {}^{236}\mathrm{U}(n,\gamma)\ {}^{237}\mathrm{U} \xrightarrow{\beta^-} {}^{237}\mathrm{Np}$$

$$70\%: \quad {}^{238}\mathrm{U}(n,2n)\ {}^{237}\mathrm{U} \xrightarrow{\beta^-} {}^{237}\mathrm{Np}$$

and extracted from irradiated fuel elements.[3]

1.2. The aqueous chemistry of the MO_2^{n+} (n=1,2,3) ions.

In contrast to the lanthanide elements, which have only a limited range of oxidation states - normally +3 - both in the solid state and in aqueous solution, the actinide elements can exist in a variety of oxidation states. This is summarised in the following table (1.1) from ref (4). The limited number of oxidation states displayed by the lanthanides is

TABLE 1.1

Oxidation States of the Actinides and Lanthanides

(The most stable oxidation states are in bold figures, those not known in solution are within parentheses.)

Actinides		Lanthanides	
89 Ac	**3**	57 La	**3**
90 Th	(3),**4**	58 Ce	**3**,**4**
91 Pa	(3),**4**,**5**	59 Pr	**3**,(4)
92 U	**3**,**4**,**5**,**6**	60 Nd	(2),**3**
93 Np	**3**,**4**,**5**,**6**,**7**	61 Pm	**3**
94 Pu	**3**,**4**,**5**,**6**,**7**	62 Sm	**2**,**3**
95 Am	(2),**3**,**4**,**5**,**6**	63 Eu	**2**,**3**
96 Cm	**3**,**4**	64 Gd	**3**
97 Bk	(2)**3**,**4**	65 Tb	**3**,(4)
98 Cf	**2**,**3**	66 Dy	**3**
99 Es	**2**,**3**	67 Ho	**3**
100 Fm	**2**,**3**	68 Er	**3**
101 Md	**2**,**3**	69 Tm	(2),**3**
102 No	**2**,**3**	70 Yb	**2**,**3**
103 Lr	**3**	71 Lu	**3**

attributed to their 4*f* electrons being more strongly shielded than the 5*f* electrons of the actinide elements, these latter also have higher energy and are therefore more available for covalent bonding. The compounds of the lanthanides involve predominantly ionic bonding, a metal ion of charge +3 being most common.

The most stable oxidation state for uranium and neptunium are +6 and +5, respectively, which occur in solution as UO_2^{2+} and NpO_2^{+}. The +6 oxidation state of neptunium (NpO_2^{2+}) can only be maintained in solution in the presence of an oxidising agent, as is illustrated by the comparative stability of the two +6 actinyl species in 1M perchloric acid.[5]

$$UO_2^{2+} + e^- = UO_2^{+} \; ; \; E^\circ = 0.163 \text{ V} \qquad (1.2.1)$$

$$NpO_2^{2+} + e^- = NpO_2^{+} \; ; \; E^\circ = 1.236 \text{ V} \qquad (1.2.2)$$

The Np(VI) species is stable enough in aqueous solution, however, for complexes to be formed which maintain the +6 oxidation in the solid state. The +5 oxidation state of uranium (UO_2^+), however, disproportionates very rapidly[6] to U^{4+} and UO_2^{2+}, being least unstable at pH 2.5.

$$2UO_2^+ + 4H^+ \rightarrow U^{4+} + UO_2^{2+} + 2H_2O \qquad (1.2.3)$$

The NpO_2^+ species is much more stable, only disproportionating at high acid concentrations (> 5M $HClO_4$) to give Np^{4+} and NpO_2^{2+}, and the hydroxide $NpO_2(OH)$ only forming when the acid concentration is reduced past pH 5.7.

The other stable oxidation state of both elements is +4, which is stable in aqueous solution in the absence of oxidising agents, but both U^{4+} and Np^{4+} in solution undergo slow oxidation by atmospheric oxygen. Uranium(IV) is oxidised directly to UO_2^{2+} and neptunium(IV) to NpO_2^+, which is thermodynamically more favourable than the oxidation of Np(IV) to Np(VI).[7]

$$UO_2^{2+} + 4H^+ + 2e^- = U^{4+} + 2H_2O \; ; \; E^\circ = 0.319V \qquad (1.2.4)$$

$$NpO_2^{2+} + 4H^+ + 2e^- = Np^{4+} + 2H_2O \; ; \; E^\circ = 0.918V \qquad (1.2.5)$$

The kinetics of the oxidative mechanisms are the major factors involved in these reactions,[8] the rate of the $NpO_2^+ \rightarrow NpO_2^{2+}$ oxidation being much faster than that of $Np^{4+} \rightarrow NpO_2^+$ or $Np^{4+} \rightarrow NpO_2^{2+}$. A major reason for the relative slowness of these latter two reactions is the presence of steps involving the formation of Np-O bonds.

The U(IV) and Np(IV) ions have a greater complexing ability than U(VI), Np(V) and Np(VI) since the latter exist as the oxo-ions UO_2^{2+}, NpO_2^+ and NpO_2^{2+} which have a lower charge and larger size than the bare ions. The actual charges on the central metal atoms in the oxygenated ions are higher than the formal ionic charges of +1 and +2 so these ions do still have a relatively high tendency toward complex ion formation, in the order U(IV) > U(VI) and Np(IV) > Np(VI) > Np(V).[9] The oxygen atoms in all the actinyl ions are non-basic and do not attract protons, even at high acidities;[7] however in aqueous solutions, both MO_2^+ and MO_2^{2+} ions coordinate with water to form acidic hydrated species.

It is possible to prepare aqueous solutions of Np(VII) by oxidation of Np(VI) with ozone in alkaline conditions[8] which produces the stable NpO_5^{3-} species. In acid conditions, Np(VII) exists as the NpO_2^{3+} ion which is much less stable. This latter species is a very strong oxidising agent which is capable of oxidising Cr(III) to Cr(VI).

1.3. Uranyl and neptunyl complexes - coordination geometry.

Large numbers of complexes containing the dioxouranium(VI) cation (UO_2^{2+}) have been prepared, and many structures have been determined.[7] There has been relatively little preparative and structural work done on the corresponding dioxoneptunium (NpO_2^{2+},

NpO_2^+) complexes.[10] The aim of the work described here has been to contribute towards remedying this lack, and to increase the amount of structural information of uranyl complexes. The effect of different types of donor ligand and coordination number on the geometry of the actinyl group will be examined, and any structural changes due to a substitution of uranium by neptunium will be discussed.

The dioxo-cation MO_2^{n+} (M = U, n = 2; M = Np, n = 1, 2) can be considered to behave as a single charged centre, as a metal ion having the characteristics of a "hard" Lewis acid.[11] As a result the ion is capable of complexing with the more electronegative elements (N, O, F^-, Cl^-) acting as donor atoms and is less likely to form complexes with those which are more polarisable and utilise π-bonding (S, P, Se, I^-). The "hard/soft" principle also suggests that a nitrogen-donor ligand will be less strongly bound to the actinyl centre than would an oxygen-donor, since oxygen has the higher base strength.[4] For this reason, M-O bonds are expected to be shorter than M-N bonds for the actinyl ions whereas for other "softer" ions M-O and M-N bonds are very similar in length (e.g. Cu(II), Co(III)).

The MO_2^{n+} ion is generally very close to linearity (O-M-O), and will accommodate between 4 and 6 donor atoms in a plane perpendicular to the axis of the ion. The ligands bond to the metal within the "equatorial plane" and the arrangement of the individual donor atoms becomes more puckered, with respect to the plane, as the coordination number is increased. The irregularities are decreased with a coordinating bidentate ligand with a small "bite", as is found in the case of $NaUO_2(CH_3COO)_3$ which has a planar ligand arrangement.[12] If the size of the donor atoms or the bite of the ligand is increased then either the puckering will be exaggerated or the coordination number in the equatorial plane will be reduced from the value found for the analogous complex with the smaller ligands.

The lengths of the M-O (MO_2^{n+}) and M-L (L = ligand atom) bonds lie in the ranges 1.6 - 2.0Å and 2.2 - 2.9Å respectively and are denoted as primary and secondary bonds. This range allows the coordination geometry in these complexes to vary from a slightly distorted octahedron, through a pentagonal bipyramidal arrangement to a hexagonal bipyramid. These possible geometries are illustrated by the examples in Figures 1.1 - 1.3. If the coordinating ligands subtend a large ligand cone angle[13] or the donor atoms are sufficiently large then a complex will be constrained to take up a distorted octahedral geometry. Examples are the structure of $NpO_2(OPPh_3)_2Cl_2$[14] and the anions of $Cs_3NpO_2Cl_4$[15] which accommodates four chlorine atoms in the equatorial plane. The ability of chlorine to coordinate in this way is determined by its large van der Waals' radius * of 1.75Å.[16] The Cl-Cl contact distances in the example are 3.89(2)Å and 3.91(2)Å, well

*The van der Waals' radius of an atom is the distance at which the repulsive inter-atomic forces balance the attractive ones. The repulsive forces come into play as the electron clouds interpenetrate.

outside the sum of the chlorine van der Waals' radii (3.5Å). An attempt to increase the number of chlorine atoms coordinated to 5, without an increase in the metal-chlorine bond length, would reduce the Cl-Cl contact distances to ca. 3.12 Å, well inside the sum of van der Waals' radii. On the other hand it is possible to coordinate an oxygen atom together with four chlorine atoms in the equator as the example of $UO_2Cl_2.H_2O$[17] demonstrates.

A coordination number of 5 is most common in the equatorial plane, particularly with oxygen donors. Where this occurs, the M-O (ligand) bond lengths are about 2.35 - 2.40Å and the non bonded O...O separations in the ligand plane will be 2.70 - 2.80Å. The contact distance here is very close to, although smaller than, the sum of van der Waals' radii for two oxygen atoms (2.84 Å) and experimental data has shown that in some cases, particularly compounds with an equatorial coordination number of 6, the oxygen-oxygen contact distances may be as low as 2.6Å. This suggests that the simple addition of two unconstrained van der Waals' radii does not describe the limiting case and that a reduction of some 8.5% is possible. However, even if this reduction is applied, the sum of the van der Waals' radii of two chlorine atoms is 3.20Å which is greater than the contact distance for the equatorial coordination of five chlorine atoms. Both monodentate ligands and bidentate ligands (with a unidentate donor occupying the fifth equatorial position) form actinyl complexes with pentagonal bipyramidal geometry. Examples of the former are $UO_2SO_4.H_2SO_4.5H_2O$ and $2NpO_2SO_4.H_2SO_4.4H_2O$[18] and of the latter $(CF_3COCHCOCF_3)_2UO_2.THF$[19] and $(CH_3COCClCOCH_3)_2UO_2.Ph_3PO$.[20]

The hexagonal bipyramid is not an energetically favoured polyhedron and is generally only observed for the case of compounds containing actinyl groups. This observation suggests that the dimensional requirements of the actinyl group cannot be accommodated within any of the lower energy polyhedra, and observation shows that neither the dodecahedron nor the square antiprism can accommodate a linear moiety without severe distortion. The alternatives of the bicapped trigonal prism and the cube would also be considerably distorted in attempting to accommodate the short U=O bonds. The few examples of hexagonal bipyramidal geometry not containing the actinyl group seem to arise as a result of some special, steric conditions. The example of tetramethylammonium triacetatodiphenylplumbate(IV) : $[Me_4N]\ [Pb(Ph)_2(CH_3COO)_3,$[21] has the special combination of two bulky monodentate and three short bite bidentate ligands about the central metal atom.

The puckering of equatorial hexagons of monodentate groups (as in α-$UO_2(OH)_2$)[22] suggest that fitting six oxygen atoms in a plane about a UO_2^{2+} ion is quite difficult, and the crowding is relieved when oxygen atoms are contributed in pairs by bidentate ligands having a small bite. Examination shows that the average O...O distance in the sulphate

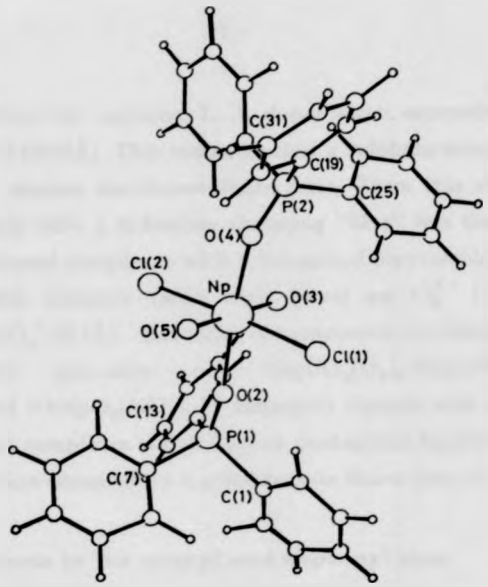

1.1. Distorted octahedral coordination geometry (from ref.14).

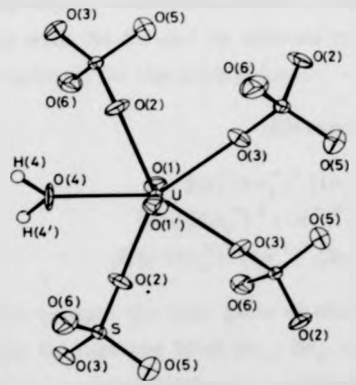

1.2. Pentagonal bipyramidal geometry (from ref.18).

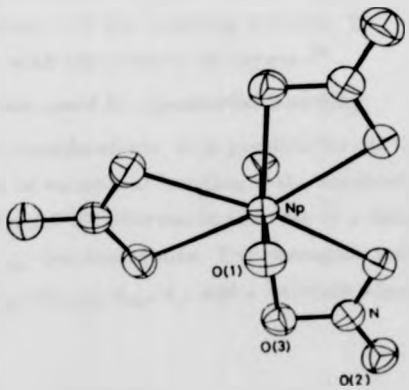

1.3. Hexagonal bipyramidal geometry (from ref.25).

ion (2.38Å) is greater than the expected L...L donor atom separation for an equatorial coordination number of 6 (2.35Å). This indicates that a sulphate group cannot give rise to this geometry, but will assume the 5-coordinate form. From this observation it can be deduced that only ligands with a bidentate chelating "bite" less than this value will be able to form hexacoordinated complexes with a hexagonal bipyramidal geometry. Typical bidentate ligands in this category (with their bites) are O_2^{2-} (1.5Å), CO_3^{2-} (2.2Å), CH_3COO^- (2.2Å) and NO_3^- (2.1Å). Examples of compounds containing these ligands in a hexagonal bipyramidal geometry are $Na_4UO_2(O_2)_3.9H_2O$,[23] $K_4UO_2(CO_3)_3$,[24] $NaNpO_2(CH_3COO)_3$ and $RbNpO_2(NO_3)_3$.[25] Bidentate ligands with larger bites (>2.3Å) will tend to form actinyl complexes which display pentagonal bipyramidal geometry with the fifth equatorial position occupied by a monodentate donor (see above).

1.4. Bonding mechanisms in the uranyl and neptunyl ions.

1.4.1. The molecular orbitals[26]

Uranium , in its ground state, has the electronic configuration $5f^3\ 6d^1\ 7s^2$ around a filled radon core and neptunium contains an extra f-electron. The electrons outside the radon core, [Rn] combine with the $2s$ and $2p$ orbitals of the oxygen atoms to give the following sets of molecular orbitals for the actinyl ions:-

Ion	Electronic configuration
UO_2^{2+}	$[Rn]\ (1\sigma_g^+)^2\ (1\sigma_u^+)^2\ (2\sigma_u^+)^2\ (2\sigma_g^+)^2(\pi_u)^4\ (\pi_g)^4$
UO_2^+, NpO_2^{2+}	$[Rn]\ (1\sigma_g^+)^2\ (1\sigma_u^+)^2\ (2\sigma_u^+)^2\ (2\sigma_g^+)^2\ (\pi_u)^4\ (\pi_g)^4\ (\phi_u)^1$
NpO_2^+	$[Rn]\ (1\sigma_g^+)^2\ (1\sigma_u^+)^2\ (2\sigma_u^+)^2\ (2\sigma_g^+)^2\ (\pi_u)^4\ (\pi_g)^4\ (\phi_u)^1\ (\delta_u)^1$

The $1\sigma_g$ and $1\sigma_u$ orbitals contain the lone pairs of electrons on the oxygen atoms triple-bonded to the metal atom through the filled $2\sigma_u$, $2\sigma_g$, π_u and π_g orbitals, making a total of six bonds. The ϕ_u and δ_u metal orbitals are non-bonding,[27] the former having a spatial distribution between the equatorial plane and the axis of the actinyl ion. The δ_g non-bonding orbital has $6d$ character and is therefore higher in energy than either ϕ_u or δ_u, which have $5f$ character. Of the bonding orbitals, $2\sigma_u^+$ is of the highest energy, as it interacts most closely with the orbitals on oxygen.[28]

1.4.2. Possible orbitals used in equatorial bonding

From symmetry considerations, it is possible for all the metal $5f$, $6d$ and $7s$ valence orbitals to participate in equatorial bonding if the equatorial coordination number around the ion is 5 or 6[26] (Figs 1.7-8), whereas in the case of a distorted octahedron, all the bonding orbitals except f_{xyz} can contribute. The strongest secondary bonds are formed with the f_{xy^2}, f_{yz^2}, f_{xz^2}, f_{yz^2}, $d_{x^2-y^2}$, d_{xy}, d_{z^2} and s orbitals which have electron density normal

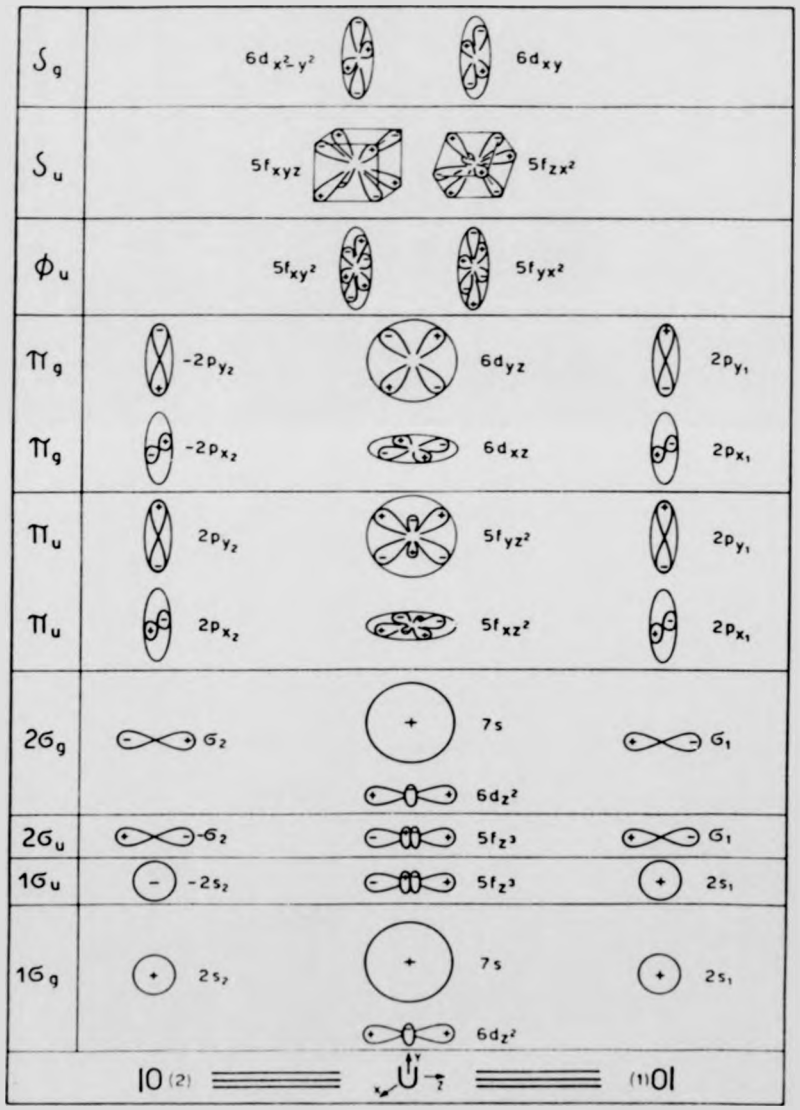

1.4. The molecular orbitals of the uranyl(VI) ion (from ref.26).

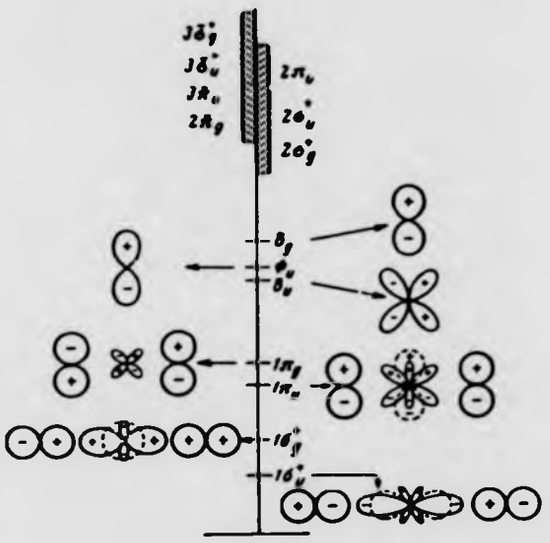

1.5. The molecular orbitals in UO_2^{2+} (from: I.I. Chernyaev, ***Complex Compounds of Uranium***, p376, Jerusalem, 1966). The $2\sigma_u$ and $2\sigma_g$ orbitals shown in Fig. 1.4 are identical to $1\sigma_u$ and $1\sigma_g$ here, the lowest energy σ-bonding orbitals.

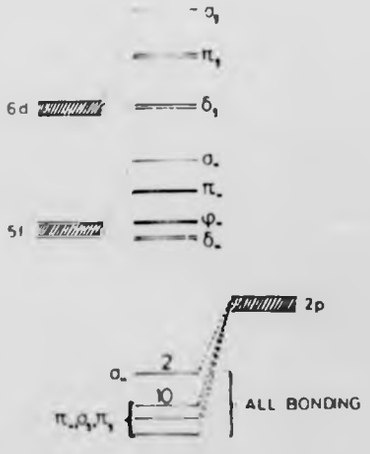

1.6. A possible energy-level scheme for actinyl ions (from ref.28).

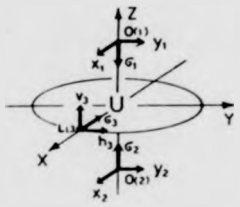

1.7. Axes describing the orientation of orbitals in the UO_2^{2+} ion (from ref.26).

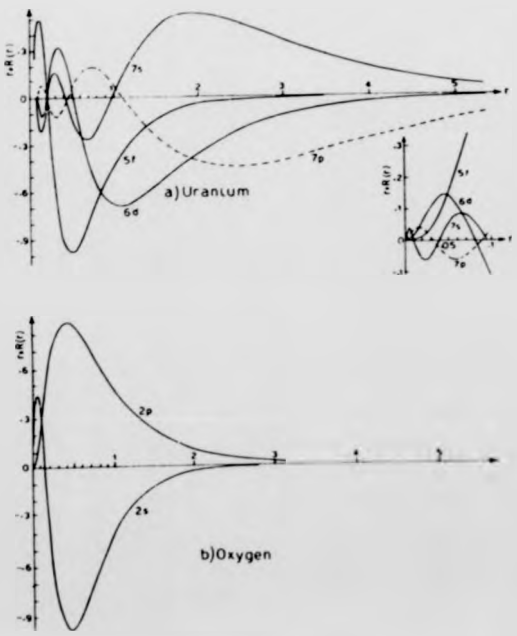

1.8. Radial distribution functions (from ref.26).

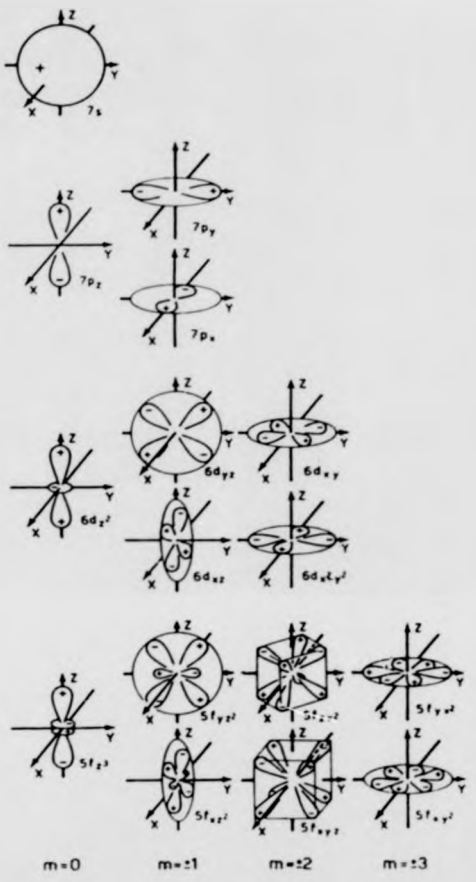

1.9. The valence orbitals of uranium (from ref.26).

1.10. Polar diagram for *spdf* hybrid orbital (from ref.29).

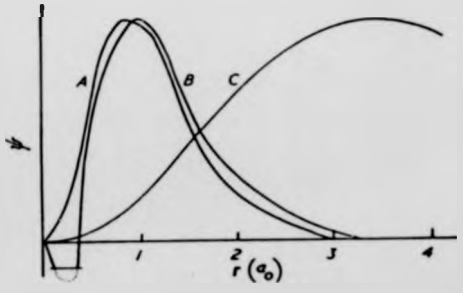

1.11. Radial part of 5*f* and 6*f* atomic orbitals for uranium (from ref.29).
(A Slater 5*f*, B Thomas-Fermi 5*f*, C Slater 6*f* wave functions)

to the z (actinyl) axis. The remaining f_{xyz}, f_{xz^2}, f_{z^3}, d_{xz}, and d_{yz} orbitals which do not have a spatial distribution in the equatorial plane may be involved in cases of staggered bonding (Fig. 1.9). The Table (1.2) shows the compositions of the orbitals used for bonding in uranyl(VI) complexes.

Table 1.2

Orbital transformation scheme according to $D_{\infty}h$ symmetry

Representation	Metal Orbitals	Ligand Orbitals	
		σ	π
σ_g^+	s, d_{z^2}	$1/\sqrt{2}(\sigma_1+\sigma_2)$	-
σ_u^+	p_z, f_{z^3}	$1/\sqrt{2}(\sigma_1-\sigma_2)$	-
π_g	d_{xz}	-	$1/\sqrt{2}(p_{x_1}-p_{x_2})$
π_g	d_{yz}	-	$1/\sqrt{2}(p_{x_1}+p_{x_2})$
π_u	p_x, f_{xz^2}	-	$1/\sqrt{2}(p_{y_1}-p_{y_2})$
π_u	p_y, f_{yz^2}	-	$1/\sqrt{2}(p_{y_1}+p_{y_2})$
δ_g	$d_{x^2-y^2}$	-	-
δ_g	d_{xy}	-	-
δ_u	f_{xyz}	-	-
δ_u	f_{xz^2}	-	-
Φ_u	f_{xy^2}	-	-
Φ_u	f_{yz^2}	-	-

Coulson and Lester[29] have suggested that the use of *spdf* hybrid orbitals is of importance in cases of equatorial hexacoordination about the actinyl ion since these orbitals would have lobes at 60° to one another in a planar arrangement, suitable for maximum overlap with the ligand orbitals. It is also suggested that the 6*f* rather than the 5*f* orbitals would be more favourably arranged for such overlap as they protrude further into space (Figs. 1.10-11).

1.4.3. The effects of oxidation state and metal type on the bond lengths in the actinyl complexes studied.

It is stated above (1.4.1) that the ϕ_u orbital is not located along the actinyl axis and so an electron occupying this orbital is likely to have little effect on the length, geometry and strength of bonds in the actinyl ion. Such an electron should not be responsible, therefore, for any differences between UO_2^{2+} and NpO_2^{2+} in identical ligand environments. Conversely, the δ_u orbital lies along the axis of the actinyl ion, and an electron occupying this has the effect of lengthening the NpO_2^+ ion primary bonds relative to those of NpO_2^{2+} by about 0.09Å. In these circumstances, a lengthening of the secondary bonds also occurs which is probably due to the repulsion of the partially filled ϕ_u orbital toward the equatorial ligands by the δ_u electron. This effects an increase in metal-ligand repulsion and therefore M-L bond length.

Between analogous uranyl(VI) and neptunyl(VI) complexes the major change in bond lengths is a result of the actinide contraction, the decrease in ionic radius that is observed from uranium to americium. [27] From protactinium (element 91) to uranium (element 92), the $5f$ orbitals become lower in energy than the $6d$ and $7s$ orbitals with the increasing nuclear charge and as a consequence the $5f$ orbitals start to fill. The $5f$ electrons do not shield themselves well, so the shells contract as the atomic number increases. This contraction results in a stabilisation of the orbitals which bond with those of oxygen in the actinyl ions, giving a poorer overlap. As a result of the poorer overlap there is a weakening of the M-O (MO_2^{2+}) bond, but nevertheless a net reduction in its length along the actinide series. A similar change is observed in the secondary bonds around MO_2^{2+}. Structural changes can also occur in analogous actinide compounds as a result of this difference in ionic radius, for example the different crystal systems of the tribromides of neptunium and plutonium. [30]

The higher energy of the $5f$ orbital compared with the $6d$ orbital in protactinium explains the absence of a linear PaO_2^+ species comparable to that of the higher actinides. The only known oxo-ion is $[Pa{=}O]^{3+}$ which occurs, for example, in $(NEt_4)_2\,PaOCl_5$. [31]

1.4.4. The length of the M-O (MO_2^{n+}) bond in actinyl complexes.

The uranium-oxygen bond lengths in the UO_2^{2+} unit have been most extensively studied, and have been found to vary between 1.50Å and 2.08Å with a mean value of 1.77Å. A recent review [32] suggests that contrary to the earlier analysis of Zachariasen [33] there is no substantial difference in U-O bond length for different coordination numbers or dependence on the type of ligands found in the coordination sphere. The mean values for the uranium bond lengths for 4,5 and 6 coordination are 1.809, 1.764 and 1.779Å respectively, but the majority of standard deviations are of the order of 0.03Å and so no trends in the bonds lengths can be inferred from these values. However, there is some evidence that

secondary bonding of the uranyl oxygen atom does increase the U-O bond length. This occurs in β-UO_2SO_4,where the uranyl oxygen atoms act as bridges to equatorial positions on neighbouring uranium atoms. [34] In this case the uranyl bond lengths are 1.80(2) and 1.73(1)Å, the former being longer than expected due to the secondary bonding of that uranyl oxygen into the pentagonal plane of an adjoining molecule which is also seen in a high-pressure form of UO_3. [35] By contrast, α-UO_2SeO_4 has uranyl U-O bonds which are more nearly equal (1.79(2) and 1.78(2)Å) despite the similar secondary bonding of one of the uranyl oxygens.

1.4.5. The geometry of the uranyl(VI) ion.

Any explanation for the constrained linearity of the uranyl ion [36] should, by extension, cover the other actinyl ions. Other dioxocations, the bent MoO_2^{2+}, for example, contains a (dsp) hybridisation set formed from the $4d$, $5s$, and $5p$ orbitals on the molybdenum which can be occupied by the $2p$ orbitals of the oxygens in the dioxocation. The minimum potential energy for the hybridisation set occurs at an angle of 110° between the lobes which is close to the observed value for the O-Mo-O bond angle (Fig. 1.12). In the UO_2^{2+} ion the available orbitals, $5f$, $6d$, $7s$ and $7p$ some of which are vacant, are higher in energy and thus unlikely to interact with the oxygen $2p$ orbitals. A ($fdsp$) hybridisation set is formed from these orbitals which has a level region in the potential energy curve in the 110-180° region. The addition of a contribution from the filled $6p_z$ uranium orbital causes the linear geometry to be favoured (Fig. 1.13). The energy of the $2\sigma_u^+$ is increased by the interaction between the $6p_z$ orbital and the $2s$ and $2p$ oxygen orbitals, as suggested previously, [28] and lowered in energy by the vacant $5f$ uranium orbitals which favours a more stable bond. It seems likely that this process determines the linearity of the UO_2^{2+} ion rather than a π-bonding mechanism through the $5f$ orbitals, which must play a different role in the bonding process.

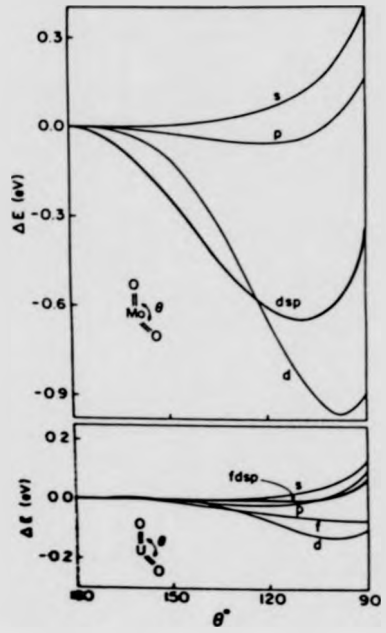

1.12. Relative total energy as a function of bond angle for Mo $4s$, $5s$, $5p$ (separately) and dsp (all together) basis sets in MoO_2^{2+} (top), and for U $5f$, $6d$, $7s$, $7p$ (separately) and $fdsp$ (all together) basis sets in UO_2^{2+} (bottom) (from ref.36).

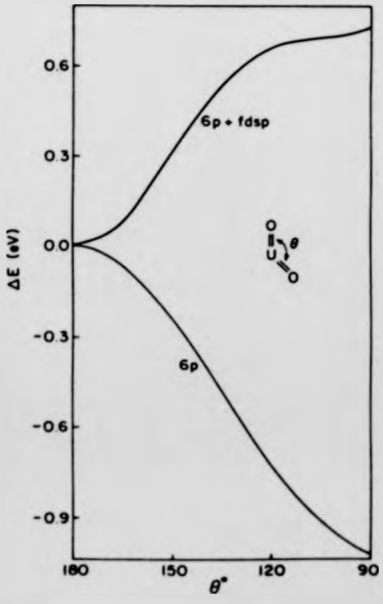

1.13. Relative total energy as a function of O-U-O bond angle for U $6p$ and $6p$ + $5f$,$6d$,$7s$,$7p$ basis sets in UO_2^{2+} (from ref.36).

References

1. E. McMillan and P. Abelson, *Phys. Rev.*, vol. 57, p. 1185, 1940.
2. M. Smutz, Chairman, "Symposium on the Production Technology of ^{237}Np and ^{238}Pu.," *Ind. Eng. Chem. Proc. Des. Dev.*, vol. 3, p. 289, Denver, 1964.
3. W.W. Schultz and G.E. Benedict, "Neptunium-237: Production and Recovery," USAEC Report TID-25955, 1972.
4. U. Casellato, M. Vidali, and P.A. Vigato, *Inorg. Chim. Acta*, vol. 18, p. 77, 1976.
5. J.R. Brand and J.W. Cobble, *Inorg. Chem.*, vol. 9, p. 912, 1970.
6. A. Ekstrom, *Inorg. Chem.*, vol. 13, p. 2237, 1974.
7. "The Actinides," in *Comprehensive Inorganic Chemistry, Vol 5*, ed. A.F. Trotman-Dickenson, Pergamon, New York, 1973.
8. C. Keller, *The Chemistry of the Transuranium Elements*, Verlag Chemie, 1971.
9. S.K. Patil, V.V. Ramakrisha, and M.V. Ramaniah, *Coord. Chem. Rev.*, vol. 25, p. 133, 1978.
10. C. Musikas and J.H. Burns, "Structure and Bonding in Compounds containing the NpO_2^+ and NpO_2^{2+} Ions," in *Transplutonium Elements*, ed. R. Lindler, pp. 237-245, North-Holland Publishing Company, Amsterdam, 1976.
11. R.G. Pearson, *J. Am. Chem. Soc.*, vol. 85, p. 3533, 1963.
12. W.H. Zachariasen and H.A. Plettinger, *Acta Cryst.*, vol. 12, p. 526, 1959.
13. K.W. Bagnall, *Inorg. Chim. Acta*, vol. 94, p. 3, 1984.
14. N.W. Alcock, M.M. Roberts, and D. Brown, *J. Chem. Soc. Dalton Trans.*, p. 25, 1982.
15. N.W. Alcock, M.M. Roberts, and D. Brown, *Acta Cryst.*, vol. B38, p. 1805, 1982.
16. A. Bondi, *J. Phys. Chem.*, vol. 68, p. 441, 1964.
17. J.C. Taylor and P.W. Wilson, *Acta Cryst.*, vol. B30, p. 169, 1974.
18. N.W. Alcock, M.M. Roberts, and D. Brown, *J. Chem. Soc Dalton Trans.*, p. 869, 1982.
19. G.M. Kramer, M.B. Dines, R.B. Hall, A. Kaldor, A.J. Jacobson, and J.C. Scanlon, *Inorg. Chem.*, vol. 19, p. 1340, 1980.
20. J.C. Taylor and A.B. McLaren, *J. Chem. Soc. Dalton Trans.*, p. 460, 1979.
21. N.W. Alcock, *J. Chem. Soc. Dalton Trans.*, p. 1189, 1972.
22. J.C. Taylor, *Acta Cryst.*, vol. B27, p. 1088, 1971.

23. N.W. Alcock, *J. Chem. Soc. (A)*, p. 1588, 1968.

24. A. Anderson, C. Chieh, D.E. Irish, and J.P.K.Tong, *Can. J. Chem.*, vol. 58, p. 1651, 1980.

25. N.W. Alcock, M.M. Roberts, and D. Brown, *J. Chem. Soc Dalton Trans.*, p. 33, 1982.

26. L. Cattalini, U. Croatto, S. Degetto, and E. Tondello, *Inorg. Chim. Acta Reviews*, vol. 5, p. 19, 1971.

27. V.I. Spitsyn and J.J. Katz, in *Proc. Mosc. Symp. Chem. Trans. Elem.*, p. 123, Pergammon Press, Oxford, 1976.

28. R.G. Denning, J.O.W. Norris, I.G. Short, and T.R. Snelgrove, "Electronic Structure of Actinyl Ions," in *ACS Symp. Series (Lanthanide Actinide Chem. Spectroscopy)*, ed. N. Edelstein, vol. 131, p. 313, 1980.

29. C.A. Coulson and G.R. Lester, *J. Chem. Soc.*, p. 3650, 1956.

30. D. Brown and J. Edwards, *J. Chem. Soc. Dalton Trans.*, p. 1757, 1972.

31. D. Brown, C.T. Reynolds, and P.T. Mosley, *J. Chem. Soc. Dalton Trans.*, p. 857, 1972.

32. R.G. Denning, "Properties of the UO_2^{n+} (n=1,2) Ions," in *Gmelin Handbuch URAN Suppl. Vol A6*, pp. 31-79, 1983.

33. W.H. Zachariasen, *Acta Cryst.*, vol. 7, pp. 795-9, 1954.

34. N.P. Brandenberg and B.O. Loopstra, *Acta Cryst.*, vol. B34, p. 3734, 1978.

35. S.Siegel, H. Hoekstra, and E. Sherry, *Acta Cryst.*, vol. 20, p. 292, 1966.

36. K. Tatsumi and R. Hoffman, *Inorg. Chem.*, vol. 19, p. 2656, 1980.

CHAPTER 2

The Crystal and Molecular Structures of Four Actinyl (VI) Complexes with 2,2'-Dipyridyl.

2.1. Introduction

A number of complexes of nitrogen donor ligands with dioxouranium(VI) have been reported including a number containing 2,2'- dipyridyl,[1] but structural information is based only on infra-red spectral analysis. No dipyridyl complexes of dioxoneptunium(VI) have been prepared, while actinyl - nitrogen bonds in general have hardly been examined. It was therefore of interest to prepare complexes of this type and examine their structures in order that changes arising from the variation of actinide element could be evaluated. The crystal structures of dinitrato dioxo(2,2'-dipyridyl)uranium(VI) (1), dinitrato dioxo(2,2'-dipyridyl)neptunium(VI) (2), diacetato dioxo(2,2'-dipyridyl)uranium(VI) (3) and diacetato dioxo(2,2'-dipyridyl)neptunium(VI) (4) are discussed here. These structures are compared and the effect of variation of the actinide element is discussed.

2.2. Experimental

2.2.1. *Preparations.*

Complex (1) was prepared by the addition of a cold ethanol (10 cm^3) solution of 2,2'-dipyridyl (9.0 mM) to an ethanol solution (10 cm^3) of uranyl(VI) nitrate hexahydrate (4.0 mM). Crystals were formed rapidly and recrystallised from methanol.[2] Complex (2) was prepared by adding an ethanol solution (1 cm^3) of 2,2'-dipyridyl (0.37 mmol) to an ethanol solution (1 cm^3) of freshly prepared neptunyl(VI) nitrate (0.25 mmol).[3] Crystals precipitated rapidly on standing. Complex (3) was prepared by adding a hot aqueous solution (10 cm^3) of 2,2'-dipyridyl (6.0 mM) to a solution of uranyl(VI) acetate (6.0 mM) in hot water. Pale yellow-green crystals were produced and recrystallised from methanol.[4] Complex (4) was prepared by adding a hot aqueous solution (1 cm^3) of 2,2'-dipyridyl (0.26 mmol) to a warm aqueous solution (1 cm^3) of freshly prepared sodium tris(acetato)dioxoneptunate(1-) (0.25 mmol).[5] The solid product formed slowly, and the supernatant was pipetted off after centrifugation. The product was washed in ice cold water to remove sodium acetate, and recrystallised from methanol.

Suitable crystals of all four complexes were mounted on quartz fibres, with (2) and (4) encapsulated in Lindemann glass capilliaries. The crystals of (2) and (4) were handled in a glove box to afford protection from the α- radiation of ^{237}Np.

2.2.2. *Data Collection and Structural Refinement.*

The crystal data and data collection conditions for each compound are given in Table 2.1.

For (1) the systematic absences, $hkl: h+k \neq 2n$ and $h0l: l \neq 2n$, indicated two possible space groups, $C2/c$ or Cc. The former was chosen and the uranium atom was placed in special position 4e with 2-fold site symmetry, based on examination of a Patterson synthesis,and the non-hydrogen atoms were located on successive Fourier syntheses. The structure of (2) was refined starting from the atomic positions of (1). The systematic absences $h0l: h+l \neq 2n$ and $0k0: k \neq 2n$ in the data collected for complex (3) indicated the space group $P2_1/n$ (a non-standard setting of $P2_1/c$). The position of the uranium atoms in the unit cell were found from a three-dimensional Patterson map, with the non-hydrogen atoms located on sucessive Fourier syntheses. The structure of (4) was refined starting from the atomic positions of the uranyl(VI) analogue (3). Final refinement of the non-hydrogen atoms with anisotropic temperature factors was by least squares methods. Unit weights were used for (1). For (2), (3), and (4) a weighting scheme of the form $w = X \cdot Y$ where $X = 1.0$ or $(\sin\theta/\lambda)/A$ for $(\sin\theta/\lambda) \geq$ A or $B/(\sin\theta/\lambda)$ for $(\sin\theta/\lambda) \geq$ B and $Y = 1.0$ or F_o/C for $F_o \leq$ C or D/F_o for $F_o \geq$ D was employed (constants in Table 2.1). These were shown to be satisfactory by a weight analysis. Calculations were carried out with the 'X-RAY '76' system[6] on a Burroughs B6700 computer. The final R values are given in Table 2.1.

Hydrogen atoms were inserted at calculated positions, in each case, with fixed isotropic temperature factors, $B = 5.0 \text{Å}^2$, and were not refined.

Final atomic coordinates are given in Tables 2.2 - 2.5, selected bond distances and angles are given in Tables 2.6 and 2.7 and least squares planes for the dipyridyl rings and the equatorial ligand rings around the metal atoms are given in Tables 2.8 and 2.9. The numbering scheme for complexes (1) and (2) is given in Figure 2.1 and for complexes (3) and (4) in Figure 2.2. The packing of (1) and (2) viewed obliquely is shown in Figure 2.3 and of (3) and (4), viewed down a, in Figure 2.4.

2.3. Discussion

Of the four structures described in this chapter the two nitrate and the two acetate complexes are isomorphous and isostructural. All four exhibit distorted hexagonal-bipyramidal geometry with the central metal atom coordinated to six oxygen atoms (two axial and four equatorial) and two nitrogen atoms. A comparison of the molecular plots in Figures 1 & 2 shows the marked similarities between the two pairs of complexes. The differences in the axial metal-oxygen distances between the compounds are typical of the actinide contraction found on substituting Np for U. The M-O (MO_2^{2+}) distance contracts

from 1.763(13)Å to 1.728(7)Å in the nitrates and from 1.770(8)(mean) to 1.729(10)(mean)Å in the acetates, a mean contraction of 0.038 Å, similar to those found in complexes with phosphine oxide ligands [7] where M-O (MO_2^{2+}) bond lengths decrease by 0.025 and 0.028Å. The M-O (nitrate) bond distances show a very slight contraction from 2.49(1) and 2.48(1)Å to 2.48(1) and 2.47(1)Å and the M-O (acetate) bond lengths apparently increase slightly from 2.450(9)(mean) to 2.455(9)(mean) Å, though neither of these changes is statistically significant. Both M-O bonds are comparable with the distances in other uranyl nitrate and acetate compounds. [8]

U-N bond lengths have been found previously in the rather wide range of 2.47 to 2.66 Å [9,10] which covers the values found in (1) and (3) (2.578(13),2.642(9) and 2.631(10)Å). The substitution of Np for U in (2) causes a small decrease in the M-N bond length is as expected from the contractions in the M-O bond distances. However there is a striking anomaly in the change in the M-N bond lengths in the acetate complexes. The substitution of Np for U causes an *increase* in the bond length of no less than 0.20Å (from 2.642(9) and 2.631(10)Å to 2.842(13) and 2.835(13)Å). Examination of the cell constants (in Table 2.1) also shows a surprising deviation. The normal expectation, on replacing U by Np, is of a slight contraction corresponding to the decrease in ionic radius between the two elements as is found for the nitrates. In the case of the acetate complexes the unit cell volume of the neptunyl compound is significantly larger than that of the uranyl analogue, and this change arises specifically from an increase of 0.1Å in the *b* axis length. The packing of the acetate compounds (Figure 2.4) shows that this axial length expansion is caused by the increases in M-N bond lengths because these are aligned broadly parallel to the *b* axis.

Evidence for the cause of this anomalous expansion may be found by examining the equatorial non-bonded contacts (Table 2.10). These show that the dipyridyl ligand has a relatively large bite (2.67 Å), and that the bite of the acetate group is compressed below the expected value (about 2.21 Å). The table also shows evidence of inter-ligand compression, particularly in the very short O---O contacts between the nitrate or acetate groups compared to an unconstrained value of 2.7-2.8 Å. The compressions have resulted in considerable distortions of the molecules from the ideal geometry of a precisely planar equatorial set of ligands. The coordinating ligand atoms are substantially displaced out of the mean equatorial plane (by up to 0.6 Å) as can be seen in Tables 2.8 and 2.9. The oxyanions are rotated about the N-O or C-C bond so that the coordinating oxygen atoms are twisted alternately above and below the equatorial plane. The 2,2'-dipyridyl ligands are twisted in two ways, firstly by twisting of the whole molecule about the centre of the 1-1' C-C bond in the direction that increases the N---O contact distance (dipyridyl twist) and secondly by rotation of the two rings of the dipyridyl group about this bond (increasing

the dipyridyl dihedral angle). These displacements are shown graphically in Figure 2.5, and Table 2.11 shows that the extent of these distortions varies between the nitrates and the acetates although the members of each pair are almost identical. The biggest difference is in the dipyridyl dihedral angle. For the nitrates this is $+12°$, in the sense that increases the distance of the two nitrogen atoms from the equatorial plane (i.e. reinforcing the dipyridyl twist), while for the acetates it is $-8°$, reversing the dipyridyl twist. The dipyridyl group is twisted overall through a greater angle in the acetate complexes, in compensation for this difference in dihedral angle, so that the nitrogen atoms are displaced out of the equatorial plane by similar amounts in the acetates and the nitrates.

The most important steric constraint affecting the deformation of the equatorial girdle seems to be repulsions involving the oxygen atoms of the MO_2^{2+} groups, which tend to keep the equatorial atoms coplanar. The distances from these atoms to the equatorial O and N atoms (Table 2.12) have a very constant minimum of about 2.8 Å. Those of the NpO_2^{2+} compounds are consistently smaller than in the UO_2^{2+} compounds, with the acetates smaller than the nitrates. In the uranyl acetate complex these steric factors have reached a critical level and the replacement of U by Np causes considerable deformation of the molecule which depends on the relative bond strengths. These must be in the order:

$$M{=}O\ (MO_2^{2+}\ \text{group}) >> M\text{-}O\ (\text{equatorial}) > M\text{-}N\ (\text{equatorial})$$

The difference in strength between the M-O (equatorial) and M-N (equatorial) has been explained by the relative softness of the N atom. [11]

Thus, on replacing U by Np, (Figure 2.6), (a) the MO_2^{2+} groups contract by a constant amount irrespective of the equatorial coordination. The equatorial bonds would also be expected to shrink, but as seen above, this cannot take place for the acetate. The first consequence of the compression (a) is to reduce the $O(MO_2^{2+})$ - O (equatorial) distance. To remove this stress, (b) the acetate or nitrate twist is slightly reduced. This in its turn decreases the O(equatorial) --- N distances. This is relieved (c) by increasing the dipyridyl twist, and the dihedral angle. However, this decreases the $O(MO_2^{2+})$ --- N distances. Then, in the acetate the two sets of oxygen atoms (axial and equatorial) act as pincers and (d) squeeze out the nitrogen-ligand, whose N-M bonds are the weakest and longest in the complex.

Figure 2.6 graphically summarises the whole process showing that the steric strain in the complex effectively causes it to behave like a coiled spring, which on compression at one point distorts at another. In this process, by a detailed comparison of the four compounds studied, the essentially static crystallographic results can become a dynamic 'moving picture'.

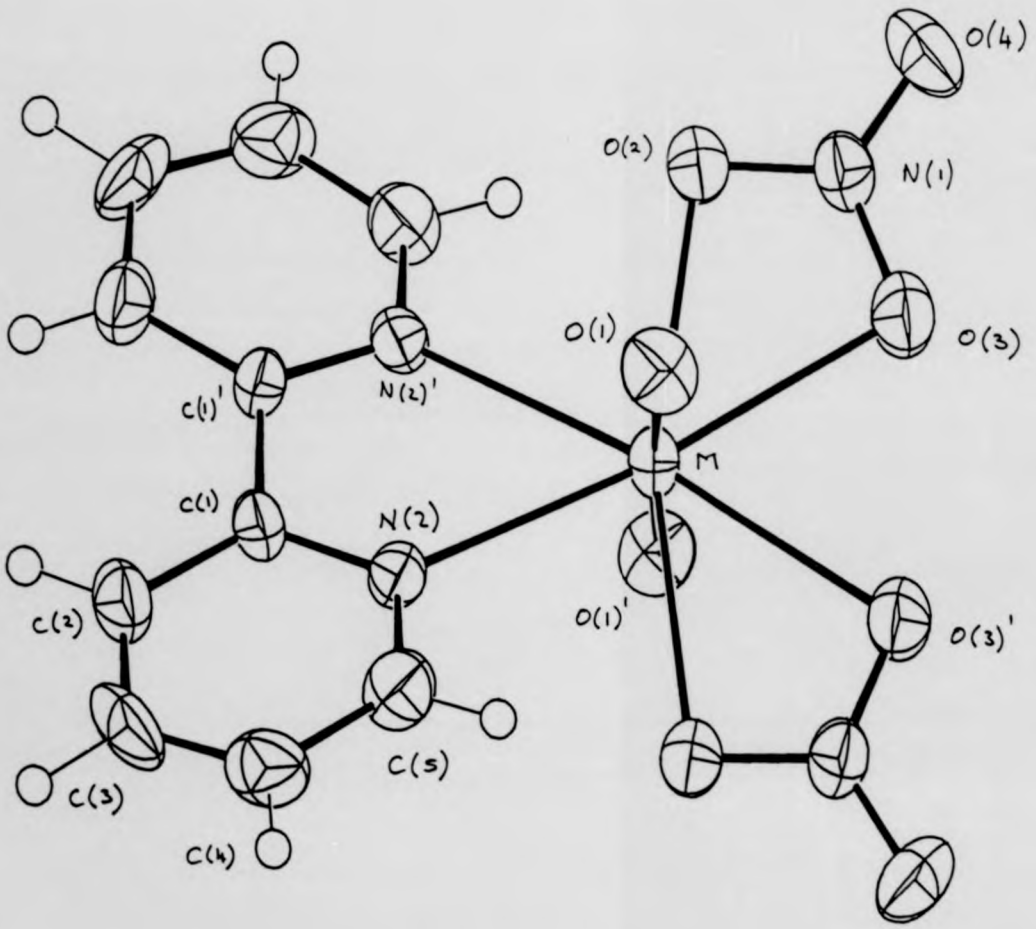

FIGURE 2.1 The $[MO_2(NO_3)_2C_{10}H_8N_2]$ (M=U or Np) molecule showing atomic numbering (primed and unprimed atoms are related by a two-fold axis).

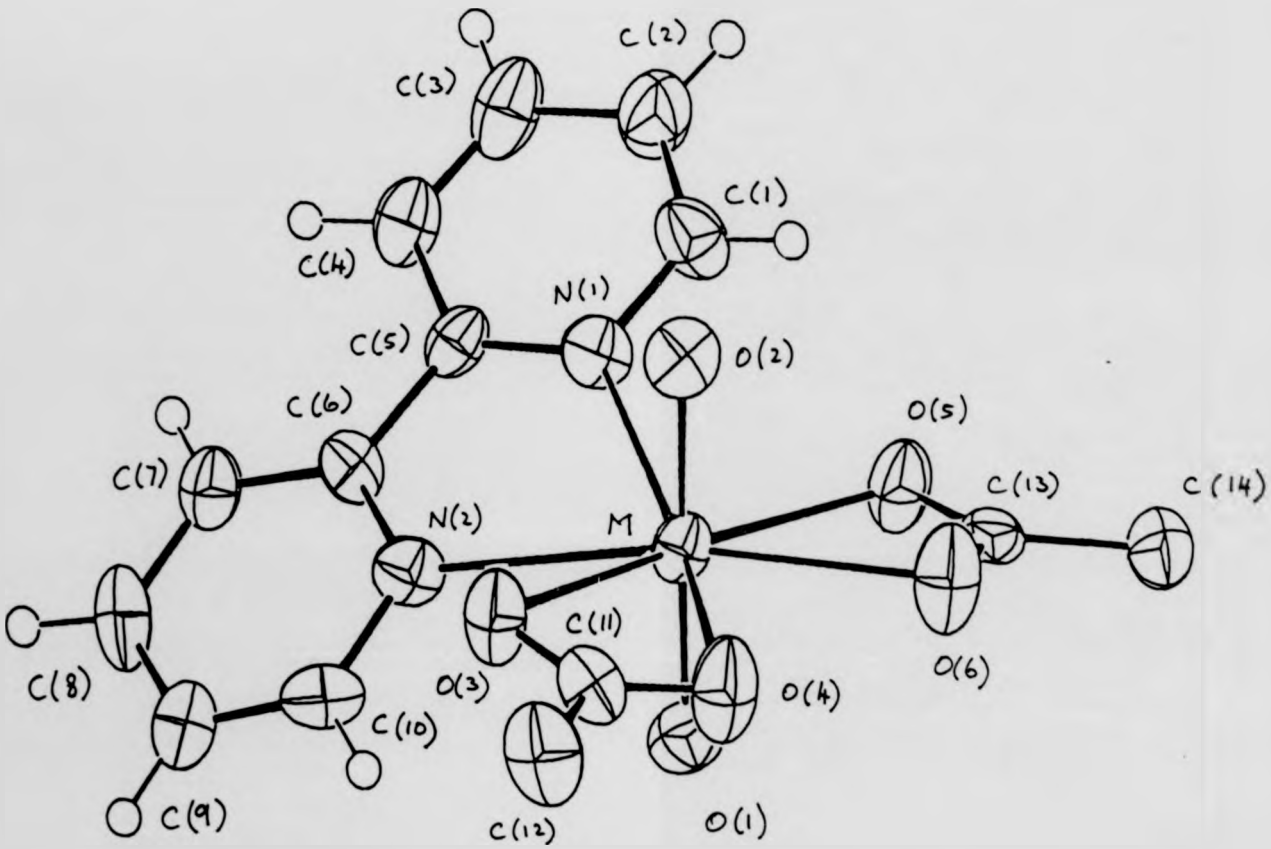

FIGURE 2.2 The $[MO_2(CH_3COO)_2C_{10}H_8N_2]$ (M=U or Np) molecule showing atomic numbering.

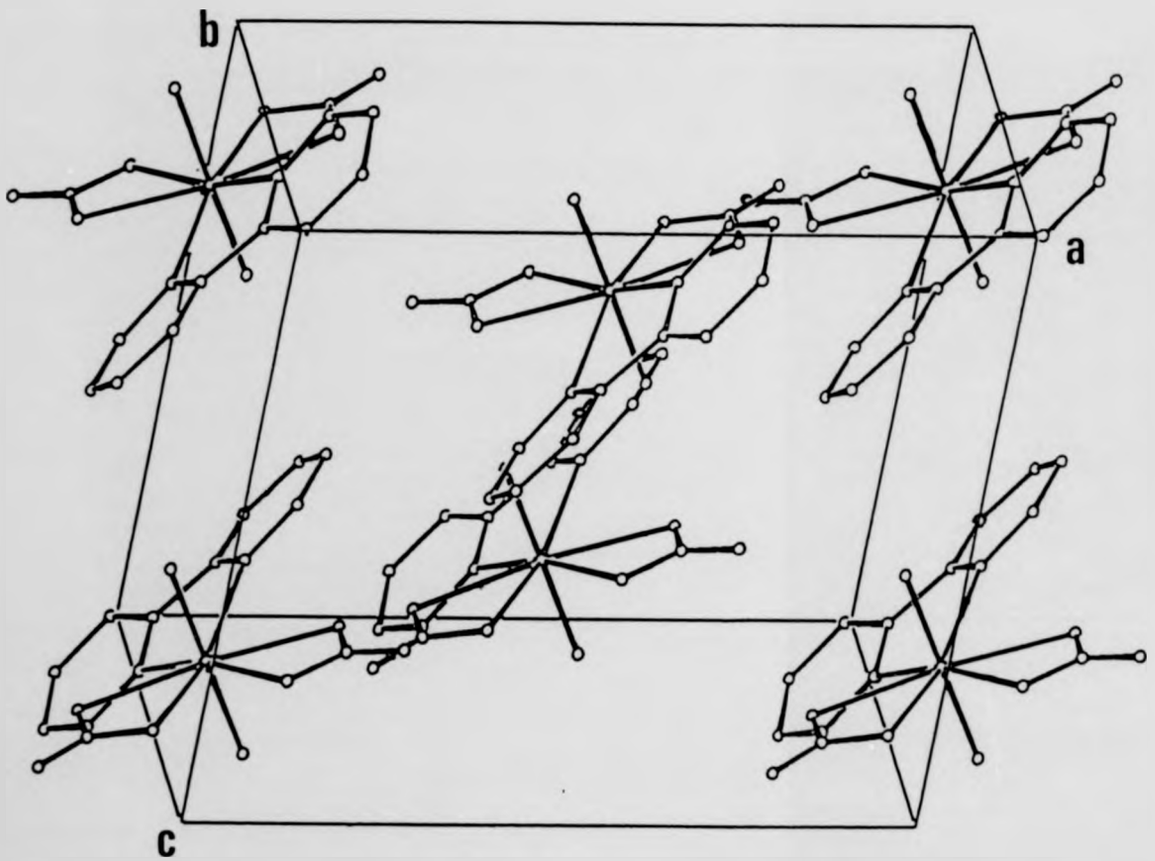

FIGURE 2.3 The packing of $[MO_2(NO_3)_2\ C_{10}H_8N_2]$ viewed obliquely.

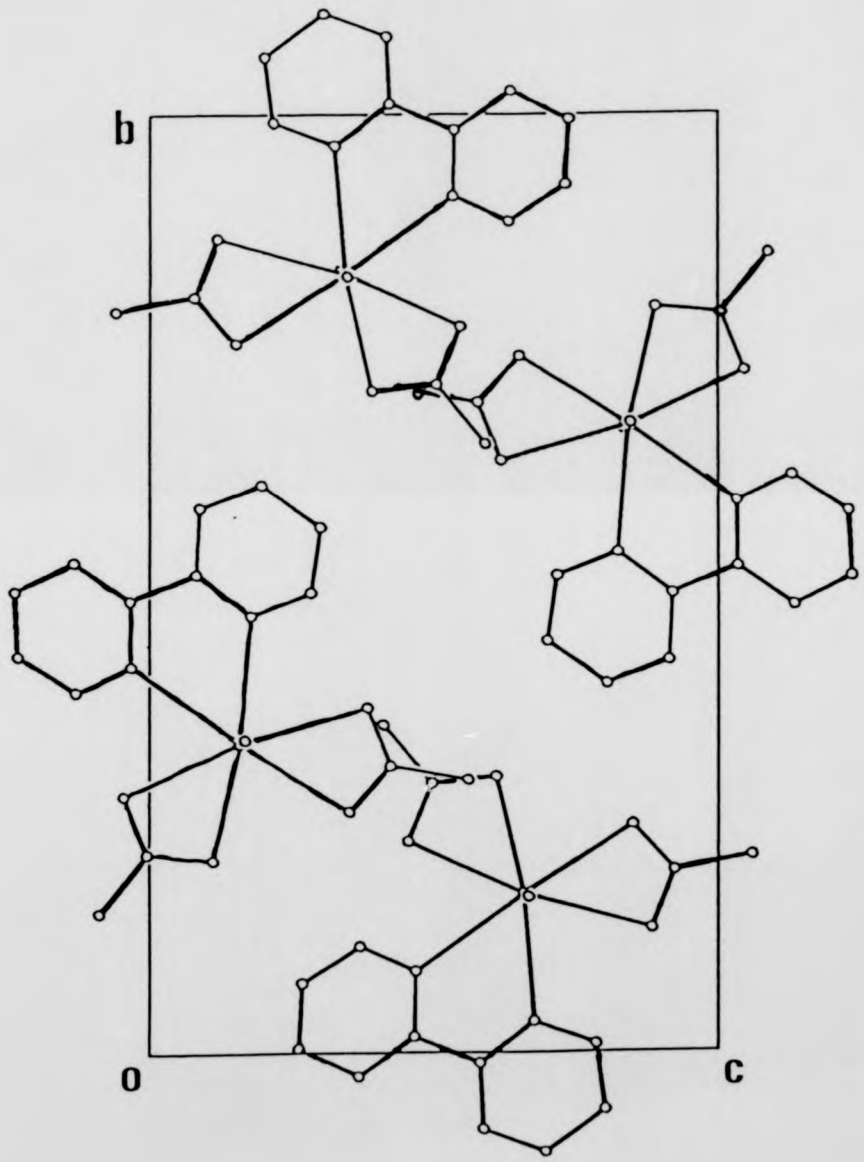

FIGURE 2.4 The packing of $[MO_2(CH_3COO)_2C_{10}H_8N_2]$ viewed down the *a* axis.

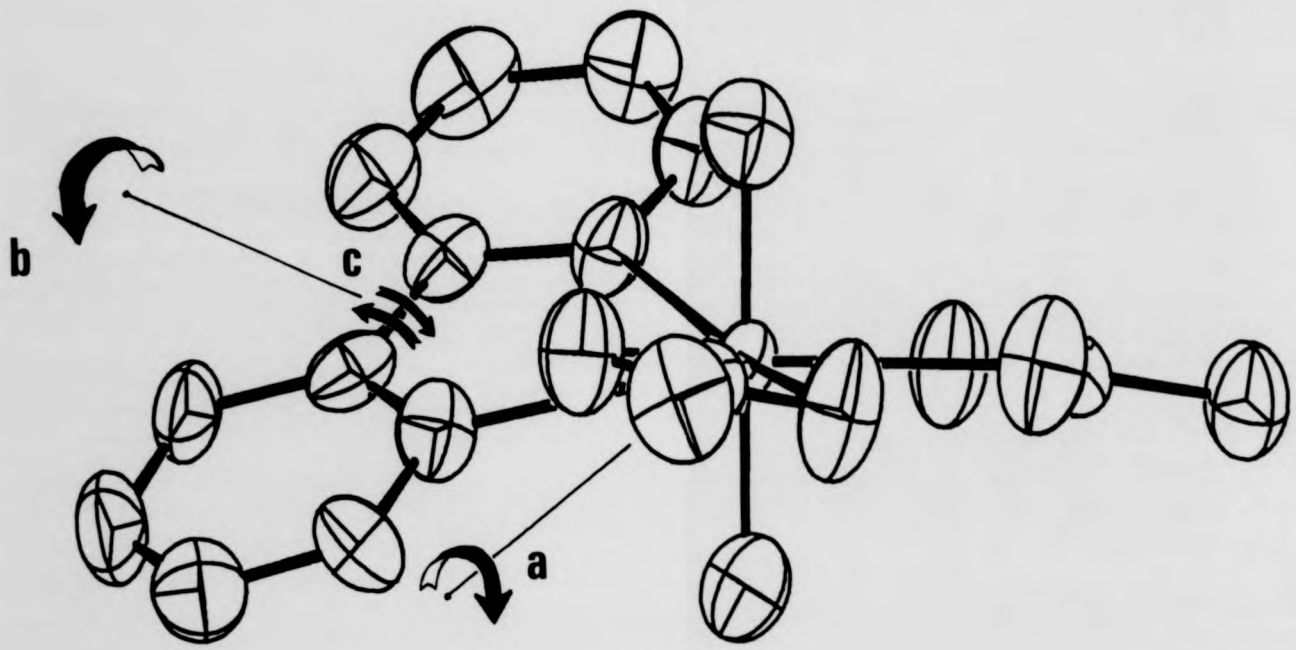

FIGURE 2.5 Distortions in the structure of $[MO_2(X)_2C_{10}H_8N_2]$ (M=U, Np, X=NO_3^-, CH_3COO^-)

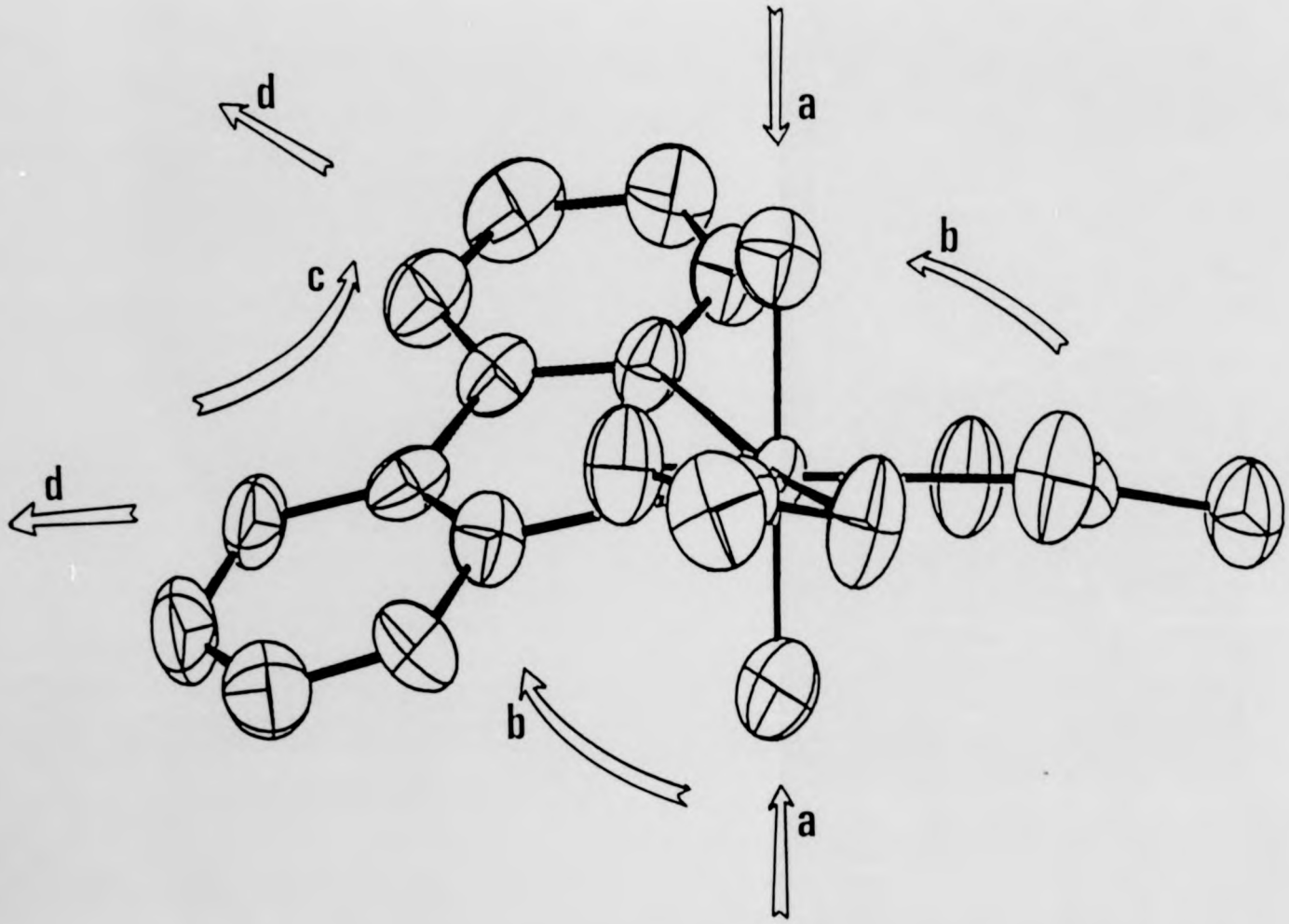

FIGURE 2.6 The sequence of reactions on compressing the $[MO_2(CH_3COO)_2C_{10}H_8N_2]$ complex by replacing U by Np.

TABLE 2.1

Crystal Data and Data Collection Conditions

Compound	(1)	(2)	(3)	(4)
Formula	$C_{10}H_8N_4O_8U$	$C_{10}H_8N_4NpO_8$	$C_{14}H_{14}N_2O_6U$	$C_{14}H_{14}N_2NpO_6$
M	550.24	549.20	544.32	543.28
System	Monoclinic	Monoclinic	Monoclinic	Monoclinic
Space Group	$C2/c$	$C2/c$	$P2_1/n$	$P2_1/n$
a/Å	13.370(2)	13.365(4)	7.949(1)	7.927(1)
b/Å	9.977(3)	9.935(5)	19.032(5)	19.126(4)
c/Å	10.538(2)	10.451(2)	10.602(3)	10.604(2)
β/°	99.81(1)	99.95(2)	95.66(2)	95.87(2)
U/Å^3	1 385.1(5)	1 366.8(8)	1 596.1(7)	1 599.2(6)
Z	4	4	4	4
D_c/g cm^{-3}	2.64	2.67	2.26	2.26
μ(Mo-K_α)/cm^{-1}	111.6	49.79	96.8	42.43
Crystal size/mm.	.12×.08×.30	.17×.02×.28	.36×.11×.10	.42×.12×.12
Max. transmission factor	0.52	0.90	0.66	0.81
Min. transmission factor	0.31	0.48	0.50	0.70
Temp.,θ_c/° C	16	-100	16	16
Scan range about K_{α_1}-K_{α_2}/°	-1.0/+1.1	±1.1	-1.0/+1.1	-1.0/+1.1
Reflections collected	1 367	1 358	3 072	3 160
Reflections observed [$I/\sigma(I)\geq 3.0$]	1 108	1 083	1 821	1 936
Weighting constants:A and B		0.20;0.60	0.37;0.37	0.05;0.99
:C and D		50.0;180.0	70.0;180.0	24.0;200.0
Final R-value	0.026	0.036	0.036	0.035

TABLE 2.2

Atomic coordinates ($\times 10^4$) for (1), with standard deviations in parentheses.

Atom	*x*	*y*	*z*
U	0.0	652.7(8)	2500.0
O(1)	745(8)	619(12)	4050(9)
O(2)	1663(8)	306(10)	1779(10)
O(3)	842(9)	-1473(11)	2062(12)
O(4)	2327(9)	-1636(12)	1478(12)
N(1)	1643(10)	-961(12)	1754(12)
N(2)	566(9)	2863(12)	1570(11)
C(1)	355(11)	4066(13)	2028(14)
C(2)	764(13)	5244(15)	1631(17)
C(3)	1380(14)	5185(17)	707(18)
C(4)	1540(13)	3974(18)	156(18)
C(5)	1121(13)	2835(16)	612(15)

TABLE 2.3

Atomic coordinates ($\times 10^4$) for (2), with standard deviations in parentheses

Atom	*x*	*y*	*z*
Np	0.0	655.9(6)	2500.0
O(1)	727(6)	625(9)	4036(7)
O(2)	1666(6)	325(7)	1796(7)
O(3)	839(7)	-1478(8)	2084(9)
O(4)	2328(7)	-1625(9)	1486(8)
N(1)	1646(8)	-959(9)	1770(9)
N(2)	567(7)	2854(9)	1556(8)
C(1)	346(8)	4074(10)	2026(9)
C(2)	771(9)	5256(10)	1629(11)
C(3)	1388(10)	5204(12)	711(12)
C(4)	1546(9)	3965(12)	161(12)
C(5)	1127(9)	2837(12)	597(10)

TABLE 2.4

Atomic coordinates ($\times 10^4$) for (3), with standard deviations in parentheses

Atom	*x*	*y*	*z*
U	2197.9(6)	1696.4(2)	3407.4(4)
O(1)	4434(10)	1723(5)	3447(8)
O(2)	-29	1658	3324
O(3)	1945(14)	2256(4)	5471(9)
O(4)	2229(13)	2945(4)	3886(8)
O(5)	2312(13)	1319(4)	1184(8)
O(6)	1962(10)	2431(5)	1514(8)
N(1)	1601(12)	333(5)	3223(10)
N(2)	3190(13)	871(5)	5328(10)
C(1)	722(18)	90(6)	2167(13)
C(2)	167(20)	-612(7)	2005(14)
C(3)	495(20)	-1066(7)	3032(14)
C(4)	1347(17)	-819(6)	4126(12)
C(5)	1886(15)	-108(6)	4184(11)
C(6)	2822(16)	170(6)	5349(12)
C(7)	3438(20)	-249(7)	6351(13)
C(8)	4436(16)	54(6)	7368(12)
C(9)	4839(19)	749(8)	7311(13)
C(10)	4165(14)	1141(6)	6314(11)
C(11)	2050(16)	2876(6)	5039(12)
C(12)	1926(20)	3503(6)	5905(13)
C(13)	2203(16)	1940(6)	778(12)
C(14)	2408(19)	2091(8)	-613(13)

TABLE 2.5

Atomic coordinates ($\times 10^4$) for (4), with standard deviations in parentheses

Atom	*x*	*y*	*z*
Np	2204.5(7)	1690.6(2)	3418.2(5)
O(1)	4379(13)	1730(6)	3476(8)
O(2)	6(12)	1658(5)	3347(8)
O(3)	1934(15)	2253(5)	5474(9)
O(4)	2228(16)	2948(5)	3886(8)
O(5)	2340(14)	1307(4)	1200(8)
O(6)	1950(15)	2421(5)	1533(9)
N(1)	1573(15)	343(5)	3218(10)
N(2)	3181(15)	871(5)	5334(10)
C(1)	729(20)	86(7)	2144(13)
C(2)	148(21)	-593(7)	2011(13)
C(3)	483(22)	-1055(7)	3017(16)
C(4)	1320(20)	-801(7)	4125(14)
C(5)	1865(16)	-110(6)	4202(11)
C(6)	2864(16)	175(6)	5363(12)
C(7)	3422(19)	-245(7)	6392(13)
C(8)	4449(21)	49(8)	7385(14)
C(9)	4794(20)	757(8)	7345(14)
C(10)	4189(18)	1147(7)	6321(13)
C(11)	2038(18)	2866(7)	5040(13)
C(12)	1949(22)	3497(7)	5894(13)
C(13)	2187(17)	1925(6)	777(12)
C(14)	2375(22)	2089(7)	-624(12)

TABLE 2.6

Bond lengths (Å) and bond angles (°) for $[MO_2(NO_3)_2C_{10}H_8N_2]$ [M=U(1) or Np(2)], with standard deviations in parentheses (Primed atoms are related to unprimed by a two-fold axis)

a)Bond lengths	(1)	(2)
i) Around M		
M-O(1)	1.763(13)	1.728(7)
M-O(2)	2.494(13)	2.484(8)
M-O(3)	2.481(12)	2.472(8)
M-N(2)	2.578(13)	2.564(9)
ii) Nitrate groups		
N(1)-O(2)	1.264(15)	1.277(12)
N(1)-O(3)	1.278(19)	1.288(14)
N(1)-O(4)	1.210(19)	1.203(14)
iii) Dipyridyl groups		
N(2)-C(1)	1.34(2)	1.36(1)
N(2)-C(5)	1.35(2)	1.35(2)
C(1)-C(1)'	1.49(2)	1.47(2)
C(1)-C(2)	1.39(2)	1.40(1)
C(2)-C(3)	1.38(3)	1.37(2)
C(3)-C(4)	1.37(3)	1.39(2)
C(4)-C(5)	1.39(3)	1.37(2)

b) Bond Angles	(1)	(2)
i) Around M		
O(1)-M-O(1)'	177.8(6)	177.9(4)
O(1)-M-O(2)	83.5(4)	83.3(3)
	96.2(4)	96.4(3)
O(1)-M-O(3)	87.3(5)	87.0(4)
	90.8(5)	91.2(4)
O(1)-M-N(2)	102.3(5)	102.5(3)
	79.7(5)	79.3(3)
O(2)-M-O(3)	50.8(4)	51.5(3)
O(2)-M-N(2)	70.6(4)	70.1(3)
O(3)-M-O(3)'	62.5(4)	61.9(3)
N(2)-M-N(2)'	62.4(4)	63.2(3)

TABLE 2.6 cont.

ii) Nitrate groups	(1)	(2)
O(2)-N(1)-O(3)	114(1)	114(1)
O(2)-N(1)-O(4)	123(1)	123(1)
O(3)-N(1)-O(4)	123(1)	123(1)
iii) Dipyridyl group		
C(5)-N(2)-C(1)	118(1)	117(1)
N(2)-C(1)-C(1)'	122(1)	116(1)
N(2)-C(1)-C(2)	116(1)	121(1)
C(2)-C(1)-C(1)'	122(1)	122(1)
C(1)-C(2)-C(3)	119(1)	120(1)
C(2)-C(3)-C(4)	119(2)	118(1)
C(3)-C(4)-C(5)	118(2)	119(1)
C(4)-C(5)-N(2)	123(1)	123(1)

TABLE 2.7

Bond lengths (Å) and angles (°) for $[MO_2(CH_3COO)_2C_{10}H_8N_2]$, [M=U(3) or Np(4)], with standard deviations in parentheses.

a)Bond lengths	(3)	(4)
i) Around M		
M-O(1)	1.774(8)	1.720(10)
M-O(2)	1.765(8)	1.737(10)
M-O(3)	2.459(9)	2.460(9)
M-O(4)	2.429(9)	2.455(9)
M-O(5)	2.475(9)	2.476(9)
M-O(6)	2.438(9)	2.430(9)
M-N(1)	2.642(9)	2.842(13)
M-N(2)	2.631(10)	2.835(13)
ii) Acetate groups	(3)	(4)
C(11)-C(12)	1.514(8)	1.514(20)
C(11)-O(3)	1.271(9)	1.264(16)
C(11)-O(4)	1.252(9)	1.259(17)
C(13)-C(14)	1.526(8)	1.542(19)
C(13)-O(5)	1.257(9)	1.265(15)
C(13)-O(6)	1.245(9)	1.268(16)
iii) Dipyridyl groups		
N(1)-C(1)	1.34(2)	1.35(1)
C(1)-C(2)	1.41(2)	1.38(1)
C(2)-C(3)	1.39(2)	1.40(2)
C(3)-C(4)	1.37(2)	1.38(2)
C(4)-C(5)	1.41(2)	1.39(2)
C(5)-N(1)	1.32(2)	1.36(2)
C(5)-C(6)	1.48(2)	1.50(2)
C(6)-N(2)	1.37(2)	1.36(2)
C(6)-C(7)	1.38(2)	1.39(2)
C(7)-C(8)	1.40(2)	1.38(2)
C(8)-C(9)	1.36(2)	1.38(2)
C(9)-C(10)	1.36(2)	1.36(2)
C(10)-N(2)	1.34(1)	1.36(2)

TABLE 2.7 cont.

b) Bond Angles	(3)	(4)
i) Around M		
O(1)-M-O(2)	178.3(3)	179.3(4)
O(3)-M-O(4)	52.5(3)	52.6(3)
O(4)-M-O(6)	67.0(3)	66.5(3)
O(5)-M-O(6)	52.3(3)	52.9(3)
N(1)-M-N(2)	60.6(3)	61.0(3)
N(1)-M-O(5)	70.6(3)	70.1(3)
N(2)-M-O(3)	67.3(3)	67.7(3)
O(1)-M-O(3)	97.9(4)	97.3(4)
O(1)-M-O(4)	88.7(4)	87.9(5)
O(1)-M-O(5)	84.2(4)	84.6(4)
O(1)-M-O(6)	89.9(3)	90.1(4)
O(1)-M-N(1)	101.6(4)	103.1(4)
O(1)-M-N(2)	77.0(4)	77.5(4)
ii) Acetate groups		
C(12)-C(11)-O(3)	120.2(4)	120.8(12)
C(12)-C(11)-O(4)	122.0(4)	120.0(12)
O(3)-C(11)-O(4)	117.8(6)	119.2(12)
C(14)-C(13)-O(5)	119.8(4)	121.2(12)
C(14)-C(13)-O(6)	120.2(4)	119.4(11)
O(5)-C(13)-O(6)	120.0(6)	119.3(12)
iii) Dipyridyl group	(3)	(4)
N(1)-C(1)-C(2)	123.9(12)	123.9(12)
C(1)-C(2)-C(3)	117.4(13)	119.0(13)
C(2)-C(3)-C(4)	119.1(12)	117.9(13)
C(3)-C(4)-C(5)	119.0(11)	120.3(13)
C(4)-C(5)-N(1)	123.4(11)	122.3(11)
C(4)-C(5)-C(6)	120.1(10)	122.0(11)
N(1)-C(5)-C(6)	116.4(10)	115.7(10)
N(2)-C(6)-C(7)	121.1(11)	122.7(11)
N(2)-C(6)-C(5)	115.3(10)	115.0(10)
C(5)-C(6)-C(7)	123.3(11)	122.3(11)
C(6)-C(7)-C(8)	119.2(11)	118.6(12)
C(7)-C(8)-C(9)	118.9(11)	118.5(13)
C(8)-C(9)-C(10)	119.4(12)	120.4(13)
C(9)-C(10)-N(2)	123.2(11)	122.2(12)
C(10)-N(2)-C(6)	118.0(10)	117.4(10)

TABLE 2.8

Deviations (Å) from mean planes for $MO_2(C_{10}H_8N_2)(NO_2)_2$ [M = U(1) or Np(2)]. (Primed atoms are related to unprimed by a two-fold axis. starred atoms define planes).

Plane 1	(1)	(2)
M *	0.000	0.000
O(2) *	0.234	0.237
O(3) *	0.054	0.066
N(2) *	-0.526	-0.540
O(2)′ *	-0.234	-0.237
O(3)′ *	-0.054	-0.066
N(2)′ *	0.526	0.540
Plane 2		
M *	0.000	0.000
N(2) *	-0.027	-0.025
C(1) *	0.049	0.046
C(1)′ *	-0.049	-0.046
N(2)′ *	0.027	0.025
Plane 3		
O(2) *	0.001	0.001
O(3) *	0.001	0.001
O(4) *	0.002	0.001
N(1) *	-0.004	-0.003
Line 4	(1)	(2)
O(1) *	0.011	0.010
M *	0.022	0.020
O(1)′ *	0.011	0.010
Angles between plane normals and line (°)		
1:2	21.98	22.63
1:3	7.09	6.48
1:4	0.93	1.09
2:3	29.00	29.00
2:4	21.05	21.54
3:4	8.02	7.54

TABLE 2.9

Deviations (Å) from mean planes for $MO_2(C_{10}H_8N_2)(CH_3COO)_2$ [M = U(3) or Np(4)]. (Starred atoms define planes).

Plane 1	(3)	(4)	**Plane 2**	(3)	(4)
M *	-0.004	0.004	N(1) *	0.000	0.000
O(3) *	-0.340	-0.339	C(5) *	0.000	0.000
O(4) *	0.046	0.049	C(4) *	0.000	0.000
O(5) *	0.244	0.261	N(2)	-0.013	-0.070
O(6) *	-0.004	-0.018	C(6)	0.057	0.047
N(1) *	-0.533	-0.548	C(7)	0.284	0.201
N(2) *	0.591	0.591			
Plane 3			**Plane 4**		
N(1)	0.337	0.155	M *	-0.036	-0.028
C(5)	0.127	0.001	N(1) *	0.065	0.058
C(4)	0.075	-0.106	C(5) *	-0.057	-0.059
N(2) *	0.000	0.000	C(6) *	-0.011	0.007
C(6) *	0.000	0.000	N(2) *	0.039	0.021
C(7) *	0.000	0.000			
Plane 5			**Plane 6**		
O(3) *	0.000	0.000	O(5) *	0.000	0.000
O(4) *	0.000	0.000	O(6) *	0.000	0.000
C(11) *	0.000	0.000	C(13) *	0.000	0.000
C(12)	-0.025	0.010	C(14)	0.032	0.074
Line 7	(3)	(4)			
O(1) *	0.009	0.003			
M *	0.018	0.007			
O(2) *	0.009	0.003			

TABLE 2.9 cont.

Angles between plane normals and line (°)

	(3)	(4)		(3)	(4)
1:2	26.13	27.65	3:4	6.76	2.62
1:3	32.27	28.67	3:5	41.29	37.95
1:4	25.59	26.13	3:6	43.75	38.88
1:5	11.10	11.21	3:7	56.88	60.55
1:6	11.49	10.32	4:5	34.52	35.34
1:7	89.14	89.07	4:6	37.08	36.36
2:3	9.74	6.62	4:7	63.55	63.08
2:4	5.75	5.86	5:6	7.82	9.02
2:5	33.54	35.42	5:7	79.46	79.03
2:6	37.33	37.96	6:7	79.37	80.53
2:7	63.02	61.17			

TABLE 2.10

Equatorial non-bonded contacts (Å)

a) Intra-ligand 'Bites'		U	Np	Avg.
N---N	Nitrate	2.67(2)	2.69(2)	2.68
	Acetate	2.66(1)	2.66(1)	2.66
O---O	Nitrate	2.13(2)	2.15(1)	2.14
	Acetate	2.16(1) 2.17(1)	2.18(1) 2.19(1)	2.175
b) Contacts between ligands				
N---O	Nitrate	2.93(2)	2.90(1)	
	Acetate	2.83(1) 2.96(1)	2.83(1) 2.93(1)	
O---O	Nitrate	2.57(2)	2.54(1)	
	Acetate	2.69(1)	2.68(1)	

TABLE 2.11

Distortions in the equatorial groups (°)

	Nitrate		Acetate	
	U	Np	U	Np
a) Oxyanion twist (dihedral angle between anion and mean equatorial plane)	7.0	6.5	11.3 (avg.)	10.8 (avg.)
b) Dipyridyl twist (dihedral angle between mean N-C-C-N plane, and mean equatorial plane)	22.0	22.7	25.6	26.1
c) Dipyridyl dihedral angle (between two rings of dipyridyl molecule)	12.7	13.2	-8.3	-8.0

TABLE 2.10

Equatorial non-bonded contacts (Å)

a) Intra-ligand 'Bites'		U	Np	Avg.
N---N	Nitrate	2.67(2)	2.69(2)	2.68
	Acetate	2.66(1)	2.66(1)	2.66
O---O	Nitrate	2.13(2)	2.15(1)	2.14
	Acetate	2.16(1) 2.17(1)	2.18(1) 2.19(1)	2.175
b) Contacts between ligands				
N---O	Nitrate	2.93(2)	2.90(1)	
	Acetate	2.83(1) 2.96(1)	2.83(1) 2.93(1)	
O---O	Nitrate	2.57(2)	2.54(1)	
	Acetate	2.69(1)	2.68(1)	

TABLE 2.11

Distortions in the equatorial groups (°)

	Nitrate		Acetate	
	U	Np	U	Np
a) Oxyanion twist (dihedral angle between anion and mean equatorial plane)	7.0	6.5	11.3 (avg.)	10.8 (avg.)
b) Dipyridyl twist (dihedral angle between mean N-C-C-N plane, and mean equatorial plane)	22.0	22.7	25.6	26.1
c) Dipyridyl dihedral angle (between two rings of dipyridyl molecule)	12.7	13.2	-8.3	-8.0

TABLE 2.12

Distances from actinyl oxygen atoms to equatorial ligand atoms (Å)

		U	Np
N---O	Nitrate	2.85(2) - 3.42(2)	2.81(1) - 3.339(1)
	Acetate	2.82(1) - 3.50(1)	2.80(1) - 3.46(1)
O---O	Nitrate	2.89(2) - 3.22(2)	2.86(1) - 3.18(1)
	Acetate	2.87(1) - 3.20(1)	2.83(1) - 3.18(1)

References

1. K. W. Bagnall, *Gmelin Handbuch URAN Suppl.*, E1, p. 40, 1979.
2. P. V. Balakrishnan, S. K. Patil, H. D. Sharma, and V. H. Venkatasetty, *Can. J. Chem.*, vol. 43, p. 2052, 1965.
3. J. B. Laidler, *J. Chem. Soc. A*, p. 780, 1966.
4. V. P. Markov and V. V. Tsapkin, *Russian J. Inorg. Chem.*, vol. 7, p. 250, 1962.
5. L. H. Jones, *J. Chem. Phys.*, vol. 23, p. 2105, 1955.
6. J.M. Stewart, "The X-RAY '76 system," TR-466, Computer Science Center, University of Maryland, U.S.A., 1976.
7. N. W. Alcock, M. M. Roberts, and D. Brown, *J. Chem. Soc., Dalton Trans.*, p. 25, 1982.
8. L. Cattalini, U. Croatto, S. Degetto, and E. Tondello, *Inorg. Chim. Acta Reviews*, vol. 5, p. 19, 1971.
9. G. Bandoli, D. A. Clemente, G. Marangoni, and G. Paolucci, *J. Chem. Soc. Chem. Commun.*, p. 235, 1978.
10. G. Bandoli, D. A. Clemente, G. Marangoni, and G. Paolucci, *J. Chem. Soc. Dalton Trans.*, p. 1304, 1980.
11. G. Bandoli, D. A. Clemente, U. Croatto, M. Vidali, and P. A. Vigato, *J. Chem. Soc. Dalton Trans.*, p. 2331, 1973.

CHAPTER 3

The Crystal and Molecular Structures of Two Uranium(VI) Complexes with 1,10-phenanthroline.

3.1. Introduction

As a result of the work described in Chap. 2, and the effect of the ability of the bidentate *N*-donor ligand to twist about the 1,1′ C-C bond allowing accomodation of a bulky ligand in the equatorial plane of a hexagonal bipyramid, it was of interest to substitute a more rigid ligand for 2,2′-dipyridyl. The ideal ligand for this comparison is 1,10-phenanthroline which has a similar geometry to the dipyridyl, but has a benzene ring joining the two pyridyl rings rather than a single C-C bond. The structure of dinitratodioxo(1,10-phenanthroline)uranium(VI) (5) is discussed here and compared with the 2,2′-dipyridyl analogue. A preparation and structure determination of diacetatodioxo(1,10-phenanthroline)uranium(VI) (6) was also attempted.

3.2. Experimental

3.2.1. *Preparation*

Compound (5) was prepared by the technique of liquid diffusion,[1] placing a saturated ethanol ($2cm^3$) solution of uranyl nitrate in a small, narrow test tube and carefully layering a saturated solution of 1,10-phenanthroline in ethanol ($2cm^3$) on top. The tube was carefully sealed and the solutions allowed to mix by diffusion, being left undisturbed for *ca.* one week. When the two solutions had mixed completely, the crystals were filtered off and washed in ice-cold ethanol. Compound (6) was prepared in a similar fashion, with a saturated solution of uranyl acetate in ethanol being layered on top of the solution of 1,10-phenanthroline. Suitable crystals of each compound were chosen and mounted on quartz fibres.

3.2.2. *Crystal Data*

[5] :$C_{12}H_8N_4O_8U$, $M = 574.25$, trigonal, space group $P3_121$, $a = 11.303(2)$, $c = 10.336(4)$ Å, $U = 1143.5(5)$ Å^3, $Z = 3$, $D_m = 2.72$ g cm^{-3}, $D_c = 2.48$ gm cm^{-3}, μ(Mo - K_α) = 101.22cm^{-1}.

[6] :$C_{28}H_{24}N_4O_{10}U_2$, $M = 1005.36$, monoclinic, space group Cc, $a = 23.320(6)$, $b = 9.945(4)$, $c = 15.978(4)$Å, $\beta = 119.14(2)°$, $U = 3237(2)$Å^3, $Z = 4$, $D_c = 2.07$ g cm^{-3}, μ(Mo - K_α) = 95.27 cm−1.

3.2.3. *Data Collection and Structural Refinement*

Data were collected with the Syntex $P2_1$ automatic four-circle diffractometer. For (5), a crystal of dimensions 0.15 × 0.16 × 0.46 mm was used which gave transmission

factors in the range 0.44 to 0.39. The scan range chosen was ±0.9° (2θ) around the $K_{\alpha_1} - K_{\alpha_2}$ angles. 3317 reflections were collected and 1215 unique reflections were considered to be observed ($I/\sigma(I) > 3.0$) and were used in the refinement. The systematic abscence $000l : l = 3n$ indicated space group $P3_121$ and the uranium atom atom was found by a Patterson synthesis to be located at special position 3a (x,0,1/3). Difference Fourier maps located the remaining non-hydrogen atoms which were refined with anisotropic temperature factors. Hydrogen atoms were inserted at calculated positions with fixed isotrpic temperature factors (U=0.07Å^2)and were not refined. Final refinement was by the least squares method. A weighting scheme of the type $W = 1/(\sigma^2(F) + g(F^2))$ with $g = 0.00165$ was applied and shown to be satisfactory by weight analysis. The final R-value was 0.035.

For (6), a crystal of dimensions 0.30 × 0.18 × 0.67 mm giving maximum and minimum transmission factors of 0.76 and 0.23 respectively was used. The scan range chosen was ± 1.1° (2θ) around the $K_{\alpha_1} - K_{\alpha_2}$ angles based on scans through two low angle reflections. 2861 reflections were collected and 1994 were considered to be observed [$I/\sigma(I) \geq 3.0$]. These observed reflections were then used in the structural refinement. The systematic absences $hkl : h + k \neq 2n$ and $h0l : l \neq 2n$ indicated a choice of possible space groups between $C2/c$ and Cc. The former of these two was chosen arbitarily but is probably incorrect and refinement was continued in the latter space group. The uranium atoms were located by Patterson methods and the non-hydrogen atoms were found by Fourier syntheses. Refinement was by cascaded least squares with isotropic temperature factors for all atoms except the uraniums which were refined with anisotropic temperature factors. The compound appears to be a hydoxy-bridged species: bis[μ-hydoxymonoacetato(1,10-phenanthroline)dioxouranium(VI)], rather than the expected diacetatodioxo(1,10-phenanthroline)uranium(VI) complex. Despite refinement to an R-value of 0.08, the structure has not been completely elucidated and shows unlikely temperature factors and apparent disorder effects. The refinement has not been completed.

Calculations for both (5) and (6) were carried out on a Data General NOVA3 minicomputer using the SHELXTL system.[2] Atomic coordinates for [5] are given in Table 3.1, and significant bond length and angles in Table 3.2. Table 3.3 contains details of the least squares planes.

3.3 Discussion

Complex (5) exhibits distorted hexagonal-bipyramidal geometry with the central uranium atom coordinated to six oxygen atoms (two axial and four equatorial) and two nitrogen atoms. This geometry is very similar to that exhibited by the complexes with 2,2'-dipyridyl (Chapter 2). The U-O(UO_2) bond length of 1.735(10)Å is rather shorter than

average for hexagonal-bipyramidal complexes[3] but the U-O(nitrate) bond lengths of 2.490(12) and 2.500(17)Å are comparable to those found in other uranyl nitrate compounds[4] and the U-N bond length of 2.557(22)Å is within the range previously described as normal,[5,6] and not significantly shorter than the values found in the 2,2'-dipyridyl complexes described above.

The bite of the 1,10-phenanthroline ligand (2.67(2)Å) is identical with that of 2,2'-dipyridyl but the bite of the nitrate anion is compressed to 2.13(2)Å. Interligand compression is also apparent with the O...O distance between the two nitrate groups (2.51(2)Å) considerably shorter than the expected 2.7-2.8Å, but the O...N distance between the nitrate group and the phenanthroline ligand (2.93(4)Å) is relatively long. This compression has resulted in a puckering of the coordinating ligands out of the mean equatorial plane in a very similar manner to that observed in bisnitrato dioxo (2,2'-dipyridyl) uranium(VI). The nitrate anions are rotated about the N-O bond so that the coordinating oxygen atoms are twisted alternately above and below the mean equatorial plane. The 1,10-phenanthroline ligand is a rigid molecule and can only be twisted as a unit about the centre of the 5-5' C-C bond. The twisting of the whole molecule to obtain the O...N interligand contact distance of 2.93(4)Å produces a similar angle between the plane of the ligand molecule and the mean equatorial plane of the complex (25.25°) to that observed in the 2,2' compound (21.98°). The distances of the equatorial ligand atoms from the uranyl oxygen atoms are greater than the observed minimum in the 2,2'-dipyridyl compounds with values of O(1)-N(2):2.87(2), O(1)-O(2'):2.98(2) and O(1)-O(3):2.90(2)Å suggesting that there is substantially less difficulty in packing the ligands about the uranium atom than in the corresponding 2,2'-dipyridyl compounds.

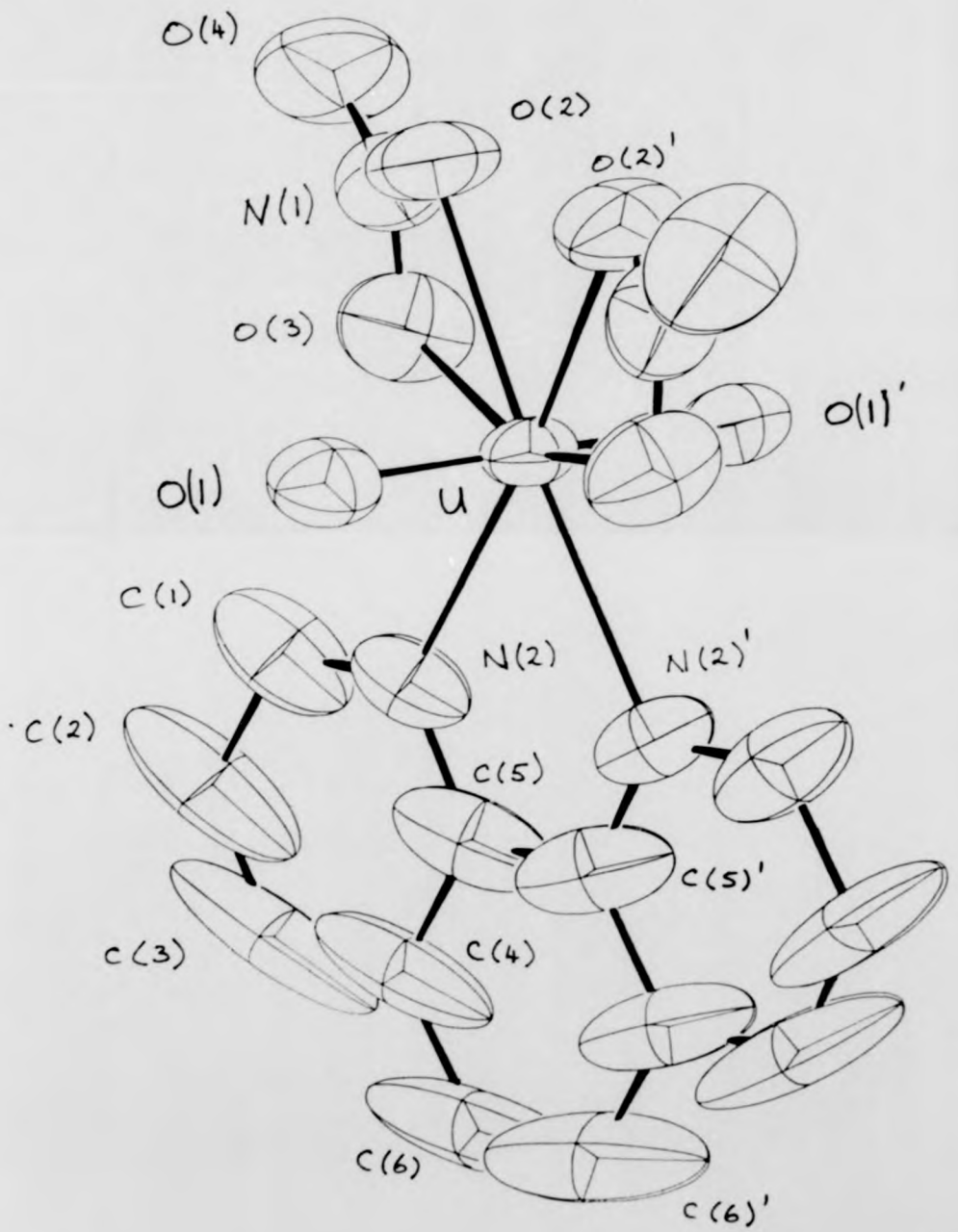

FIGURE 3.1. The $[UO_2(NO_3)_2C_{12}H_8N_2]$ [5] molecule showing atomic numbering (primed and unprimed atoms are related by a two-fold axis).

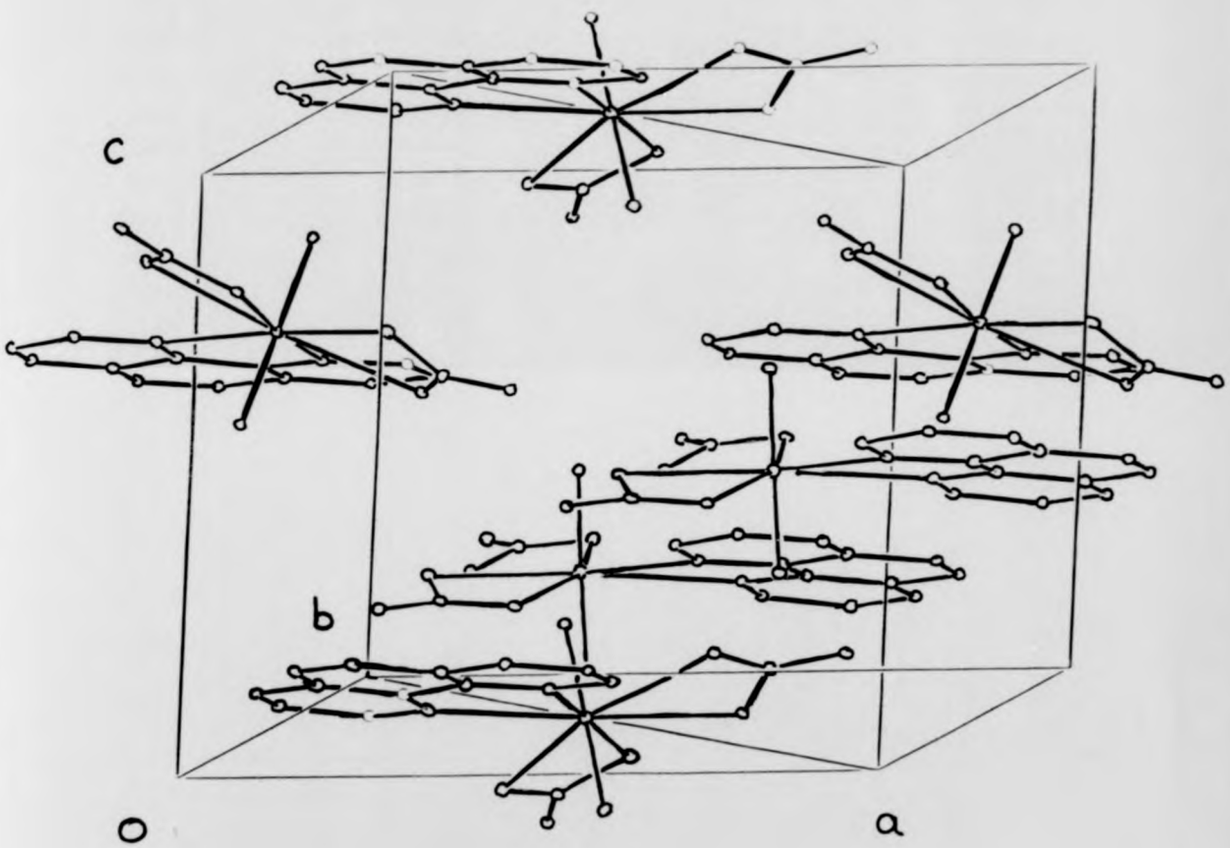

FIGURE 3.2. The packing of $[UO_2(NO_3)_2\ C_{12}H_8N_2]$ viewed obliquely.

TABLE 3.1

Atomic coordinates ($\times 10^4$) for [5]

Atom	x	y	z
U	4323(1)	0	3333
O(1)	4572(10)	533(10)	4934(10)
O(2)	5610(12)	-1255(12)	3568(13)
O(3)	3566(12)	-2306(11)	42556(12)
O(4)	4818(18)	-3257(15)	4435(17)
N(1)	4646(17)	-2327(15)	4156(16)
N(2)	3076(16)	1363(16)	3283(10)
C(1)	3772(29)	2729(24)	3310(14)
C(2)	3062(37)	3474(30)	3356(17)
C(3)	1696(39)	2827(37)	3343(16)
C(4)	953(28)	1413(34)	3347(14)
C(5)	1672(24)	700(23)	3295(15)
C(6)	-506(31)	655(45)	3318(34)

TABLE 3.2

Bond lengths (Å) and angles (°) for [5] with standard deviations in parentheses. (Primed atoms are related to unprimed by a two-fold axis).

a)Bond lengths.

U-O(1)	1.735(10)
U-O(2)	2.500(17)
U-O(3)	2.490(12)
U-N(2)	2.557(22)
O(2)-N(1)	1.31(2)
O(3)-N(1)	1.24(3)
O(4)-N(1)	1.20(3)
N(2)-C(1)	1.34(3)
N(2)-C(5)	1.37(3)
C(1)-C(2)	1.43(6)
C(2)-C(3)	1.34(5)
C(3)-C(4)	1.39(5)
C(4)-C(5)	1.40(5)
C(4)-C(6)	1.43(4)
C(5)-C(5)'	1.37(4)
C(6)-C(6)'	1.28(9)

TABLE 3.2 cont.

b)Bond angles

O(1)-U-O(1)'	178.7(7)
O(1)-U-O(2)	93.7(5)
O(1)-U-O(2)'	87.4(5)
O(1)-U-O(3)	84.8(4)
O(1)-U-O(3)'	95.4(4)
O(1)-U-N(2)	81.5(5)
O(1)-U-N(2)'	97.3(4)
O(2)-U-O(3)	50.4(4)
O(2)-U-N(2)	175.2(4)
O(2)-U-O(2)'	60.1(6)
O(2)-U-O(3)'	109.1(4)
O(2)-U-N(2)'	118.7(5)
O(3)-U-N(2)	129.3(4)
O(3)-U-O(2)'	109.1(5)
O(3)-U-O(3)'	159.3(6)
O(3)-U-N(2)'	70.9(5)
N(2)-U-O(2)'	118.7(5)
N(2)-U-O(3)'	70.9(5)
N(2)-U-N(2)'	62.9(7)
U-O(2)-N(1)	97(1)
U-O(3)-N(1)	99(1)
U-N(2)-C(1)	121(2)
U-N(2)-C(5)	120(1)
O(2)-N(1)-O(3)	113(2)
O(2)-N(1)-O(4)	120(2)
O(3)-N(1)-O(4)	126(1)
C(1)-N(2)-C(5)	119(2)
N(2)-C(1)-C(2)	120(2)
C(1)-C(2)-C(3)	121(3)
C(2)-C(3)-C(4)	120(4)
C(3)-C(4)-C(5)	118(3)
C(3)-C(4)-C(6)	123(4)
C(5)-C(4)-C(6)	119(3)
N(2)-C(5)-C(4)	122(2)
N(2)-C(5)-C(5)'	118(2)
C(4)-C(5)-C(5)'	120(1)
C(4)-C(6)-C(6)'	121(5)

TABLE 3.3

Deviations (Å) from mean planes for $UO_2(C_{12}H_8N_2)(NO_2)_2$ [5]. (Primed atoms are related to unprimed by a two-fold axis, starred atoms define planes).

Plane 1	
U *	-0.070
O(2) *	0.036
O(3) *	0.000
N(2) *	0.035
O(2)' *	-0.036
O(3)' *	0.000
N(2)' *	-0.035
Plane 2	
N(2) *	0.000
C(1) *	0.000
C(5) *	0.000
C(5)' *	0.000
C(1)' *	0.000
N(2)' *	0.000
Plane 3	
O(2) *	-0.010
O(3) *	-0.011
O(4) *	-0.012
N(1) *	0.033
Line 4	
O(1) *	0.000
U *	0.000
O(1)' *	0.000
Angles between plane normals and line (°)	
1:2	25.45
1:3	3.69
1:4	11.57
2:3	27.08
2:4	18.81
3:4	18.77

References

1. P.G. Jones, *Chem. Brit.*, vol. 17, p. 222, 1981.
2. G.M. Sheldrick, in *SHELXTL User Manual*, Nicolet Instrument Co., 1981.
3. R.G. Denning, "Properties of the UO_2^{n+} (n=1,2) Ions." in *Gmelin Handbuch URAN suppl. Vol A6*, pp. 31-79, 1983.
4. L. Cattalini, U. Croatto, S. Degetto, and E. Tondello, *Inorg. Chim. Acta. Reviews*, vol. 5, p. 19, 1971.
5. G. Bandoli, D. A. Clemente, G. Marangoni, and G. Paolucci, *J. Chem. Soc. Chem. Commun.*, p. 235, 1978.
6. G. Bandoli, D. A. Clemente, G. Marangoni, and G. Paolucci, *J. Chem. Soc. Dalton Trans.*, p. 1304, 1980.

CHAPTER 4

The Crystal and Molecular Structures of Four Actinyl (VI) Complexes with Pentan-2,4-dione.

4.1. Introduction.

A large number of complexes of dioxo-uranium(VI) with pentan-2,4-dione have been reported[1] but in most cases the only investigations carried out have been of the infra red spectra, usually involving the identification of $\nu_{as\,OUO}$ and $\nu_{s\,OUO}$. Dioxobis(pentane-2,4-dionato)pyridine uranium(VI) [7] was first reported in 1927[2] and infra red data were obtained later.[3,4] Interpretation of these data in the light of theoretical calculations[5] led to the conclusion that the O-U-O uranyl(VI) group was not linear. The determination of the structure from single crystal X-Ray data demontrates that this group is indeed significantly non-linear. No previous work on the corresponding neptunyl compounds has been carried out and so the determination of the structure of dioxobis(pentane-2,4-dionato)pyridineneptunium(VI) [8] allows the identification of structural changes arising from the change in actinide element. Two further structure determinations have been carried out on compounds of dioxouranium(VI) with pentan-2,4-dione, dioxobis(pentane-2,4-dionato)monoaquouranium(VI) [9] and dinitrato(pentan-2,4-dionato)uranium(VI) 2,4,6-trimethylpyridinium [10]. The structure of compound [9] was determined as an earlier determination of a crystal modification of the same compound in a different space group[6] had been carried out photographically in only two dimensions. Compound [10] was formed whilst attempting to prepare an analogue of compound [7] where the pyridine molecule was replaced by a 2,6-substituted pyridine. In this instance the substituted pyridine chosen was γ-collidine (2,4,6-trimethylpyridine).

4.2. Experimental.

4.2.1. *Preparation.*

Compound [7] was prepared following the method of Hager.[2] A methanol solution (5 cm^3) of uranyl(VI) nitrate (1.25 mmol) was added to a mixture of pentane-2,4-dione (2.5 mmol) and pyridine (1.25 mmol) and crystals formed immediately. These were recrystallised from methanol. The neptunyl analogue [8] was prepared by essentially the same method, using 0.25 mmol of freshly prepared neptunyl (VI) nitrate[7] and reducing the quantities of the other reagents to the same proportions. In both cases a large number of crystals had to be examined to obtain a suitable single crystal for structure determination as the majority were found to be twinned. Compound [9] was prepared using the method of Comyns et al.[8] to produce the monoclinic form 1B. A warm, dilute, aqueous solution (5

cm^3) of sodium hydroxide (1M) was added to a warm aqueous solution (10 cm^3) of uranyl(VI) nitrate (2.5 mmol) and pentane-2,4-dione (2.5 mmol). Crystals formed as the solution cooled and were recrystallised from water. This form is not identical to that studied by Frasson et al. [6] but is more useful for comparison purposes as this prior structure determination does not give any atomic coordinates. Compound [10] was prepared in a similar manner to [7] with 2,4,6-trimethylpyridine substituted for pyridine. On concentration amorphous lumps of an orange material were precipitated and recrystallisation from hot toluene gave thin lath-shaped dark orange crystals.

Infrared spectra of [7] were taken with a Perkin-Elmer 180 spectrophotometer using Nujol mulls between KBr plates for the region 1000-400 cm^{-1} and between silicon plates for the region 500-150 cm^{-1}. These confirmed the spectra obtained previously; [3,4] the expected absorption at *ca.* 210 cm^{-1} (characterised as ν_2) [4] was observed at 235 cm^{-1}.

4.2.2. *Data Collection and Structural Refinement*

The crystal data and data collection conditions for each compound are given in Table 4.1 . For complex [7], the systematic absences: $hkl:h+k, k+l \neq 2n$; $0kl:k+l \neq 4n$; $h0l:h+l \neq 4n$ indicated the space group $Fdd2$. A further strong pseudo-absence: $hkl:h+k+l \neq 2n+1$ or $4n$ suggested that the uranium atom was in special position 8*a* with two-fold site symmetry. Successive Fourier syntheses with the uranium placed at 0,0,0 (z arbitrarily chosen and fixed as 0) located the light atoms around the uranium. Hydrogen atoms were inserted at calculated positions with fixed isotropic temperature factors B = 5.0$Å^2$ and were not refined.

During the refinement, the pyridine ligand was found in a false position bonding to the uranium atom between O(3) and O(3)' giving the included angle O(3)-U-N(1) = 37.1°. This occurred by virtue of the special symmetry of the molecule in the cell, but was corrected by transposing the position of the pyridine ligand so that the nitrogen atom bonded to uranium between O(2) and O(2)' giving angles O(2)-U-N(1) = 72.1°.

The space group chosen for the solution is non-centrosymmetric and it was necessary to check that the structure had been solved in the correct hand. Refinement with the opposite handed molecule led to an increase in R so the hand originally used in solution is taken to be correct. The atomic positions of [7] were used as the starting point for the structure refinement of [8] by the least squares method with non-hydrogen atoms given anisotropic temperature factors. Hydrogen atoms were given fixed isotropic temperature factors of U=0.07$Å^2$, and were not refined.

For complex [9], the systematic absences $h0l:l \neq 2n$ and $0k0:k \neq 2n$ indicated the space group $P2_1/c$ and the uranium atom position was determined from a three-dimensional Patterson map. The non-hydrogen atoms were found on successive difference Fourier maps

and all were refined anisotropically. Hydrogen atoms, with the exception of those of the water molecule, were inserted in calculated positions with fixed isotropic temperature factors, U=0.08 Å^2, and were not refined.

For compound [10], the systematic absences $h0l: h+l \neq 2n$ ($00l: l \neq 2n$) indicated the space group $Pmmn$ and a three-dimensional Patterson map located the uranium atom at $0,\frac{1}{2},z$ in special position $2b$. The positions of the remaining non-hydrogen atoms in the cation were determined from successive difference Fourier maps, but no peaks corresponding to the anion atoms could be discovered in any of the Fourier maps and the R-factor was most unsatisfactory. Various attempts were made to reduce the symmetry and space groups $Pm2_1n$ and $P2_1mn$ were examined. In both of these space groups the mm symmetry at the uranium atom is relaxed to a mirror plane either parallel or perpendicular to the uranyl group. The former space group produced no improvement in the refinement, but in the latter the position of the non-hydrogen atoms of the anion were determined. However the position of one of the oxygen atoms of the uranyl group could not be found and the temperature factors of a number of atoms in both ions were found to be distinctly irregular. This indicated the presence of a false symmetry element and a re-examination of the raw data suggested that the systematic absence $hk0: h+k \neq 2n$ corresponding to the n-glide plane was not reliable.

In order to resolve these difficulties an alternate lower symmetry space group, $P2_12_12$, was investigated. The uranium atom was maintained at special position $2b$ and all non-hydrogen atoms were located from a difference Fourier map, and as the refinement showed only normal temperature factors the space group was taken to be correct. Non-hydrogen atoms were refined with anisotropic temperature factors except C(4) and C(41) which were refined isotropically. Hydrogen atoms were found and were refined as rigid groups with fixed isotropic temperature factors, U = 0.07Å^2. Refinement of the imaginary dispersion coefficient ($\Delta F''$) with all other parameters fixed showed little change from the initial value indicating that the structure has been solved in the correct hand.

For [7] a weighting scheme of the form $w = X \cdot Y$, where $X = 1.0$ or $(\sin\theta/\lambda)/0.35$ for $(\sin\theta/\lambda) < 0.35$ or $0.99/(\sin\theta/\lambda)$ for $(\sin\theta/\lambda) > 0.99$, and $Y = 1.0$ or $600/F_{obs}$ for $F_{obs} > 600.0$. This was shown to be satisfactory by a weighting analysis.

A weighting scheme of the type $w = 1/(\sigma^2(F) + g(F^2))$ was applied to complexes (8), (9) and (10) and shown to be satisfactory by weight analysis. The weighting constants and the final R-factors are given in Table 4.1.

The calculations were carried out with the X-RAY 76 system,[9] on a Burroughs B6700 computer and with the SHELXTL system[10] on a Data General NOVA3 minicomputer.

Final atomic coordinates are given in Table 4.2 - 4.5, bond lengths and angles in Tables 4.6 - 4.8 and details of least squares planes in Tables 4.9 and 4.10 Views of the molecules and the unit cells are given in Figs. 4.1 - 4.6.

4.3. Discussion.

The two complexes [7] and [8] are isomorphous and isostructural exhibiting pentagonal-bipyramidal coordination about the actinide atom involving two bidentate pentane-2,4-dionate ions and a pyridine molecule about the actinyl(VI) ion. The structures have a similar geometry to uranyl(VI) bis(pentane-2,4-dionate) hydrate, the only other uranyl pentane -2,4-dionate to have been studied structurally.[6] The ligand dimensions in the complexes are normal, as are the equatorial metal-ligand distances; M-N is somewhat longer than the average M-O (equatorial), as expected from the covalent radii. However, of these two complexes the uranyl(VI) group itself is most unusual. It has longer U-O distances [1.83(1)Å] than is usual (*ca.* 1.76Å)[11] for complexes with five equatorial ligands and the O-U-O angle [173.5(8)°] deviates considerably form linearity. This might be due to packing effects, but the complex shows no close intermolecular interactions involving O(1) and, as Figure 4.2 illustrates, the main contacts are between the pentan-2,4-dionate groups. The direction of the bend in the O-U-O group is more informative and Figure 4.1 shows the clear bend *away* from the pyridine substituent. This is confirmed by the N(1)-U-O(1) angle of 93.2(5)°, deviating from 90° by almost precisely half the deviation of the O-U-O angle from 180°. Furthermore the pyridine ring is twisted by 45° out of the equatorial plane, presumably to avoid interference with the pentane-2,4-dionate groups. This must, however, increase repulsions between the *ortho*-hydrogen atoms on the pyridine and the uranyl oxygen atoms, and must be responsible for the observed bent O-U-O group. It presumably also causes the unusually long U-O distance, although the lengthening seems somewhat large for the degree of bending observed. Also of significance is that the deviation of 6.5° from linearity is sufficient to produce the observed spectroscopic effects.

A number of other examples of bent uranyl(VI) groups have been reported, but consideration of those listed in a recent review,[11] coupled with a search of the later literature, shows that most occur in polymerised systems. Only three have been found with bond angles $<175°$ in monomeric systems, and of these uranyl diperchlorate heptahydrate[12] with a uranyl(VI) bond angle of 161(3)° should hardly be considered as it contains extensive hydrogen bonding involving the uranyl(VI) oxygens. [3-Oxapentane-1,5-diyl-*N*,*N'*-bis (salicylideneiminato)]dioxouranium(VI)[13] exists in two crystal modifications, each with a bent uranyl(VI) group [174.2(6) and 173.8(5)°]. Infrared and Raman spectral data again show the predicted absorptions for non-linear uranyl(VI) groups. These groups do not, however, have abnormal U-O bond lengths. Clearly the deviations from linearity in these structures must also be of intramolecular origin, and an interaction is suggested with two

oxygen atoms in the equatorial girdle, which are forced by the molecular geometry to have short U-O distances (mean 2.20 *vs.* 2.34-2.44Å in compound [7]). The final example, dioxobis (8-quinolinato)(8-quinolinol)uranium(VI),[14] has a reported O-U-O angle of 174.8°. The standard deviation is unstated, but may be as large as ±2°, and so the reality of the deviation from linearity is not fully established. However the molecular geometry is rather similar to that of the bis(salicylidene) derivative and the cause may be the same.

In the neptunyl(VI) complex the O-Np-O angle of 176.5(19)° does not deviate from linearity to the same extent, but the Np-O bond length does deviate from the value found in the compounds with 2,2'-dipyridyl of *ca.* 1.72Å (Chap 2). The Np-O (NpO_2^{2+}) bond length is 1.78(2)Å, a decrease of 0.05Å from the corresponding bond length in complex [7] which is in line with observed reductions on substituting neptunium for uranium.[15] The Np-O (equatorial) distances are also slightly shorter than those seen in the uranium complex, whereas the Np-N bond length of 2.56(2)Å is greater than the corresponding distance in the uranium compound reflecting the relative weakness of the actinyl-nitrogen bond. Examination of the angle between the pyridine molecule and the equatorial plane (Table 4.9) shows there is an increase of 5.1°. this indicates that the balance of interactions between the *ortho*-hydrogens of the pyridine and the terminal methyls of the pentane-2,4-dionates and the actinyl oxygens is resolved by the increase in the Np-N and Np-O (NpO_2^{2+}) bond lengths from the expected values and the slight bend of the NpO_2^{2+} group away from the pyridine molecule.

Complex [9] has the pentagonal bipyramidal geometry expected for a compound with two bidentate ligands and one monodentate ligand. There is some deviation in the U-O(ligand) bond lengths (2.34-2.49Å) but these are not significant when compared with the differences in bond lengths found in the equatorial girdle of compound [7]. Alternate oxygen atoms of the pentan-2,4-dionate groups are found above and below the equatorial plane and the uranium atom and the oxygen atom of the water ligand are also found marginally below the plane. The dioxouranium(VI) group has an angle of 179.0(3)° and makes an angle of 88.0° with the equatorial plane.

Complex (10) is composed of dinitratodioxo(pentane-2,4-dionato)uranium(VI) anions and 2,4,6-trimethyl pyridinium cations. The view of the anion (Figure 4.5) and the numbering scheme shows the coordination about the uranium atom to be hexagonal bipyramidal, with one pentan-2,4-dionate ion and two nitrate ions coordinated in the equatorial plane. The view of the unit cell down the *a* axis (Figure 4.6) shows the arrangement of the anions and the 2,4,6-trimethyl pyridinium cations. This arrangement suggests that the negative charge on the anion is localised in the region of C(3) of the pentane-2,4-dionate group and that the positive charge on the cation is located at the protonated nitrogen atom.

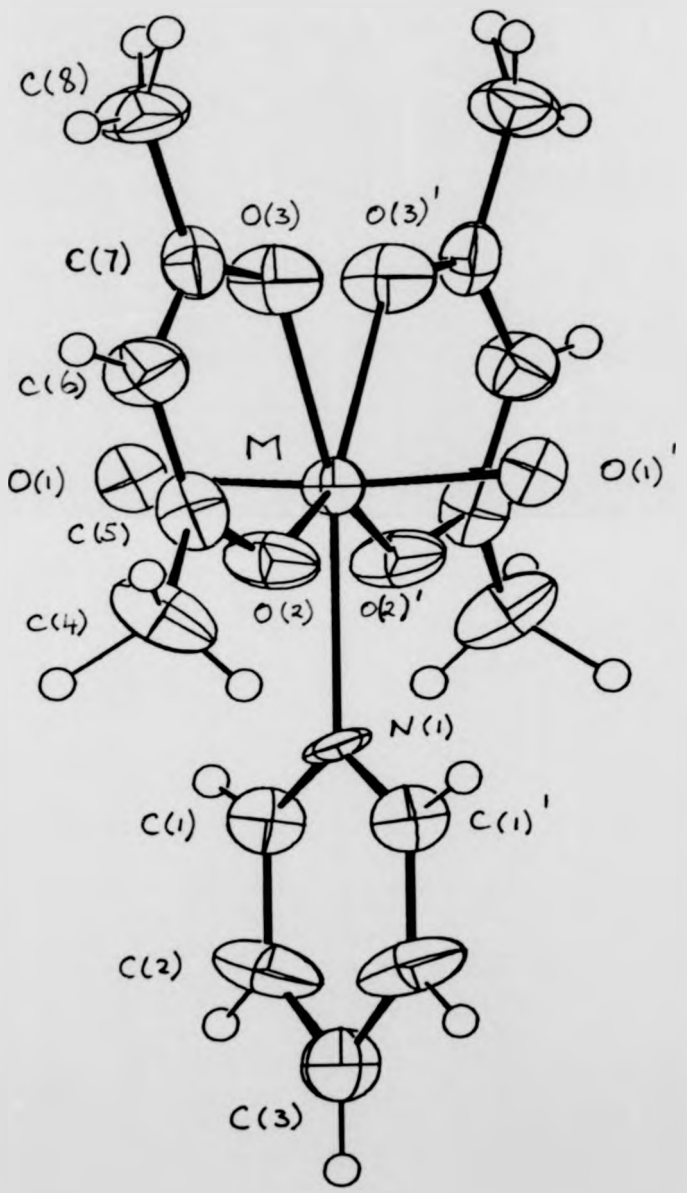

FIGURE 4.1. The $[MO_2(CH_3COCHCOCH_3)_2C_5H_5N]$ [M=U(7) or Np(8)] molecule showing atomic numbering (primed and unprimed atoms are related by a two-fold axis).

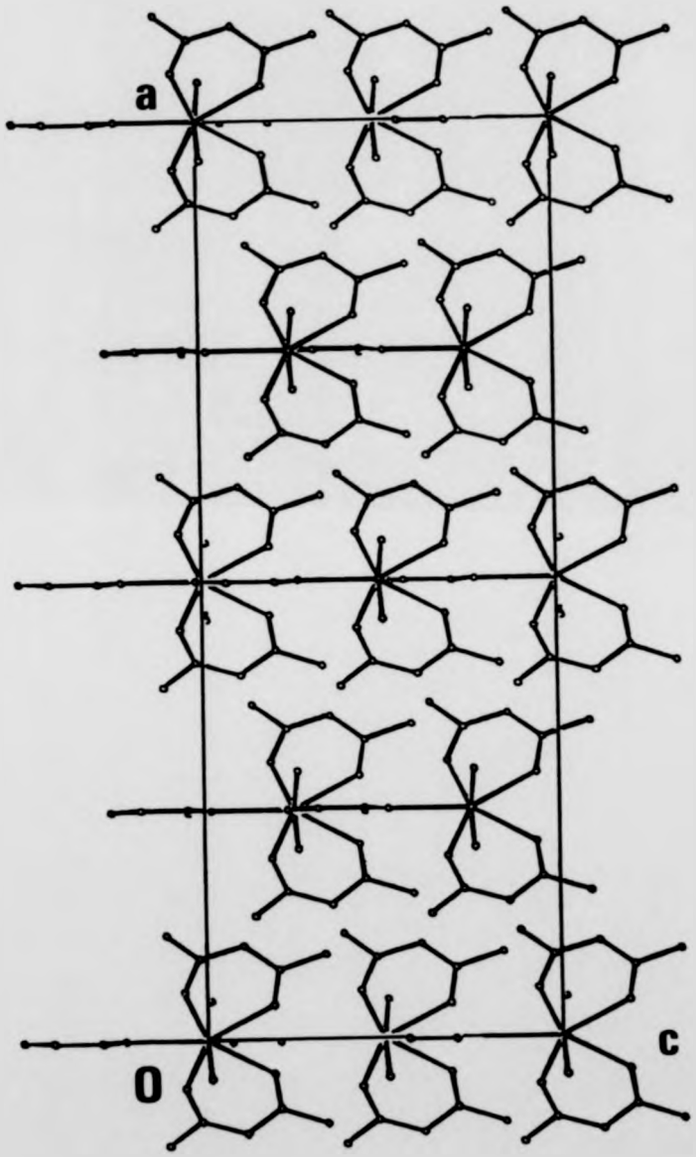

FIGURE 4.2. The packing of $[MO_2(CH_3COCHCOCH_3)_2C_5H_5N]$ [M=U(7) or Np(8)] viewed down the *b* axis.

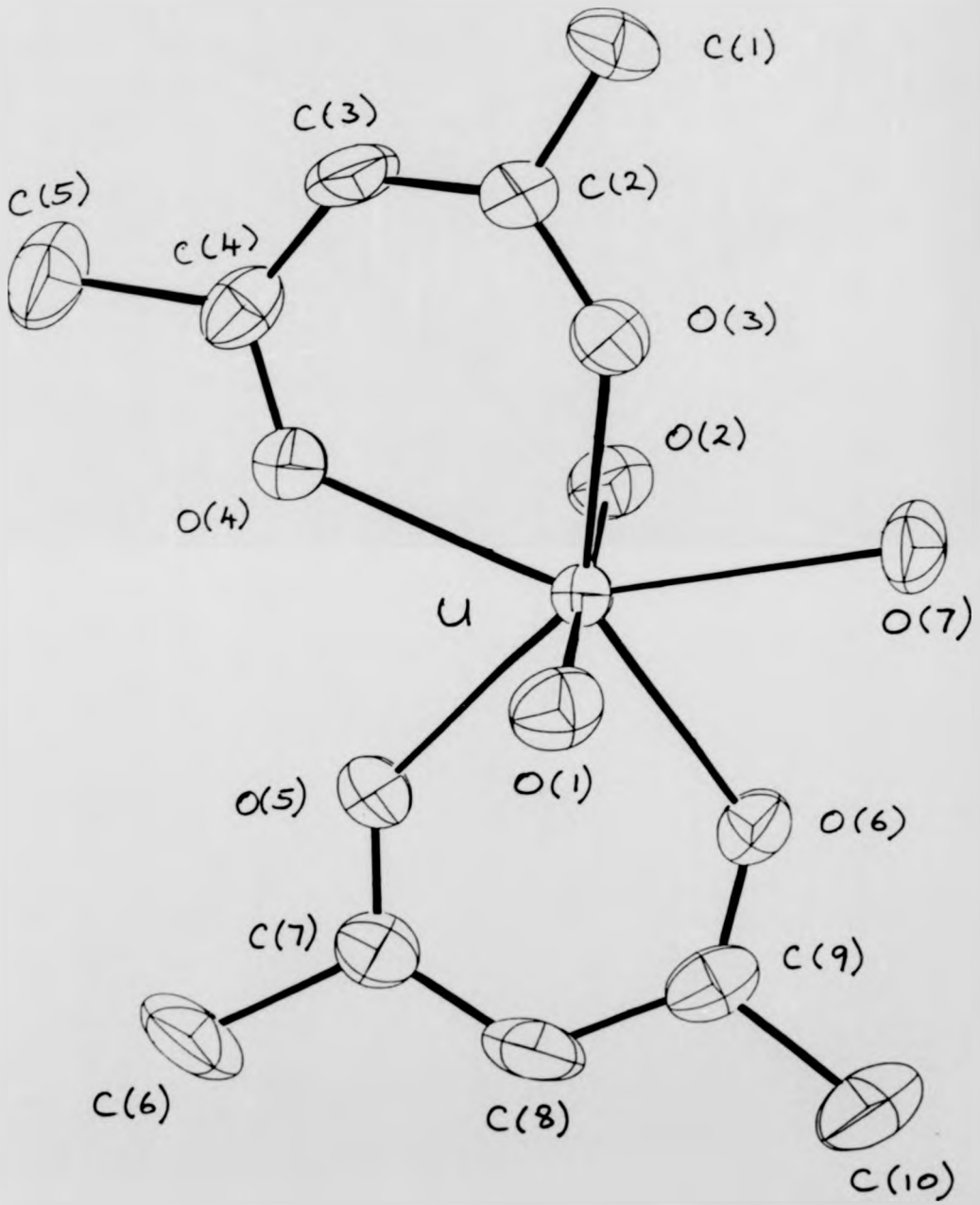

FIGURE 4.3. The $[UO_2(CH_3COCHCOCH_3)_2.H_2O]$ [9] molecule showing atomic numbering

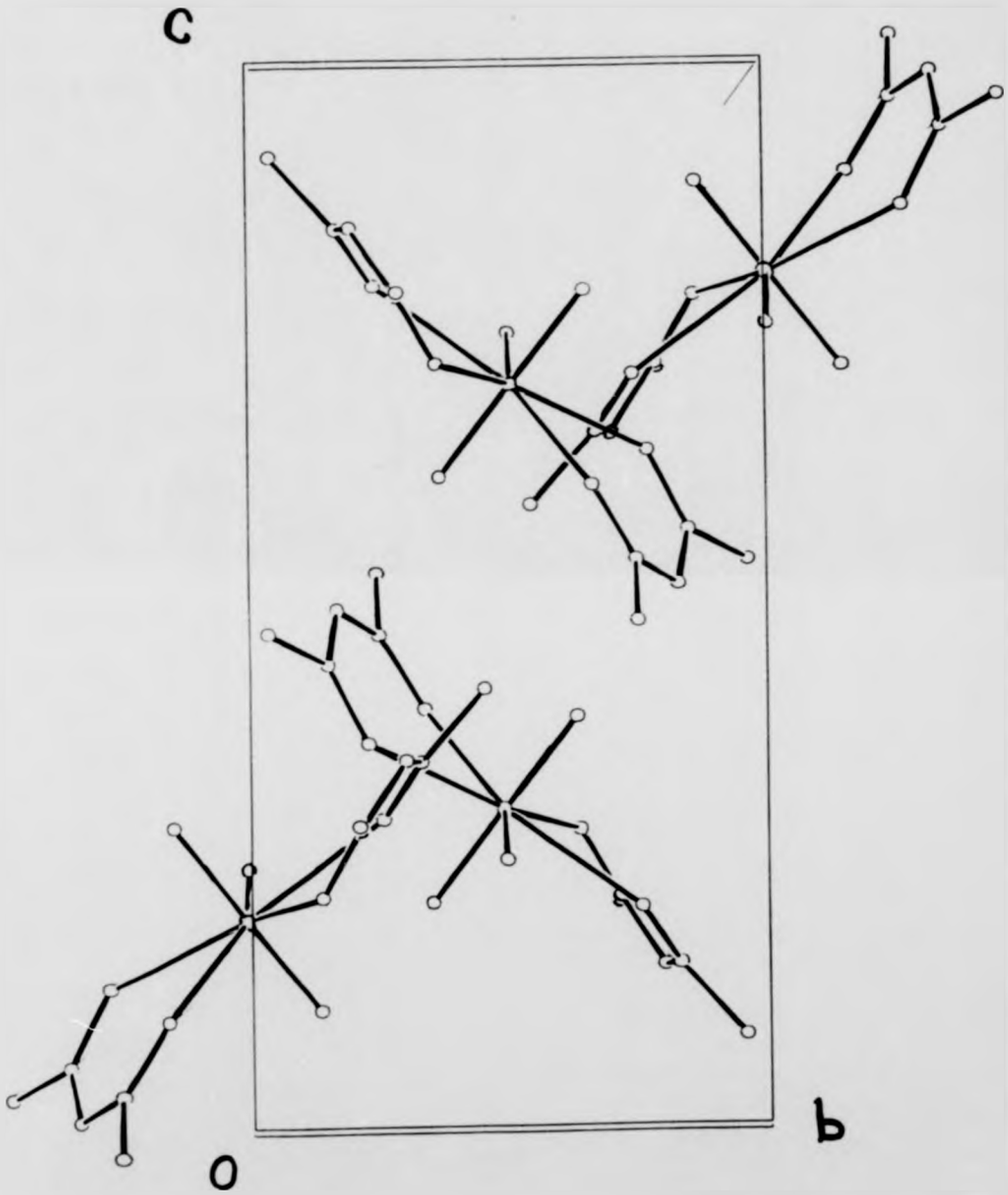

FIGURE 4.4. The packing of $[UO_2(CH_3COCHCOCH_3)_2.H_2O]$ viewed down the a axis.

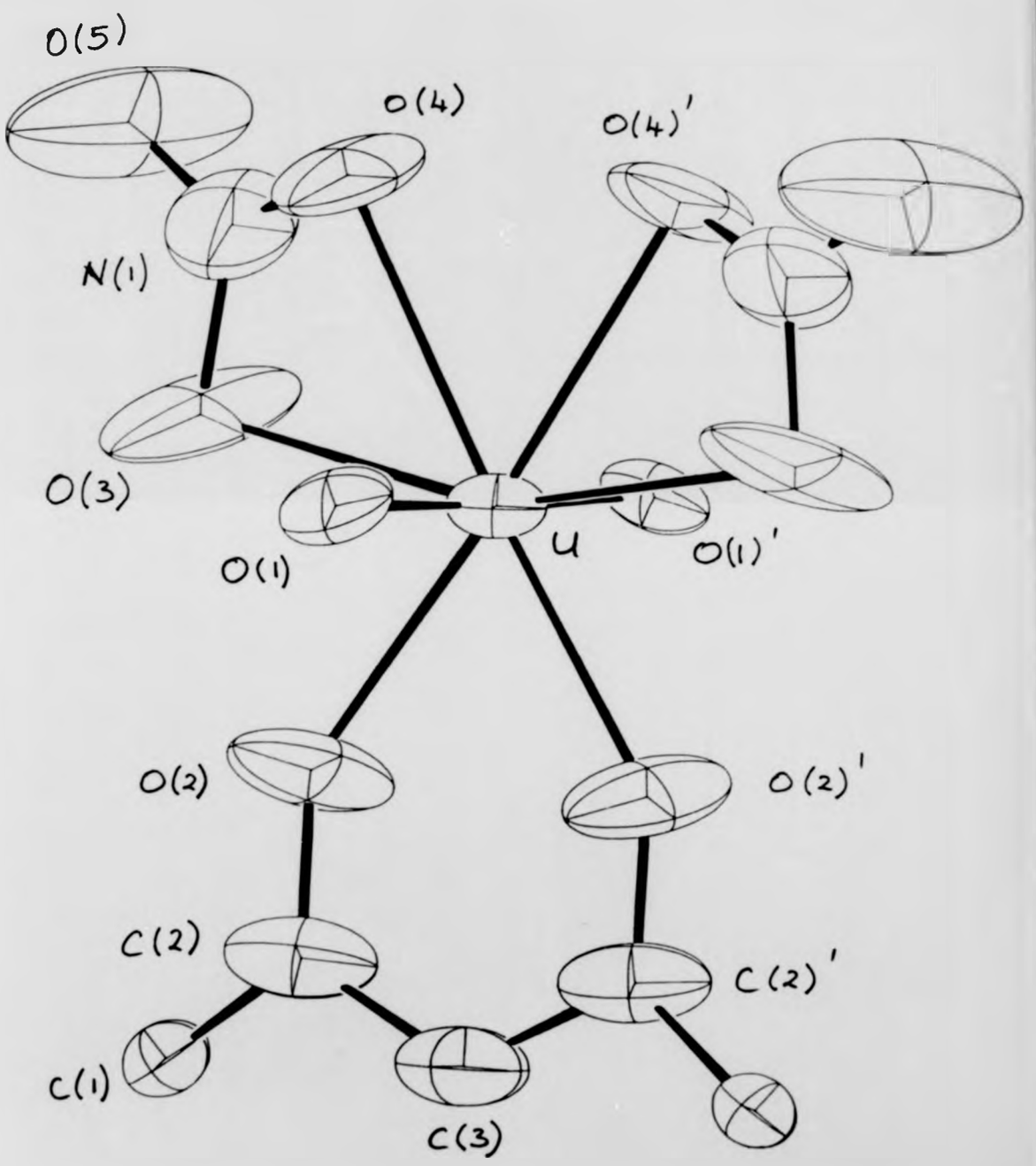

FIGURE 4.5. The $[UO_2CH_3COCHCOCH_3(NO_3)_2]$ [10] anion showing atomic numbering (primed and unprimed atoms are related by a two-fold axis)

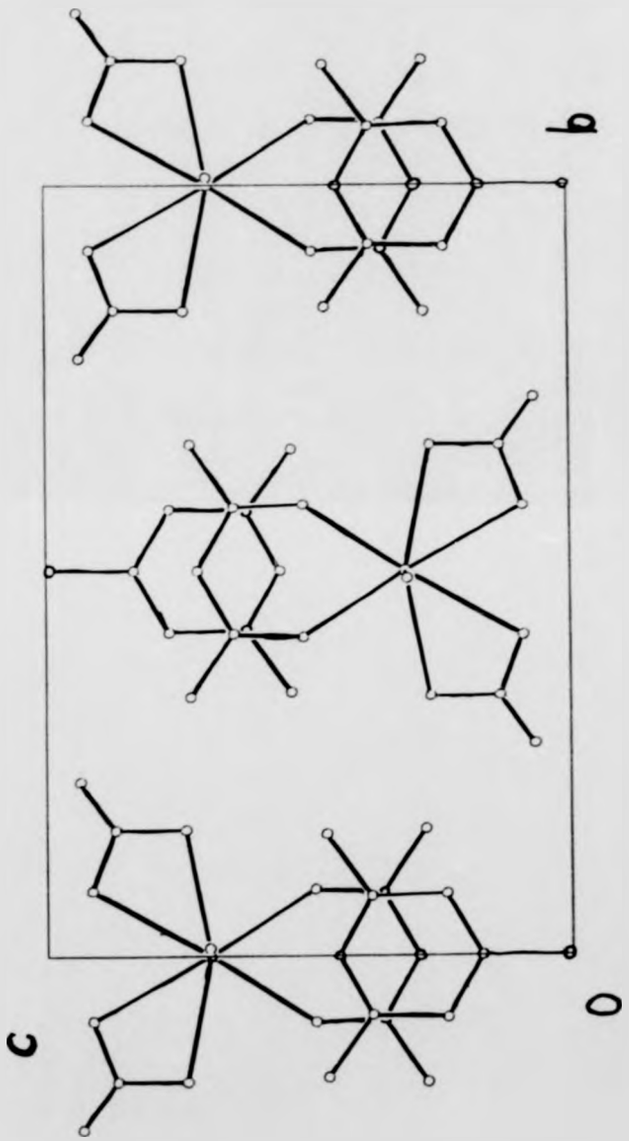

FIGURE 4.6. The packing of $[UO_2CH_3COCHCOCH_3(NO_3)_2]^-$ $[(CH_3)_2C_5H_3N]^+$ viewed down the a axis.

TABLE 4.1

Crystal Data and Data Collection Conditions

Compound	(7)	(8)	(9)	(10)
Formula	$C_{15}H_{19}NO_4U$	$C_{15}H_{19}NNpO_4$	$C_{10}H_{16}O_7U$	$C_{13}H_{19}N_3O_{10}U$
M	549.38	548.35	486.27	615.34
System	Orthorhombic	Orthorhombic	Monoclinic	Orthorhombic
Space Group	$Fdd2$	$Fdd2$	$P2_1/c$	$P2_12_12$
a/Å	29.702(4)	29.617(5)	12.895(3)	6.879(2)
b/Å	11.433(2)	11.406(2)	7.042(2)	15.241(4)
c/Å	10.593(2)	10.595(4)	16.633(3)	9.613(2)
β/°			109.46(2)	
U/Å^3	3 597.3(10)	3579.4(16)	1424.2(6)	1007.9(4)
Z	8	8	4	2
D_c/g cm^{-3}	2.02	2.03	2.27	2.03
D_m/g cm^{-3}	2.03			
μ(Mo - K_α)/cm^{-1},	85.8	37.95	108.27	76.86
Max. 2θ/°	55.0	50.0	50.0	50.0
Crystal size/mm.	.12×.08×.30	.17×.02×.28	.36×.11×.10	.42×.12×.12
Max. transmission factor	0.57	0.74	0.28	0.65
Min. transmission factor	0.28	0.65	0.10	0.53
Temp.,θ_c/° C	16	-100	16	16
Scan range about K_{α_1}-K_{α_2}/°	-1.0/+1.1	±1.1	-1.0/+1.1	-1.0/+1.1
Reflections collected	1 367	1 358	3 072	3 160
Reflections observed [$I/\sigma(I)\geq 3.0$]	1 108	1 083	1 821	1 936
Weighting constant: g		0.00287	0.00436	0.00088
Final R-value	0.032	0.046	0.043	0.039

TABLE 4.2

Atomic coordinates ($\times 10^4$) for [7], with standard deviations in parentheses.

Atom	*x*	*y*	*z*
U	0	0	0
N(1)	0	0	-2334(13)
O(1)	-425(4)	1158(10)	97(17)
O(2)	524(4)	1393(13)	-668(13)
O(3)	376(4)	821(12)	1846(12)
C(1)	19(7)	-1012(12)	-2992(14)
C(2)	13(10)	-1040(19)	-4319(15)
C(3)	0	0	-5184(15)
C(4)	1151	2562(20)	-1145(17)
C(5)	886(5)	1834(14)	-214(18)
C(6)	1026(6)	1777(18)	1044(18)
C(7)	760(5)	1306(15)	2010(17)
C(8)	-925(7)	-1317(22)	3348(18)

TABLE 4.3

Atomic coordinates ($\times 10^4$) for [8], with standard deviations in parentheses.

Atom	*x*	*y*	*z*
Np	0	0	0
O(1)	-421(6)	1107(18)	51(28)
O(2)	522(8)	1373(18)	-731(20)
O(3)	375(6)	829(18)	1765(18)
N(1)	0	0	-2420(24)
C(1)	-25(8)	994(23)	-3042(28)
C(2)	-24(13)	1058(29)	-4351(29)
C(3)	0	0	-4978
C(4)	1151(13)	2531(38)	-1242(32)
C(5)	886(8)	1838(24)	-301(22)
C(6)	1015(10)	1772(25)	992(26)
C(7)	760(8)	1270(26)	1956(27)
C(8)	924(12)	1308(30)	3253(28)

TABLE 4.4

Atomic Coordinates ($\times 10^4$) for [9] with standard deviations in parentheses.

Atom	x	y	z
U	2922.1(2)	5086.7(4)	6976.5(2)
O(1)	2971(5)	6509(9)	7853(4)
O(2)	2900(5)	3677(9)	6117(4)
O(3)	3528(5)	2443(9)	7912(4)
O(4)	1389(5)	3634(9)	7165(4)
O(5)	1393(5)	6643(9)	6024(4)
O(6)	3546(5)	7712(8)	6358(4)
O(7)	4968(6)	5041(7)	7469(7)
C(1)	3879(11)	460(16)	9131(8)
C(2)	3132(8)	1711(12)	8445(5)
C(3)	2069(8)	2000(15)	8451(6)
C(4)	1259(7)	2877(11)	7797(6)
C(5)	105(7)	2889(18)	7826(8)
C(6)	81(7)	7528(19)	4736(8)
C(7)	1263(7)	7497(12)	5326(6)
C(8)	2084(8)	8297(14)	5088(5)
C(9)	3141(7)	8492(12)	5613(6)
C(10)	3925(10)	9626(16)	5325(9)

TABLE 4.5

Atomic Coordinates ($\times 10^4$) for [10] with standard deviations in parentheses.

Atom	x	y	z
U	0	5000	3113(1)
O(1)	2530(20)	4904(22)	3084(11)
O(2)	-133(81)	4138(8)	5092(11)
O(3)	-38(69)	6631(8)	2648(13)
O(4)	133(87)	5843(9)	847(12)
O(5)	-398(135)	7256(8)	633(17)
N(1)	-346(91)	6632(15)	1291(20)
N(2)	5000	5000	55561(19)
C(1)	251(98)	3358(12)	7253(16)
C(2)	-191(113)	4183(14)	6424(18)
C(3)	0	5000	7117(22)
C(4)	4751(62)	5769(10)	6196(16)
C(41)	4706(58)	6581(12)	5337(19)
C(5)	4759(59)5802(15)	7652(19)	
C(6)	5000	5000	8354(23)
C(61)	5000	5000	9955(26)

TABLE 4.6

Bond lengths (Å) and bond angles (°) with standard deviations in parentheses for $MO_2(CH_3COCHCOCH_3)_2C_5H_5N$ [M=U(7) or Np(8)]
(Primed atoms are related to unprimed by a two-fold axis)

a)Bond lengths	(7)	(8)
M-O(1)	1.83(1)	1.78(2)
M-O(2)	2.34(1)	2.33(2)
M-O(3)	2.44(1)	2.37(2)
M-N(1)	2.47(1)	2.56(3)
N(1)-C(1)	1.35(2)	1.31(3)
C(1)-C(2)	1.41(2)	1.39(4)
C(2)-C(3)	1.50(2)	1.38(3)
C(4)-C(5)	1.51(3)	1.49(5)
C(5)-O(2)	1.28(2)	1.29(3)
C(5)-C(6)	1.40(3)	1.42(4)
C(6)-C(7)	1.40(3)	1.39(4)
C(7)-O(3)	1.28(2)	1.26(3)
C(7)-C(8)	1.50(3)	1.46(4)

b) Bond Angles	(7)	(8)
O(1)-M-O(1)'	177.8(6)	177.9(4)
O(1)-M-O(1)'	173.5(8)	176.5(19)
O(2)-M-O(3)	71.1(4)	71.6(7)
O(2)-M-N(1)	72.4(3)	70.6(5)
O(2)-M-O(2)'	144.7(5)	141.2(10)
O(3)-M-O(3)'	73.4(4)	75.9(9)
O(1)-M-O(2)	89.1(5)	89.9(9)
O(1)-M-O(3)	89.6(6)	91.2(10)
O(1)-M-N(1)	93.2(5)	91.7(10)
C(4)-C(5)-C(6)	120(2)	122(3)
C(4)-C(5)-O(2)	114(2)	115(2)
C(6)-C(5)-O(2)	126(2)	123(2)
C(5)-C(6)-C(7)	123(2)	126(3)
C(6)-C(7)-C(8)	120(2)	122(3)
C(6)-C(7)-O(3)	125(2)	120(3)
C(8)-C(7)-O(3)	115(2)	118(3)
C(1)-N(1)-C(1)'	118(1)	120(3)
N(1)-C(1)-C(2)	122(1)	123(3)
C(1)-C(2)-C(3)	126(2)	116(3)
C(2)-C(3)-C(2)'	105(1)	122(3)
C(1)-N(1)-M	121(1)	120(2)

TABLE 4.7

Bond lengths (Å) and bond angles (°) for $UO_2(CH_3COCHCOCH_3)_2 \cdot H_2O$ with standard deviations in parentheses

a)Bond lengths

U(1)-O(1)	1.752(6)
U(1)-O(2)	1.733(6)
U(1)-O(3)	2.385(6)
U(1)-O(4)	2.338(6)
U(1)-O(5)	2.349(5)
U(1)-O(6)	2.383(6)
U(1)-O(7)	2.489(8)
C(1)-C(2)	1.51(1)
C(2)-O(3)	1.27(1)
C(2)-C(3)	1.39(1)
C(3)-C(4)	1.38(1)
C(4)-O(4)	1.24(1)
C(4)-C(5)	1.51(1)
C(6)-C(7)	1.51(1)
C(7)-O(5)	1.27(1)
C(7)-C(8)	1.37(1)
C(8)-C(9)	1.36(1)
C(9)-O(6)	1.30(1)
C(9)-C(10)	1.49(2)

b)Bond angles

O(1)-U-O(2)	179.0(3)
O(1)-U-O(3)	89.4(3)
O(1)-U-O(4)	86.3(3)
O(1)-U-O(5)	94.8(2)
O(1)-U-O(6)	89.5(3)
O(1)-U-O(7)	89.6(3)
O(2)-U-O(3)	90.2(3)
O(2)-U-O(4)	94.5(3)
O(2)-U-O(5)	86.1(2)
O(2)-U-O(6)	90.2(3)
O(2)-U-O(7)	89.4(3)
O(3)-U-O(4)	71.2(2)
O(3)-U-O(5)	145.4(2)
O(3)-U-O(6)	143.4(2)
O(3)-U-O(7)	72.2(2)
O(4)-U-O(5)	74.8(2)
O(4)-U-O(6)	145.1(2)
O(4)-U-O(7)	143.2(2)
O(5)-U-O(6)	71.1(2)
O(5)-U-O(7)	142.0(3)
O(6)-U-O(7)	71.2(2)

TABLE 4.7 cont.

b)Bond angles cont.

U-O(3)-C(2)	130.7(6)
U-O(4)-C(4)	131.5(5)
U-O(5)-C(7)	131.6(6)
U-O(6)-C(9)	130.9(5)
O(3)-C(2)-C(1)	117.4(9)
O(3)-C(2)-C(3)	125.0(8)
C(1)-C(2)-C(3)	117.6(10)
C(2)-C(3)-C(4)	123.4(10)
O(4)-C(4)-C(3)	125.5(9)
O(4)-C(4)-C(5)	116.1(8)
C(3)-C(4)-C(5)	118.3(10)
O(5)-C(7)-C(6)	113.4(9)
O(5)-C(7)-C(8)	125.5(7)
C(6)-C(7)-C(8)	121.1(9)
C(7)-C(8)-C(9)	124.3(8)
O(6)-C(9)-C(8)	124.8(9)
O(6)-C(9)-C(10)	115.8(8)
C(8)-C(9)-C(10)	119.4(9)

TABLE 4.8

Bond lengths (Å) and bond angles (°) for $UO_2(CH_3COCHCOCH_3)(NO_3)_2$ [10] with standard deviations in parentheses (Primed and unprimed atoms are related by a two fold axis)

a)Bond lengths

i) Anion

U(1)-O(1)	1.75(1)
U(1)-O(2)	2.31(1)
U(1)-O(3)	2.53(1)
U(1)-O(4)	2.53(1)
C(1)-C(2)	1.52(3)
C(2)-O(2)	1.28(2)
C(2)-C(3)	1.42(2)
N(1)-O(3)	1.32(3)
N(1)-O(4)	1.32(3)
N(1)-O(5)	1.14(3)

ii) Cation

N(2)-C(4)	1.33(2)
C(4)-C(41)	1.49(1)
C(4)-C(5)	1.40(2)
C(5)-C(6)	1.41(3)
C(6)-C(61)	1.54(3)

TABLE 4.8 cont.

b)Bond angles

i) Anion

O(1)-U-O(1')	178.1(7)
O(1)-U-O(2)	90.3(15)
O(1)-U-O(3)	95.1(15)
O(1)-U-O(4)	89.6(15)
O(2)-U-O(3)	134.7(4)
O(2)-U-O(4)	175.9(6)
O(2)-U-O(2')	69.3(6)
O(3)-U-O(4)	49.3(4)
O(4)-U-O(4')	61.2(6)
U-O(2)-C(2)	142.4(13)
C(1)-C(2)-C(3)	117.5(23)
C(1)-C(2)-O(2)	118.3(23)
C(3)-C(2)-O(2)	120.8(20)
C(2)-C(3)-C(2')	124.0(21)
U-O(3)-N(1)	100.2(12)
U-O(4)-N(1)	100.1(12)
O(3)-N(1)-O(4)	106.0(24)
O(3)-N(1)-O(5)	123.5(23)
O(4)-N(1)-O(5)	126.1(27)

ii) Cation

C(4)-N(2)-C(4')	125.5(20)
N(2)-C(4)-C(5)	119.2(17)
N(2)-C(4)-C(41)	118.7(10)
C(41)-C(4)-C(5)	121.7(11)
C(4)-C(5)-C(6)	116.7(19)
C(5)-C(6)-C(61)	118.7(11)
C(5)-C(6)-C(5')	122.6(23)

TABLE 4.9

Deviations (Å) from mean planes for $MO_2(CH_3COCHCOCH_3)_2C_5H_5N$ [M = U(7) or Np(8)]. (Primed atoms are related to unprimed by a two-fold axis, starred atoms define planes).

Plane 1	(7)	(8)
M*	0.02	0.00
O(2)*	0.03	-0.06
O(2′)*	0.06	0.06
O(3)*	-0.06	0.09
O(3′)*	-0.08	-0.09
N(1)*	0.03	0.00
Plane 2		
U*	0.00	0.00
N(1)*	0.00	0.00
C(1)*	0.06	0.00
C(1′)*	-0.06	0.00
C(2)*	0.04	0.00
C(2′)*	-0.04	0.00
C(3)*	0.00	0.00
Line 3		
O(1)*	0.05	0.02
U*	0.00	0.04
O(1′)*	0.05	0.04
Angles between plane normals and line (°)		
1 - 2	44.6	49.7
1 - 3	4.8	0.8
2 - 3	45.8	49.0

TABLE 4.10

Deviations (Å) from mean planes for $UO_2(CH_3COCHCOCH_3)_2.H_2O$ [9]

Plane 1		**Line 2**	
U*	0.00	O(1)*	0.01
O(3)*	-0.07	U*	0.01
O(4)*	0.12	O(2)*	0.01
O(5)*	-0.13		
O(6)*	-0.09		
O(7)*	0.01		
Angle between plane normal and line (°)			
1 - 2	88.0		

References

1. K. W. Bagnall, *Gmelin Handbuch URAN Suppl.*, E1, p. 40, 1979.
2. K. Hager, *Z. Anorg. Allgem. Chem.*, vol. 162, p. 82, 1927.
3. L. Sacconi, G. Caroti, and P. Paoletti, *J. Chem. Soc.*, p. 4257, 1958.
4. L. Sacconi, G. Caroti, and P. Paoletti, *J. Inorg. Nucl. Chem.*, vol. 8, p. 93, 1958.
5. G.K.T. Conn and C.K. Wu, *Trans. Faraday Soc.*, vol. 34, p. 1483, 1938.
6. E. Frasson, G. Bombieri, and C. Panattoni, *Coord. Chem. Reviews*, vol. 1, p. 145, 1966.
7. J.B. Laidler, *J. Chem. Soc. A*, p. 780, 1966.
8. A.E. Comyns, B.M. Gatehouse, and E. Wait, *J. Chem. Soc. (Part 4)*, p. 4655, 1958.
9. J.M. Stewart, "The X-RAY '76 system," TR-466, Computer Science Center, University of Maryland, U.S.A., 1976.
10. G.M. Sheldrick, *SHELXTL User Manual*, Nicolet Instrument Co., 1981.
11. R.G. Denning, "Properties of the UO_2^{n+} (n=1,2) Ions," in *Gmelin Handbuch URAN Suppl. Vol A6*, pp. 31-79, 1983.
12. N.W. Alcock and S. Esperas, *J. Chem. Soc. Dalton Trans.*, p. 893, 1977.
13. A.M. Brock, D.H. Cook, D.E. Fenton, G. Bombieri, E. Forsellini, and F. Benetollo, *J. Inorg. Nucl. Chem.*, vol. 40, p. 1551, 1978.
14. D. Hall, A.D. Rae, and T.N. Waters, *Acta Crystallogr.*, vol. 22, p. 258, 1967.
15. N.W. Alcock, M.M. Roberts, and D. Brown, *J. Chem. Soc Dalton Trans.*, p. 869, 1982.

CHAPTER 5

The Crystal Structures of Two Further Neptunium Compounds

5.1. The crystal and molecular structure of: Trischloromono (η^5-cyclopentadienyl)neptunium(IV) bis(methyldiphenylphosphineoxide)

5.1.1. Introduction.

A recent review[1] gives an indication of the large number of organouranium compounds that have been prepared and the number of crystal structure determinations that have been carried out. However, there has been little extension of this work to transuranium elements and , in particular, very few neptunium compounds have been prepared. In addition no X-ray structure determinations have been undertaken. As a result of this deficiency I undertook the structure determination of such a compound which had been prepared by a colleague at A.E.R.E. Harwell as part of his own research project.

5.1.2.Experimental

5.1.2.1.*Preparation.*

The title compound was prepared and recrystallised by Mr. G.F. Payne[2] who supplied a small sample. A suitable crystal was mounted on a quartz fibre and encapsulated in a Lindermann capillary. As the compound reacts rapidly with oxygen or atmospheric moisture these operations were carried out in a dry, nitrogen-filled glove box.

5.1.2.2.*Crystal Data*

$C_{31}H_{31}NpO_2P_2$, Space group: $P2_1/c$, a = 10.199(4),b= 33.208(13),c= 20.661(7) Å, β=113.04(2)°, U = 6 439.62(39)Å^3, M = 840.90, Z = 4, D_c = 1.735 g cm $^{-3}$, Mo- K_α radiation, λ = 0.710 69 Å, μ (Mo- K_α)= 24.69 cm $^{-1}$.

5.1.2.3. *Data Collection and Structural Refinement*

Data were collected with a Syntex $P2_1$ four circle diffractometer, with scan range -1.0/+1.1 ° (2θ) around the K_{α_1} - K_{α_2} angles. Of the 12 325 reflections collected, 4 511 were deemed to be observed [$I/\sigma(I)\geq 3.0$) and were used in the subsequent refinement, The maximum and minimum transmission factors were 0.66 and 0.46 respectively. The crystal dimensions were: 0.17 x 0.58 x 0.40 m.m. The systematic absences: $h0l:l\neq 2n$, $0k0:k\neq 2n$ ($00l:l\neq 2n$) indicate the space group is $P2_1/c$. Two neptunium atoms were located in the asymmetric unit by Patterson techniques and the remaining non-hydrogen atoms were found on successive Fourier syntheses. Hydrogen atoms were inserted at calculated

positions with fixed isotropic temperature factors, B= 5.0 $Å^2$, and were not refined. Final refinement was by least squares methods with the phenyl and cyclopentadienyl groups treated as rigid bodies.

A weighting scheme of the form w = $X \cdot Y$ was applied where X = 1.0 or $(\sin\theta/\lambda)/0.35$ for $(\sin\theta/\lambda) > 0.35$ and Y = 1.0 or 110.0/ F_{obs} if $F_{obs} \geq 110.0$ and was shown to be satisfactory by a weighting analysis. The final R-value was 0.062. Final atomic coordinates are given in Table 5.1, and selected bond lengths and angles in Table 5.2.

5.1.3. Discussion.

Figure 5.1 shows a view of molecule 1 with the atomic numbering. The neptunium atom is octahedrally coordinated to two oxygen atoms of the methyldiphenyl phosphineoxide (mdppo) ligands, which occupy *cis* positions, to three chlorine atoms and to the cyclopentadienyl (cp) ligand (considered as bonded to the centre of the ring) which is *trans* with respect to one mdppo ligand. The octahedral geometry is distorted due to the relative bulk of the ligands, particularly the cp ligand, causing deviation of the inter-ligand angles from 90°. The angles between the centroid of the cp ligand and the three chlorine atoms and between the centroid and O(2) of the mtppo ligand are all *ca.* 100°, indicating that the bulk of the cp ligand has forced these ligands below the plane of the central neptunium atom. This, in turn, reduces the angles between the chlorine atoms and the oxygen atoms whilst maintaining the angles between chlorine atoms close to 90°. This deviation from true octahedral geometry reflects the relative bulk of the ligands about the neptunium atom in the order:

$$(\text{cyclopentadiene}) > Cl^- > \text{mtppo}$$

The neptunium to chlorine bond lengths have a range of 2.65-2.67Å and the neptunium to oxygen lengths range from 2.26Å to 2.28Å.

The structure of the uranium(IV) analogue has not been determined, but the structure of $U(C_5H_5)Cl_3.(OPPh_3)_2.C_4H_8O$ has been reported [3] and shows a general similarity to compound [11].

The view of the unit cell down *a* (Figure 5.2) shows the two orientations of the molecules within the cell and the small variation between the two independent molecules in each asymmetric unit.

5.2. The Crystal and Molecular Structure of a Mixed Oxidation State Neptunium Salt: $Cs_7Np^{(V)}O_2(Np^{(VI)}O_2)_2Cl_{12}$

5.2.2. Introduction.

A recent paper[4] reported the preparation of the title complex and its characterisation by infra-red spectroscopy and X-ray powder photography, comparing this compound to the cubic modification of $Cs_2AmO_2Cl_4$.[5] It was suggested that both compounds should be considered to contain $M^{(V)}$ and $M^{(VI)}$. In conjunction with optical and infra-red studies[6] which have confirmed the Russian observations of NpO_2^+ and NpO_2^{2+} bonding a structure determination of this compound has been carried out.

5.2.2. Experimental

5.2.2.1. *Preparation*

Crystals of $Cs_7(NpO_2)_2Cl_{12}$ were prepared by dissolving dioxoneptunium(V)hydroxide (0.25 mmol) in ethanol (3 cm^3)containing equimolar quantities of caesium chloride and hydrochloric acid (1.0 mmol). The solvent was evaporated to give a deposit of yellow-green crystals which were washed in ice-cold ethanol and air dried. The thin, plate-like crystal used was the result of a further preparation by Mr. G.S. Topping. The crystal selected was mounted on a quartz fibre and encapsulated in a Lindermann glass capillary.

5.2.2.2. *Crystal Data*

$Cs_7Np^{(V)}O_2(Np^{(VI)}O_2)_2Cl_{12}$, Cubic, $I\bar{4}3d$, a = 15.084(4)Å, U = 3432.3(1.5)Å^3, Z = 4, D_c = 4.18 g cm^{-3}, Mo-K_α radiation, λ = 0.71069Å, μ(Mo-K_α) = 140.65 cm^{-1}, M = 2162.73

5.2.2.3. *Data Collection and Structural Refinement*

Reflections were collected with a Syntex $P2_1$ automatic four circle diffractometer, using a crystal measuring 0.19 × 0.26 × 0.28 mm which gave transmission factors in the range 0.167 to 0.646. The scan range used was -0.9/+1.1°(2θ) about the $K_{\alpha_1}-K_{\alpha_2}$ positions. 1709 reflections were collected of which 1674 were deemed to be observed [$I/\sigma(I)\geq 3.0$] and were used in the subsequent refinement. Four standard monitored every 100 reflections showed only slight decreases in intensity; the data were rescaled to correct for this. The systematic absences $h+k+l\neq 2n$ for hkl and $2h+l\neq 4n$ for hkl (cyclically permuted) allow only space group $I\bar{4}3d$. A Patterson synthesis located three heavy atom peaks in the asymmetric unit in special positions 12*a*, 12*b* and 16*c*. These peaks were assumed to correspond to the three neptunium atoms and refinement was attempted on this basis. The refinement did not produce the expected decrease in the R-factor and examination of the temperature factors suggested that only the identification of the peak at 12*a* was correct and that the peaks at 12*b* and 16*c* corresponded to

caesium atoms.

The remaining atoms were found by Fourier synthesis and refined by least squares methods. The coordinates of the neptunium atom and caesium atom (2) were fixed in special positions 12*a* and 12*b*, respectively, and the position of caesium atom (1) in special position 16*e*, was refined with a site occupation factor of 1/3 and coordinates *x*,*x*,*x*. The oxygen atom was inserted at a special position with *y* and *z* fixed at 0.5 and 0.25 respectively with a site occupation factor of 0.5. The chlorine atom was inserted in a general position. Refinement with anisotropic temperature factors for all the atoms gave a final *R*-value of 0.035. A weighting scheme of the form $W = 1/(\sigma^2(F) + g\ F^2)$ with $g = 0.00069$ was applied and shown to satisfactory by a weight analysis. The final difference Fourier synthesis showed ripples of $0.85e\ Å^{-3}$ around the neptunium atom and $\leq 1.18e\ Å^{-3}$ near the caesium atoms.

The final atomic coordinates and temperature factors are listed in Table 5.3; bond lengths and angles are given in Table 5.4. An oblique view of the cell showing the positions of the ions is given in Figure 5.3.

5.2.3. **Discussion.**

The structure of $Cs_7Np^{(V)}O_2\ (Np^{(VI)}O_2)_2Cl_{12}$ consists of Cs^+ cations and isolated $[NpCl_4O_2]^{n-}$ anions with octahedral geometry. Since the three neptunium atoms are in the special position 12*a* they are crystallographically identical and it is impossible to distinguish the one Np(V) and the two Np(VI) atoms. The site symmetry of the neptunium atoms requires the neptunyl (V) and (VI) group to be linear and at right angles to the mean equatorial plane. Alternate Cl atoms are 0.080Å above and below the mean equatorial plane, producing a mild puckering of the square plane of Cl atoms [O(1)-Np-Cl(1) = 88.3(1)° and Cl(1)-Np-Cl(1′) = 176.5(3)°].

The Np-O bond length [1.790(15)Å] is intermediate between the values for NpO_2^+ and NpO_2^{2+} reported recently:- 1.814(34)Å for Np(V) in $Cs_3NpO_2Cl_4$[7] and 1.721(16) and 1.751(18)Å for Np(VI) in $NpCl_2O_2.2tppo$.[8] The Np-Cl bonds show the same intermediate length [2.685(5)Å] when compared with the neptunyl(V) [2.752(13) and 2.760(19)Å] and neptunyl(VI) [2.622(14) and 2.645(13)Å] compounds above. The thermal ellipsoids of the chloride and oxygen ligands might be expected to show abnormal elongations because of the disorder, but this is not seen; the greatest elongation is at right angles to the bonds rather than parallel to them. Presumably the expected 0.05 - 0.15Å differences in Np-Cl distances are swamped by the normal thermal motion. The caesium(1) cation is 9-coordinate and positioned on a 3-fold axis at the centre of a tricapped trigonal prism. Coordination to the oxygen and chlorine atoms gives Cs-O contact distances of 3.17(1)Å and Cs-Cl contact distances of 3.73(1) and 3.74(1)Å. Caesium(2) is 8-coordinate with $\bar{4}$ symmetry at the centre of a dodecahedron of chlorine atoms with Cs-Cl contact distances

of 3.54(1)Å.

Computing was with SHELXTL[9] on a Data General NOVA 3 mini-computer and the X-RAY 76 system[10] on a Burroughs B6800 computer.

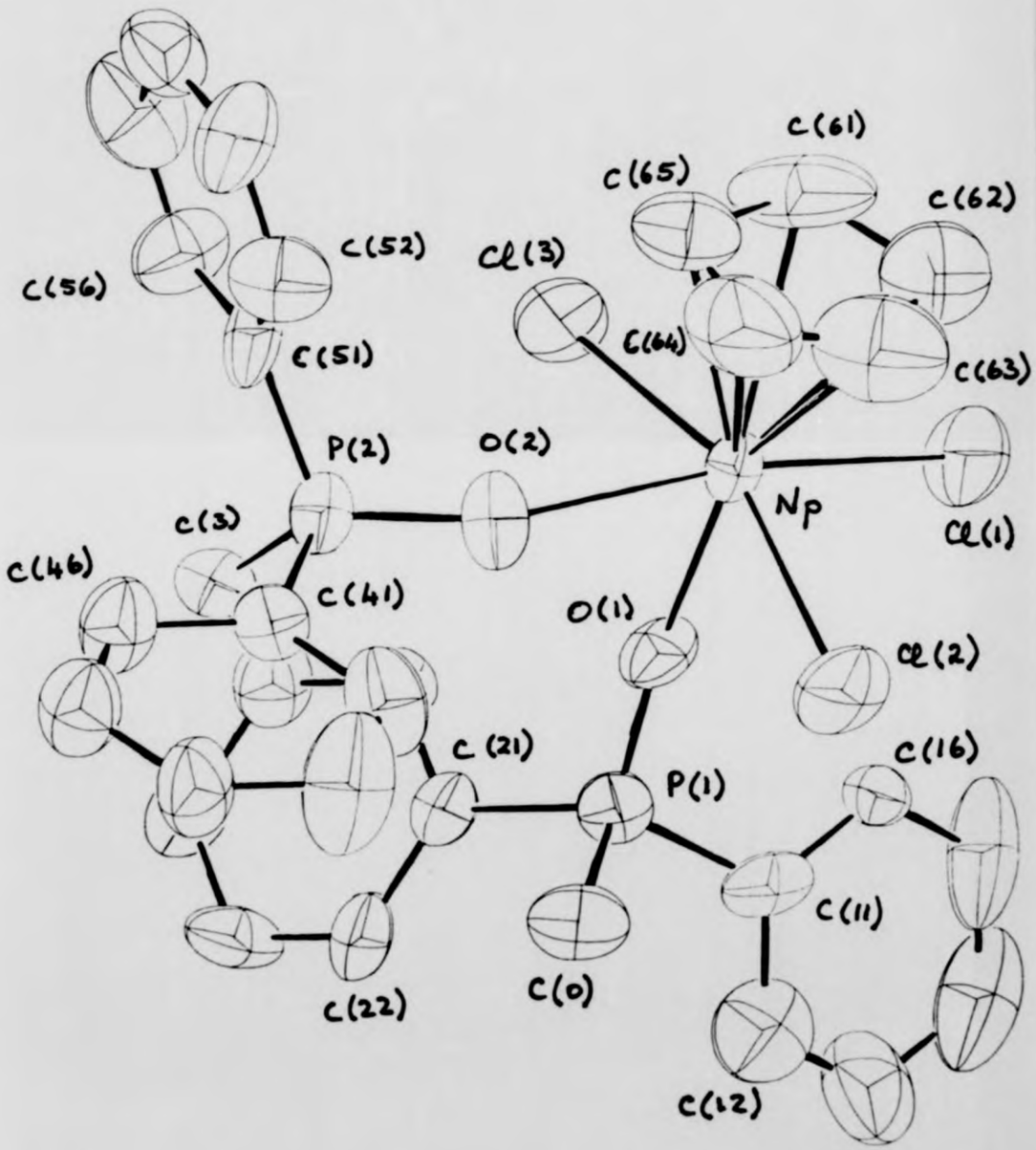

FIGURE 5.1. The $[(C_5H_5)Cl_3Np(OPPh_3)_2]$ [11] molecule showing atomic numbering.

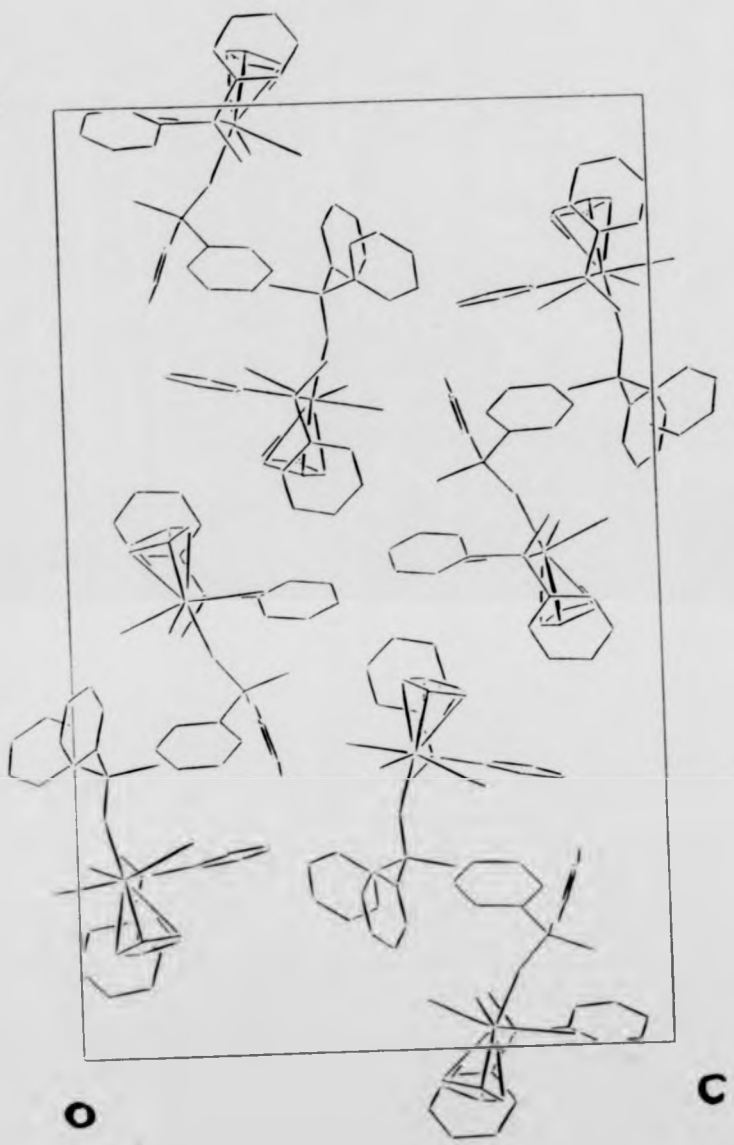

FIGURE 5.2. View of the unit cell of $[(C_5H_5)Cl_3Np(OPPh_3)_2]$ [11] down the *a* axis.

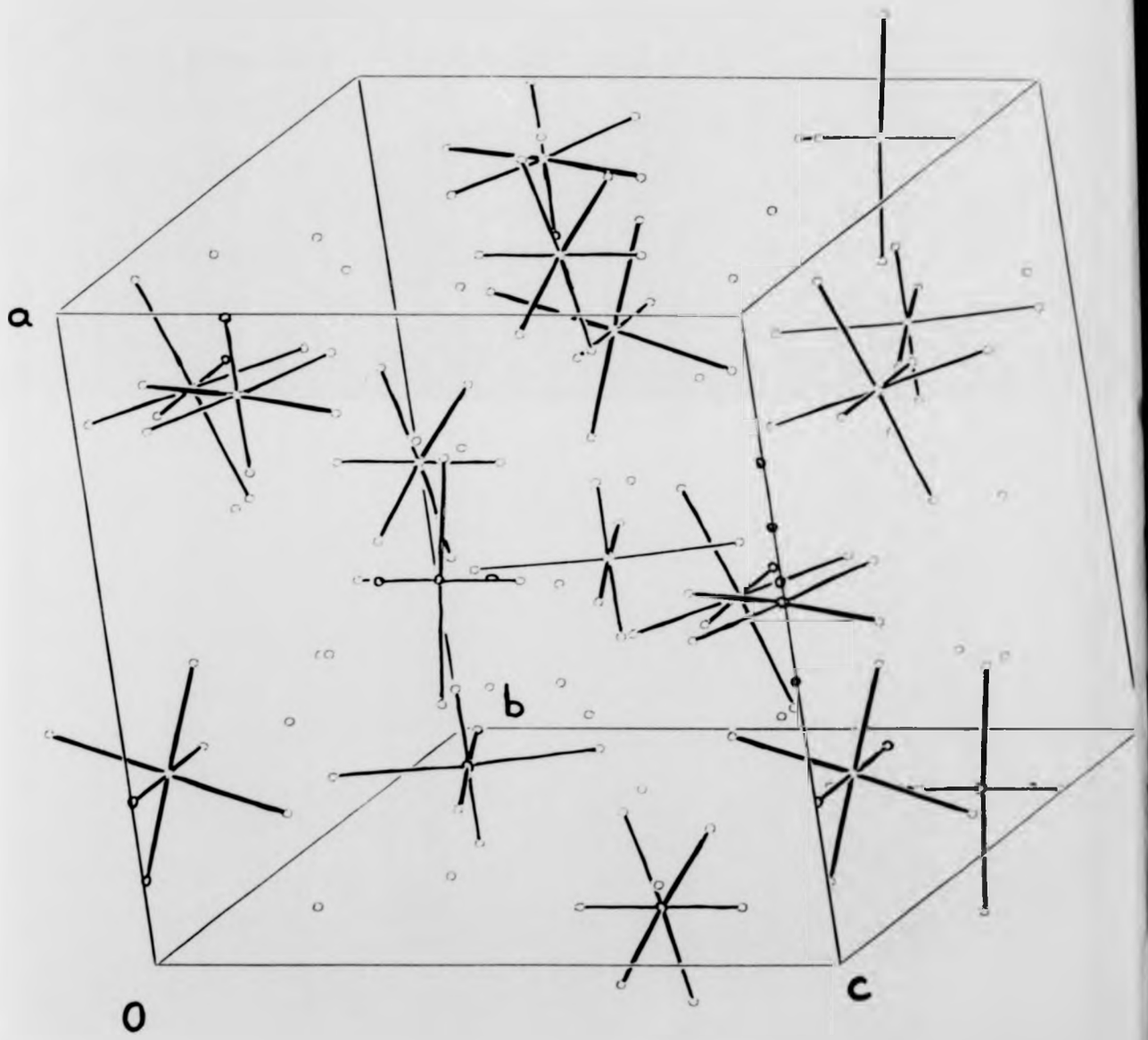

FIGURE 5.3. Oblique view of the unit cell of $[Cs_7Np^{(VI)}O_2(Np^{(VI)}O_2)_2Cl_{12}]$ [12]

TABLE 5.1

Atomic coordinates ($\times 10^4$) (with standard deviations in parentheses) for Trischloromono(η^5-cyclopentadienyl)neptunium(IV) bis(methyl diphenylphosphineoxide).[11]

a) Molecule 1

Atom	x	y	z
Np	1348.1(31)	6876.7(10)	5787.2(16)
Cl(1)	-1401(23)	7026(8)	5153(15)
Cl(2)	1499(28)	6744(8)	4554(12)
Cl(3)	1631(31)	7256(8)	6969(13)
O(1)	1507(56)	7528(14)	5472(27)
P(1)	1905(23)	7976(7)	5581(10)
C(1)	3113(122)	8095(38)	6454(49)
C(11)	2629(67)	8127(24)	4968(33)
C(12)	2456(88)	7892(23)	4391(39)
C(13)	2948(89)	8029(31)	3865(44)
C(14)	3683(97)	8369(30)	3971(48)
C(15)	3937(98)	8628(24)	4566(52)
C(16)	3400(92)	8506(30)	5070(45)
C(21)	306(94)	8278(23)	5360(39)
C(22)	-1023(77)	8099(24)	5005(39)
C(23)	-2211(108)	8353(34)	4778(64)
C(24)	-2095(124)	8757(44)	4933(64)
C(25)	-838(143)	8921(39)	5277(77)
C(26)	461(114)	8680(31)	5540(55)
O(2)	3743(53)	6929(19)	6148(28)
P(2)	5212(20)	6914(7)	6106(11)
C(3)	5381(89)	7267(27)	5500(48)
C(41)	5605(79)	6428(29)	5842(45)
C(42)	5456(118)	6346(28)	5161(52)
C(43)	5727(133)	5980(38)	4992(58)
C(44)	6123(119)	5661(28)	5486(61)
C(45)	6220(106)	5753(35)	6148(62)
C(46)	6023(116)	6129(31)	6341(48)
C(51)	6555(77)	7016(26)	6964(38)
C(52)	6133(106)	7114(36)	7510(47)
C(54)	8607(103)	7155(30)	8275(48)
C(55)	9035(96)	7054(33)	7749(52)
C(56)	7964(89)	7002(29)	7071(50)
C(61)	2180(123)	6094(26)	6003(59)
C(62)	684(117)	6074(30)	5606(56)
C(63)	-38(109)	6208(31)	6046(87)
C(64)	1166(134)	6287(41)	6696(62)
C(65)	2294(160)	6224(52)	6578(90)

TABLE 5.1 cont.

b) Molecule 2

Atom	x	y	z
Np	4920(4)	208(1)	3035(2)
Cl(1)	4783(32)	545(8)	4178(13)
Cl(2)	4537(33)	111(10)	1695(14)
Cl(3)	7446(27)	543(10)	3338(16)
O(1)	4172(61)	836(17)	2596(28)
P(1)	3382(23)	1172(7)	2107(11)
C(2)	2067(102)	982(37)	1293(56)
C(11)	4595(87)	1464(26)	1890(40)
C(12)	4369(93)	1855(27)	1659(43)
C(13)	5302(100)	2089(31)	1508(48)
C(14)	6579(102)	1922(30)	1564(44)
C(15)	6860(104)	1523(28)	1770(50)
C(16)	5923(101)	1287(26)	1960(48)
C(21)	2559(89)	1485(26)	2541(44)
C(22)	3208(86)	1513(28)	3266(43)
C(23)	2694(108)	1752(34)	3648(58)
C(24)	1448(128)	1950(36)	3304(54)
C(25)	725(107)	1919(29)	2558(66)
C(26)	1314(111)	1691(32)	2171(53)
O(2)	2534(66)	141(19)	2679(33)
P(2)	1069(24)	166(8)	2696(14)
C(3)	977(121)	586(37)	3186(74)
C(41)	719(75)	-268(24)	3125(47)
C(42)	1327(115)	-302(36)	3856(63)
C(43)	1033(157)	-619(54)	4162(62)
C(44)	264(107)	-961(38)	3765(58)
C(46)	-115(99)	-595(24)	2727(43)
C(51)	-230(77)	192(29)	1804(42)
C(52)	-1441(141)	383(54)	1709(71)
C(53)	-2433(188)	450(51)	966(96)
C(54)	-2155(152)	257(54)	434(75)
C(55)	-984(161)	72(64)	539(88)
C(56)	56(133)	-2(41)	1290(67)
C(61)	5279(127)	-400(31)	3928(52)
C(62)	4435(130)	-575(24)	3276(61)
C(63)	5310(160)	-589(34)	2904(68)
C(64)	6666(139)	-447(33)	3320(84)
C(65)	6736(159)	-322(26)	3965(88)

TABLE 5.2

Bond lengths (Å) and angles (°) (with standard deviations in parentheses) for Trischloromono(η^5-cyclopentadienyl)neptunium(IV) bis(methyldiphenylphosphine oxide) [11]

a) Bond lengths	Molecule 1	Molecule 2
(i) Around Np		
Np-Cl(1)	2.64(2)	2.67(3)
Np-Cl(2)	2.65(3)	2.66(3)
Np-Cl(3)	2.66(3)	2.65(3)
Np-O(1)	2.28(5)	2.28(6)
Np-O(2)	2.26(5)	2.26(6)
Np-C(61)	2.72(9)	2.66(11)
Np-C(62)	2.74(10)	2.73(9)
Np-C(63)	2.79(12)	2.70(12)
Np-C(64)	2.77(14)	2.72(12)
Np-C(65)	2.66(17)	2.73(12)
Np-C(mean)	2.74(12)	2.71(11)
(ii) Cyclopentadienyl group		
C(61)-C(62)	1.42(15)	1.41(14)
C(62)-C(63)	1.45(22)	1.39(24)
C(63)-C(64)	1.44(16)	1.39(18)
C(64)-C(65)	1.28(24)	1.37(25)
C(65)-C(61)	1.23(23)	1.48(22)
(iii) Methyldiphenylphosphine oxide groups		
O(1)-P(1)	1.53(5)	1.51(6)
P(1)-C(0)	1.78(9)	1.80(9)
P(1)-C(11)	1.77(8)	1.76(10)
P(1)-C(21)	1.81(8)	1.78(10)
C(11)-C(12)	1.38(10)	1.37(12)
C(12)-C(13)	1.44(14)	1.36(15)
C(13)-C(14)	1.32(14)	1.38(15)
C(14)-C(15)	1.44(14)	1.39(13)
C(15)-C(16)	1.41(16)	1.41(16)
C(16)-C(11)	1.45(12)	1.43(14)
C(21)-C(22)	1.40(11)	1.38(11)
C(22)-C(23)	1.40(13)	1.36(16)
C(23)-C(24)	1.37(18)	1.36(15)
C(24)-C(25)	1.32(17)	1.43(16)
C(25)-C(26)	1.46(17)	1.40(18)
C(26)-C(21)	1.38(13)	1.38(13)

TABLE 5.2 cont.

a) Bond lengths cont.	Molecule 1	Molecule 2
Methyldiphenylphosphine oxide (ii)		
O(2)-P(2)	1.53(6)	1.51(8)
P(2)-C(3)	1.77(10)	1.75(14)
P(2)-C(41)	1.80(10)	1.80(9)
P(2)-C(51)	1.80(7)	1.80(8)
C(41)-C(42)	1.38(15)	1.40(15)
C(42)-C(43)	1.33(17)	1.32(22)
C(43)-C(44)	1.42(16)	1.44(19)
C(44)-C(45)	1.37(19)	1.31(15)
C(45)-C(46)	1.35(16)	1.36(15)
C(46)-C(41)	1.38(13)	1.42(11)
C(51)-C(52)	1.39(15)	1.33(18)
C(52)-C(53)	1.44(12)	1.49(20)
C(53)-C(54)	1.37(16)	1.39(28)
C(54)-C(55)	1.36(17)	1.28(24)
C(55)-C(56)	1.41(12)	1.52(19)
C(56)-C(51)	1.37(12)	1.37(18)

TABLE 5.2 cont.

b) Bond angles	Molecule 1	Molecule 2
(i) Around Np		
Cl(1)-Np-Cl(2)	90.2(9)	91.7(11)
Cl(1)-Np-Cl(3)	94.6(9)	89.9(10)
Cl(1)-Np-O(1)	81.9(4)	81.0(16)
Cl(1)-Np-O(2)	161.7(7)	84.6(19)
Cl(1)-Np-C(61)	118(2)	75(3)
Cl(1)-Np-C(62)	88(2)	99(3)
Cl(1)-Np-C(63)	74(2)	124(3)
Cl(1)-Np-C(64)	97(3)	114(4)
Cl(1)-Np-C(65)	121(4)	85(4)
Cl(2)-Np-Cl(3)	159.2(9)	159.3(9)
Cl(2)-Np-O(1)	81.1(6)	78.8(16)
Cl(2)-Np-O(2)	82.4(6)	87.0(19)
Cl(2)-Np-C(61)	82(3)	124(3)
Cl(2)-Np-C(62)	79(3)	96(3)
Cl(2)-Np-C(63)	106(4)	75(3)
Cl(2)-Np-C(64)	125(3)	87(4)
Cl(2)-Np-C(65)	108(4)	116(4)
Cl(3)-Np-O(1)	79.6(6)	81.5(16)
Cl(3)-Np-O(2)	86.9(7)	160.5(17)
Cl(3)-Np-C(61)	113(3)	107(3)
Cl(3)-Np-C(62)	121(3)	126(3)
Cl(3)-Np-C(63)	95(4)	105(4)
Cl(3)-Np-C(64)	74(3)	78(3)
Cl(3)-Np-C(65)	87(4)	77(3)
O(1)-Np-O(2)	80(2)	79(2)
O(1)-Np-C(61)	154(3)	154(3)
O(1)-Np-C(62)	158(3)	152(3)
O(1)-Np-C(63)	155(3)	153(3)
O(1)-Np-C(64)	153(3)	155(4)
O(1)-Np-C(65)	154(3)	154(3)
O(2)-Np-C(61)	78(3)	89(3)
O(2)-Np-C(62)	107(3)	73(3)
O(2)-Np-C(63)	124(3)	93(4)
O(2)-Np-C(64)	100(3)	121(3)
O(2)-Np-C(65)	77(4)	121(4)

TABLE 5.2 cont.

b) Bond angles cont.	Molecule 1	Molecule 2
*Cnd-Np-Cl(1)	100(1)	100(1)
Cnd-Np-Cl(2)	101(1)	100(1)
Cnd-Np-Cl(3)	98(1)	99(1)
Cnd-Np-O(1)	177(1)	179(1)
Cnd-Np-O(2)	98(2)	100(2)
(ii) Cyclopentadienyl groups		
C(61)-C(62)-C(63)	108(10)	105(11)
C(62)-C(63)-C(64)	100(10)	110(12)
C(63)-C(64)-C(65)	107(13)	111(15)
C(64)-C(65)-C(61)	119(13)	103(11)
C(65)-C(61)-C(62)	104(13)	110(12)
(iii) Methyldiphenylphosphine oxide groups		
O(1)-P(1)-C(0)	114(5)	112(4)
O(1)-P(1)-C(11)	109(4)	109(4)
O(1)-P(1)-C(21)	110(4)	109(4)
C(0)-P(1)-C(11)	110(5)	107(5)
C(0)-P(1)-C(21)	109(5)	110(4)
C(11)-P(1)-C(21)	104(5)	109(4)
P(1)-C(11)-C(12)	121(6)	125(7)
P(1)-C(11)-C(16)	120(6)	119(7)
C(11)-C(12)-C(13)	121(8)	126(9)
C(12)-C(13)-C(14)	119(9)	118(9)
C(13)-C(14)-C(15)	124(10)	119(10)
C(14)-C(15)-C(16)	118(8)	123(10)
C(15)-C(16)-C(11)	119(8)	117(8)
C(16)-C(11)-C(12)	120(8)	117(9)
P(1)-C(21)-C(22)	119(6)	118(6)
P(1)-C(21)-C(26)	118(6)	122(7)
C(21)-C(22)-C(23)	117(8)	123(8)
C(22)-C(23)-C(24)	122(9)	118(10)
C(23)-C(24)-C(25)	120(12)	121(12)
C(24)-C(25)-C(26)	122(12)	120(9)
C(25)-C(26)-C(21)	116(9)	117(9)
C(26)-C(21)-C(22)	123(8)	121(10)

*Cnd is the centroid of the cyclopentadienyl group with coordinates .1257, .6177, .6186 for molecule 1 and .5685, -.0466, .3479 for molecule 2.

TABLE 5.2 cont.

Bond angles cont.	Molecule 1	Molecule 2
Methyldiphenylphosphine oxide (ii)		
O(2)-P(2)-C(3)	113(4)	110(5)
O(2)-P(2)-C(41)	113(4)	111(4)
O(2)-P(2)-C(51)	109(4)	109(4)
C(3)-P(2)-C(41)	107(5)	107(6)
C(3)-P(2)-C(51)	109(4)	112(5)
C(41)-P(2)-C(51)	107(4)	109(4)
P(2)-C(41)-C(42)	122(7)	121(7)
P(2)-C(41)-C(46)	117(8)	121(7)
C(41)-C(42)-C(43)	120(10)	120(10)
C(42)-C(43)-C(44)	122(11)	122(11)
C(43)-C(44)-C(45)	116(10)	117(12)
C(44)-C(45)-C(46)	123(11)	124(11)
C(45)-C(46)-C(41)	119(10)	119(8)
C(46)-C(41)-C(42)	120(9)	118(9)
P(2)-C(51)-C(52)	119(6)	116(9)
P(2)-C(51)-C(56)	120(7)	118(7)
C(51)-C(52)-C(53)	119(10)	116(15)
C(52)-C(53)-C(54)	117(11)	119(15)
C(53)-C(54)-C(55)	125(8)	123(14)
C(54)-C(55)-C(56)	117(9)	119(17)
C(55)-C(56)-C(51)	121(10)	116(12)
C(56)-C(51)-C(52)	121(7)	125(9)

TABLE 5.3

Atomic coordinates ($\times 10^4$) and anisotropic temperature factors ($Å^2 \times 10^3$)† (with standard deviations in parentheses) for $Cs_7Np^{(V)}O_2(Np^{(VI)}O_2)_2Cl_{12}$ [12]

a) Coordinates

Atom	x	y	z
Np	1250	5000	2500
O(1)	2346(10)	5000	2500
Cl(1)	1304(4)	5598(3)	824(3)
Cs(1)	1020(1)	1020(1)	1020(1)
Cs(2)	8750	5000	7500

b) Temperature Factors

Atom	U_{11}	U_{22}	U_{33}	U_{23}	U_{13}	U_{12}
Np	23(1)	36(1)	36(1)	0	0	0
O(1)	17(6)	62(10)	78(14)	49(12)	0	0
Cl(1)	80(4)	57(3)	38(2)	-3(2)	1(2)	23(3)
Cs(1)	53(1)	53(1)	53(1)	13(1)	13(1)	13(1)
Cs(2)	40(1)	39(1)	39(1)	0	0	0

TABLE 5.4

Bond lengths (Å) and angles (°) (with standard deviations in parentheses) for $Cs_7Np^{(V)}O_2(Np^{(VI)}O_2)_2Cl_{12}$ [12] (Primed atoms are related to unprimed by a two fold axis, double primed atoms are related to unprimed by a four fold axis).

a) Bond lengths

Np-O(1)	1.790(15)
Np-Cl(1)	2.685(5)

b) Bond angles

O(1)-Np-O(1)'	180.0
O(1)-Np-Cl(1)	88.3(1)
O(1)-Np-Cl(1)''	91.7(1)
Cl(1)-Np-Cl(1)'	176.5(3)

†The anisotropic temperature factor exponent takes the form: $-2(ha \times U_{11} + kb \times U_{22} + \cdots + 2hka \times b \times U_{12})$

References

1. T.J. Marks and R.D. Ernst, "Actinides," in *Comprehensive Organometallic Chemistry, Vol 3, Chap. 21.4*, ed. F.G.A. Stone, p. 211, Pergammon Press, Oxford, 1982.
2. G.F. Payne, *Thesis for Degree of Ph.D.*, University of Manchester, 1984.
3. K.W. Bagnall, F. Benetollo, G. Bombieri, and G. dePaoli, *J. Chem. Soc., Dalton Trans.*, p. 67, 1984.
4. R.F. Melkaya, Yu.F. Volkov, E.I. Sokolov, I.I. Kapshukov, and A.G. Rykov, *Soviet Radiochemistry*, vol. 23, p. 579, 1981.
5. K.W. Bagnall, J.B. Laidler, and M.A.A. Stuart, *J. Chem. Soc. A*, p. 133, 1968.
6. R.G. Denning and G.S. Topping, *Unpublished Results.*
7. N.W. Alcock, M.M. Roberts, and D. Brown, *Acta. Cryst.*, vol. B38, p. 1805, 1982.
8. N.W. Alcock, M.M. Roberts, and D. Brown, *J. Chem. Soc. Dalton Trans.*, p. 25, 1982.
9. G.M. Sheldrick, *SHELXTL User Manual,* Nicolet Instrument Co., 1981.
10. J.M. Stewart, "The X-RAY '76 system," TR-466, Computer Science Center, University of Maryland, U.S.A., 1976.

CHAPTER 6

Further compounds with uranium

6.1. The Crystal and Molecular Structure of Bisnitrato dioxo tetrakis(glycinato)uranium(VI),

6.1.1. Introduction

Complexation of dioxouranium(VI) (or uranyl) ion, $[UO_2^{2+}]$, by carboxylic acids has been widely studied and has been thoroughly reviewed recently.[1] Of particular interest has been the site and extent of coordination by ambidentate ligands , especially with *N*-donor atoms.[1,2] The simplest amino-acid, glycine, has attracted over 20 investigations of which the most recent[3] provides a reasonably unified picture of the situation prevailing in fairly dilute solution, namely that ligation proceeds through the carboxylate group with no involvement of the amino group. This potentiometric study[3] indicates that 1:1 and 1:2 complexes are formed which agrees well with polarographic results.[4] No higher complexes were detected, in contrast with the situation both for Th(IV)[3] and, according to one report,[5] for complexation of glycine with monosulphatodioxouranium(VI). In both of these cases tris-glycinato formulations are given. While the majority of the evidence clearly favours coordination *via* the carboxylate group, Sergeev and Korshunov suggest participation of the amino group both in the glycinatouranyl(VI) complex[6] and in glycinatothorium(IV)complexes.[7] This is based both on the observed stability constants and on the $N-H$ frequency in the i.r. spectra. Such *N*- coordination is established[8] for the bis(glycinato)complex of Cu(II), which is bis-chelated in a single plane, and reaction of glycine with *cis* $[Pt(NH_3)_2(H_2O)_2]^{+}$ in water gives initially *cis* $[Pt(NH_3)_2(O$-glycine$)(H_2O)]^{2+}$ which converts slowly into the $(N-O)$-chelate complex.[9]

In view of the uncertainty about the mode of complexation of glycine with uranyl(VI) a study of the interaction utilising absorptiometric and luminescence methods in solution was carried out by Mr. M.A. Shand in addition to the crystal structure determination.

6.1.2. Experimental

6.1.2.1. *Preparation.*

The solution studies carried out[10] indicated the presence of a 1:4 complex and a solution made up to this formulation was allowed to evaporate slowly to leave a bright yellow amorphous solid. This was redissolved in the minimum quantity of water and placed in an n.m.r. tube (diameter 5mm); acetonitrile as a precipitant was layered on the top of the

CHAPTER 6

Further compounds with uranium

6.1. The Crystal and Molecular Structure of Bisnitrato dioxo tetrakis(glycinato)uranium(VI),

6.1.1. Introduction

Complexation of dioxouranium(VI) (or uranyl) ion, $[UO_2^{2+}]$, by carboxylic acids has been widely studied and has been thoroughly reviewed recently.[1] Of particular interest has been the site and extent of coordination by ambidentate ligands , especially with *N*-donor atoms.[1,2] The simplest amino-acid, glycine, has attracted over 20 investigations of which the most recent[3] provides a reasonably unified picture of the situation prevailing in fairly dilute solution, namely that ligation proceeds through the carboxylate group with no involvement of the amino group. This potentiometric study[3] indicates that 1:1 and 1:2 complexes are formed which agrees well with polarographic results.[4] No higher complexes were detected, in contrast with the situation both for Th(IV)[3] and, according to one report,[5] for complexation of glycine with monosulphatodioxouranium(VI). In both of these cases tris-glycinato formulations are given. While the majority of the evidence clearly favours coordination *via* the carboxylate group, Sergeev and Korshunov suggest participation of the amino group both in the glycinatouranyl(VI) complex[6] and in glycinatothorium(IV)complexes.[7] This is based both on the observed stability constants and on the $N-H$ frequency in the i.r. spectra. Such *N*- coordination is established[8] for the bis(glycinato)complex of Cu(II), which is bis-chelated in a single plane, and reaction of glycine with *cis* $[Pt(NH_3)_2(H_2O)_2]^{+}$ in water gives initially *cis* $[Pt(NH_3)_2(O$-glycine$)(H_2O)]^{2+}$ which converts slowly into the $(N-O)$-chelate complex.[9]

In view of the uncertainty about the mode of complexation of glycine with uranyl(VI) a study of the interaction utilising absorptiometric and luminescence methods in solution was carried out by Mr. M.A. Shand in addition to the crystal structure determination.

6.1.2. Experimental

6.1.2.1. *Preparation.*

The solution studies carried out[10] indicated the presence of a 1:4 complex and a solution made up to this formulation was allowed to evaporate slowly to leave a bright yellow amorphous solid. This was redissolved in the minimum quantity of water and placed in an n.m.r. tube (diameter 5mm); acetonitrile as a precipitant was layered on the top of the

aqueous solution and the tube was left for 2-3 days. Small crystals grew at the interface. [11] The liquid layers were withdrawn carefully to leave a number of yellow lath-shaped crystals which were washed with acetonitrile and allowed to dry in a desiccator.

6.1.2.2. *Crystal Data.*

($C_8H_{20}N_6O_{16}U$) $UO_2(NH_2CH_2COOH)_4(NO_3)_2$, Space group:$P\bar{1}$; a = 5.875(1); b = 13.095(3); c = 13.285(2)Å, α = 72.76(1); β = 88.36(1); γ = 88.27(2)°, U = 975.4(3)Å^3, M = 686.25, Z = 2, D_c = 2.34 g cm^{-3}, Mo - K_α radiation, λ = 0.71069Å, μ(Mo-K_α) = 79.78 cm^{-1}.

6.1.2.3. *Data Collection and Structure Refinement.*

Data were collected with the Syntex $P2_1$ four circle diffractometer, with scan range -1.0/+1.05°(2θ) around the K_{α_1} - K_{α_2} angles. Of the 3447 reflections collected, 2281 were deemed to be observed ($I/\sigma(I)>3.0$) and were used in refinement. The crystal dimensions were 0.82 × 0.20 × 0.24 mm giving maximum and minimum transmission factors of 0.58 and 0.19. The density could not be determined because the crystals dissolved in the flotation reagents available.

A centred, apparently monoclinic cell was found initially with dimensions a = 5.874(1), b = 15.652(3), c = 23.883(4)Å, α = 89.17(2), β = 117.30(1), γ = 90.08(2)°. The deviation of α from 90° was disturbing and a careful check of an oscillation photograph about b showed that although many intensities corresponded fairly closely to m symmetry, a number departed significantly. It was concluded that the correct symmetry was triclinic; $P\bar{1}$ was chosen arbitrarily, and shown to be correct by the successful refinement. The pseudo-symmetry is explicable with hindsight, because the uranium atoms virtually conform to monoclinic symmetry. Averaging the reflection data using monoclinic symmetry gave an overall internal agreement of 8.1% (i.e. considerably worse than the final agreement achieved), after rejection of 70 pairs of reflections with large differences between corresponding pairs. Thue the intensity symmetry only conforms very approximately to the monoclinic case.

A Patterson synthesis showed near perfect I - centering, and indicated that the structure contained two cations each with $\bar{1}$ symmetry rather than one unconstrained cation. With two uranium atoms placed at 0,0,0 and ½,½,½, the light atoms were located on successive Fourier syntheses. The false I - centering caused some difficulty, particularly in the later stages when the correct peaks had to be selected on chemical grounds. Difference syntheses showed all the H-atoms, including those of the four NH_3^+ groups; H-atoms were included with fixed temperature factors, U = 0.07Å^2 and were refined as rigid CH_2 groups(C-H = 0.96Å) or NH_3^+ groups (N-H = 0.91Å). Final refinement was by cascaded least squares, and the largest peak on a final difference synthesis was of height 3.27 eÅ^{-3}

near a uranium atom.

A weighting scheme of the form $W = 1/(\sigma^2(F) + gF^2)$ with $g = 0.00026$ was applied, and this was shown to be satisfactory by a weight analysis. The final R-value was 0.0264. Final atomic coordinates are given in Table 6.1, and bond lengths and angles in Table 6.2.

6.1.3. Discussion.

The view of the cation $[UO_2(NH_2CH_2COOH)_4]^{2+}$ (Figure 6.1) shows the atomic numbering. The coordination about the uranium atom is seen to be hexagonal bipyramidal with four zwitterionic glycine molecules coordinated in the equatorial plane, all via their carboxylate oxygen atoms. Two glycine molecules are monodentate and two are bidentate. The two cations found in the unit cell (Figure 6.2) are very similar, each having asymmetric coordination to the bidentate glycine molecules with one longer and one shorter distance. U(1) to O(12) and O(13) are 2.562(5) and 2.489(6)Å respectively and U(2) is 2.502(6)Å from O(22) and 2.561(5)Å from O(23). The distances to the unidentate glycines are shorter, 2.436(4) and 2.438(4)Å.

These small but statistically significant differences are the only obvious variations between the two cations. There is, however, a larger difference between the two nitrate anions in their orientation in the cell, which can be seen in Figure 6.2. One of them makes a larger angle to the b-axis than the other and is also oriented differently in the $a-b$ plane. Presumably this provides the driving force for the distortions from the monoclinic symmetry. It is possible for the nitrate anions to take up these alternative orientations because they sit in relatively large cavities without strong interactions. The shortest contact distances they make are O---H distances of 1.998(10)Å [O(101)---H(111)] and 1.992(10)Å [O(202)---H(213)].

The cations are linked into infinite chains by hydrogen bonding (Table 6.3), N(11)-H(13)---O(25) and N(21)-H(212)---O(15). This can be seen in the view of the cell down the a axis (Figure 6.2) where the hydrogen bonds are shown as broken lines.

6.2. The Crystal and Molecular Structure of 4,4'-dipyridinium bis(dinitratohydroxydioxouranate(VI)) .

6.2.1. Introduction

Chapter 2 describes the determination of the structures of compounds between 2,2'-dipyridyl and uranyl(VI) and neptunyl(VI) nitrates and acetates[12] and it was felt that an extension of that study to include compounds containing 4,4'-dipyridyl would be of interest. In addition, the structures of a number of compounds of 4,4'-dipyridyl with lanthanide nitrates have been determined[13] and comparison might be possible between the two systems.

6.2.2. Experimental.

6.2.2.1. *Preparation*.- The production of dinitratodioxouranium(VI)1.5 4,4'-dipyridyl has been described previously,[14] and the reaction of uranyl(VI) nitrate hexahydrate (0.5 mmol) and excess (2.5 mmol) 4,4'-dipyridyl in 5 cm^{-3} of hot ethanol proceeds straightforwardly giving a yellow amorphous product. However, this product has proved very difficult to recrystallise and the only solvent in which the powder obtained dissolved was water. A crystalline product was obtained upon recrystallisation from water but this had a different infrared spectrum to that of the original product. Examination of this spectrum did suggest that the 4,4'-dipyridyl group was still present in the crystalline material and so the structure determination was carried out on the recrystallised product.

6.2.2.2. *Crystal Data*.- $C_{10}H_{12}N_6O_{18}U$; Space group: Pn; a = 13.336(3), b = 5.555(2), c = 15.433(3)Å, β = 94.25(1)°; U = 1 140.1(5)Å^3; M = 978.28; Z = 2; D_c = 2.849 g cm^{-3}; D_m = 2.847 g cm^{-3}; Mo- K_α radiation, λ = 0.710 69 Å; μ (Mo- K_α) = 24.69 cm^{-1}.

6.2.2.3. *Data Collection and Structural Refinement* - Data were collected with a Syntex $P2_1$ four circle diffractometer, with scan range -1.0/+1.1 (2θ) around the K_{α_1} - K_{α_2} angles. Of the 2 342 reflections collected, 1 920 were deemed to be observed [$(I)/\sigma(I) \geq 3.0$] and were used in subsequent refinement The crystal dimensions were: 0.11 × 0.29 × 0.05 mm which gave maximum and minimum transmission factors of 0.87 and 0.71 respectively. The systematic absences: $h0l: h+l \neq 2n$, ($h00: h \neq 2n$) ($00l: l \neq 2n$) indicate the space group is Pn . The uranium atoms were located by Patterson techniques and the remaining non-hydrogen atoms were found on successive Fourier syntheses. Hydrogen atoms were inserted at calculated positions with fixed isotropic temperature factors, U= 0.08Å^2 , and were not refined. Final refinement was by least squares methods.

A weighting scheme of the form w = $X \cdot Y$ was used where X = 1.0 or $(\sin\theta/\lambda)/0.35$ for $(\sin\theta/\lambda) \leq 0.35$ or $0.58/(\sin\theta/\lambda)$ for $(\sin\theta/\lambda) \geq 0.58$ and Y = 1.0 or $F_{obs}/30.0$ for $F_{obs} \leq 30.0$ or $125.0/F_{obs}$ if $F_{obs} \geq 125.0$, and was shown to be satisfactory by a weighting

analysis. The final R-value was 0.032.

Final atomic coordinates are given in Table 6.4, and selected bond lengths and angles in Table 6.5.

6.2.3. Discussion

The compound formed in the recrystallisation consists of bis[μ-hydroxy bis(nitrato)dioxouranium(VI)] anions and 4,4'-dipyridinium cations and Figure 6.3 shows the structure of the anion and the associated numbering scheme. The two dioxouranium(VI) groups are bonded by the bridging hydroxide groups so that the uranium atoms are at the centres of neighbouring hexagonal bipyramids with one common edge. The U-O distance in the uranyl groups is 1.78(2)Å and the U-O ligand distances are 2.52(2)Å for nitrate and 2.36(3)Å for hydroxide. The view of the cell (Figure 6.4) down the *b*-axis shows the arrangement of the ion pairs. The dipyridinium ion is slightly twisted about the C-C bond [C(103)-C(107)] between the two rings, the dihedral angle is 4.8 degrees. Comparison with the lanthanide nitrate 4,4'-dipyridyl compounds[13] is not possible as all have unprotonated, uncoordinated 4,4'-dipyridyl molecules present in the structure.

A hydrolysis reaction of the form:

$$UO_2(NO_3)_2.(4,4'-\text{dipyridyl})_{1.5} \xrightarrow{H_2O} [UO_2(NO_3)_2OH]_2^{2-}\ [4,4'-\text{dipyridyl}]^{2+}$$

appears to be responsible for the formation of the ionic material, but the mechanism has not been determined. Upon closer examination of the original material, a small number of crystals were found and these have the same cell parameters as the title compound. Such crystals were probably formed as the result of hydrolysis with the trace quantities of water present in the original reaction mixture.

6.3. Mono(trichloracetato)monochlorodioxo bis(triphenylphosphineoxide) uranium(VI)

6.3.1. Introduction

The structure of the title compound was determined in order to ascertain the final product of the photo-oxidisation of the compound tetrakis (trichloracetato) bis(triphenylphosphineoxide) uranium(VI)

6.3.2. Experimental

6.3.2.1 *Preparation* A research student working for Professor K.W. Bagnall at the University of Manchester prepared the compound tetrakis (trichloracetato) bis(triphenylphosphineoxide) uranium(IV) from uranium(IV), trichloracetic acid and tppo, and after recrystallisation a sample was provided for structure determination. Examination suggested that the compound had been oxidised to the +6 oxidation state, possibly during the recrystallisation from dichloromethane, as the compound now had the characteristic yellow colour of a dioxouranium(VI) compound. This observation was confirmed by an examination of the infrared spectrum which showed the characteristic $\nu_{as}OUO$ absorption at *ca.* 910cm^{-1}.

6.3.2.2. *Crystal Data:* $C_{36}H_{32}Cl_6O_6P_2U$, Space group:$P2_1/n$. a=10.029(2), b=18.924(4), c=22.454(5) Å, β=96.72(2)° U=4232.5(15)Å^3, M=1151.38, Z=4, D_c = 1.741 g cm^{-3}, Mo-K_α radiation, λ = 0.710 69 Å, μ (Mo-K_α)= 41.36 cm^{-1}. F(000) = 2152

6.3.2.3. *Data Collection and Structure Refinement* - Data were collected with a Syntex $P2_1$ four circle diffractometer, with scan range ± 1.1 (2 θ) around the K_{α_1} - K_{α_2} angles. Of the 8180 reflections collected, 5182 were deemed to be observed [$I/\sigma(I)\geq 3.0$] and were used in subsequent refinement. The maximum and minimum transmission factors were 0.50 and 0.37 respectively and the crystal dimensions were: 0.57 × 0.36 × 0.30 mm

The systematic absences: $h0l:h+l\neq 2n$ and $0k0:k\neq 2n$ ($00l:l\neq 2n$) indicate the space group is $P2_1/n$ (a special case of $P2_1/c$). The uranium atom was located by Patterson techniques and the remaining non-hydrogen atoms were found on successive Fourier syntheses. Hydrogen atoms were inserted at calculated positions with fixed isotropic temperature factors, B= 5.0 Å^2, and were not refined. Final refinement was by least squares methods.

A weighting scheme of the form w = $X\cdot Y$ was applied, where X = 1.0 or $(\sin\theta/\lambda)/0.35$ for $(\sin\theta/\lambda)\geq 0.35$ and Y = 1.0 or 110.0/ F_{obs} if $F_{obs}\geq$ 110.0, and was shown to be satisfactory by a weighting analysis. The final R-value was 0.062.

Final atomic coordinates are given in Table 6.6, and selected bond lengths and angles in Table 6.7.

6.3.3. Discussion.

A view of the molecule showing atomic numbering is given in Figure 6.5, and Figure 6.6 shows a view of the cell down the *b*-axis. The oxidation was reported[15] as being due to the rather facile photochemical reaction shown:

$$U(CCl_3COO)_4.2tppo \xrightarrow{h\nu/O_2} UO_2(CCl_3COO)Cl.2tppo$$

The stoichiometry of the oxidation product reflects the constituents of the original reaction with three of the chlorines of uranium(IV) chloride substituted in the equatorial plane, one by trichloracetate and two by triphenyl phosphine oxide groups, and the insertion of uranyl oxygens at the apices of a pentagonal bipyramid. The remaining chlorine atom is *trans* to the trichloracetate in the equatorial plane separated by the triphenyl phosphine oxide ligands. The mean uranyl U-O distance is 1.71(1)Å and the U-O(ligand) distances for the trichloracetate are 2.51(1) and 2.54(1)Å. The U-O(phosphine oxide) distances ar 2.30(1) and 2.31(1)Å and the U-Cl distance is 2.675(4)Å. The U-O(ligand) and U-Cl distances are very similar to those found in $UO_2(OPPh_3)_2(NO_3)_2$[16] and $UO_2(OPPh_3)_2Cl_2$.[17] The U-O(tppo) distances are 2.359(7) and 2.300(8)Å respectively, U-O(NO_3) distances 2.524(7) and 2.536(11)Å and the U-Cl distance 2.645(5)Å.

Computing for each structure was with the SHELXTL system[18] on a Data General NOVA3 mini-computer and the X-RAY 76 system,[19] on a Burroughs B6700 computer.

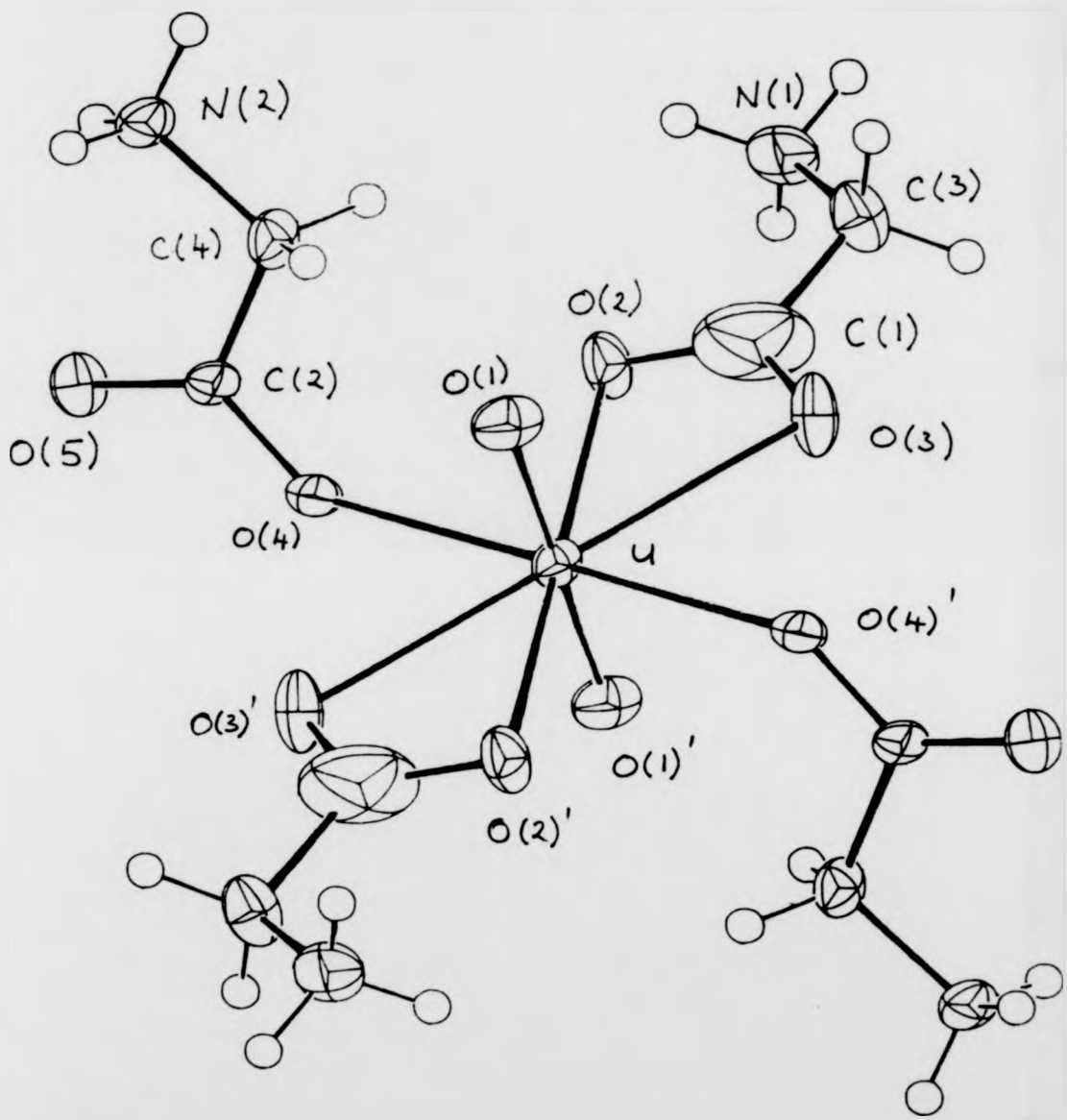

FIGURE 6.1. The $[UO_2(O_2CCH_2NH_3)_4]^{2+}$ [13] cation showing atomic numbering (Primed atoms are related to unprimed atoms by an inversion centre).

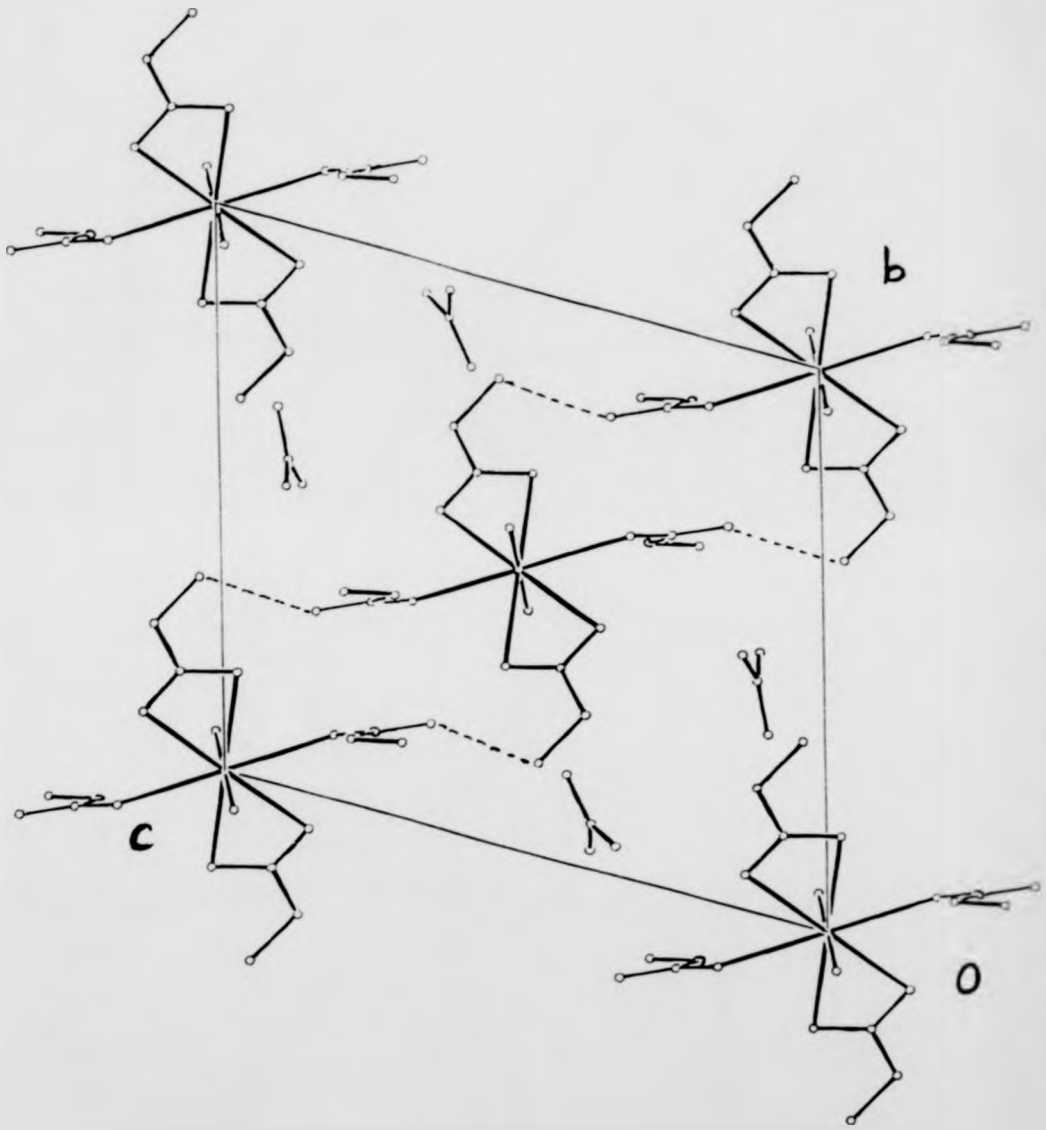

FIGURE 6.2. View of the unit cell of $[UO_2(O_2CCH_2NH_3)_3]^{2+}$ $[NO_3]_2^-$ [13] down *a* showing hydrogen atoms as broken lines.

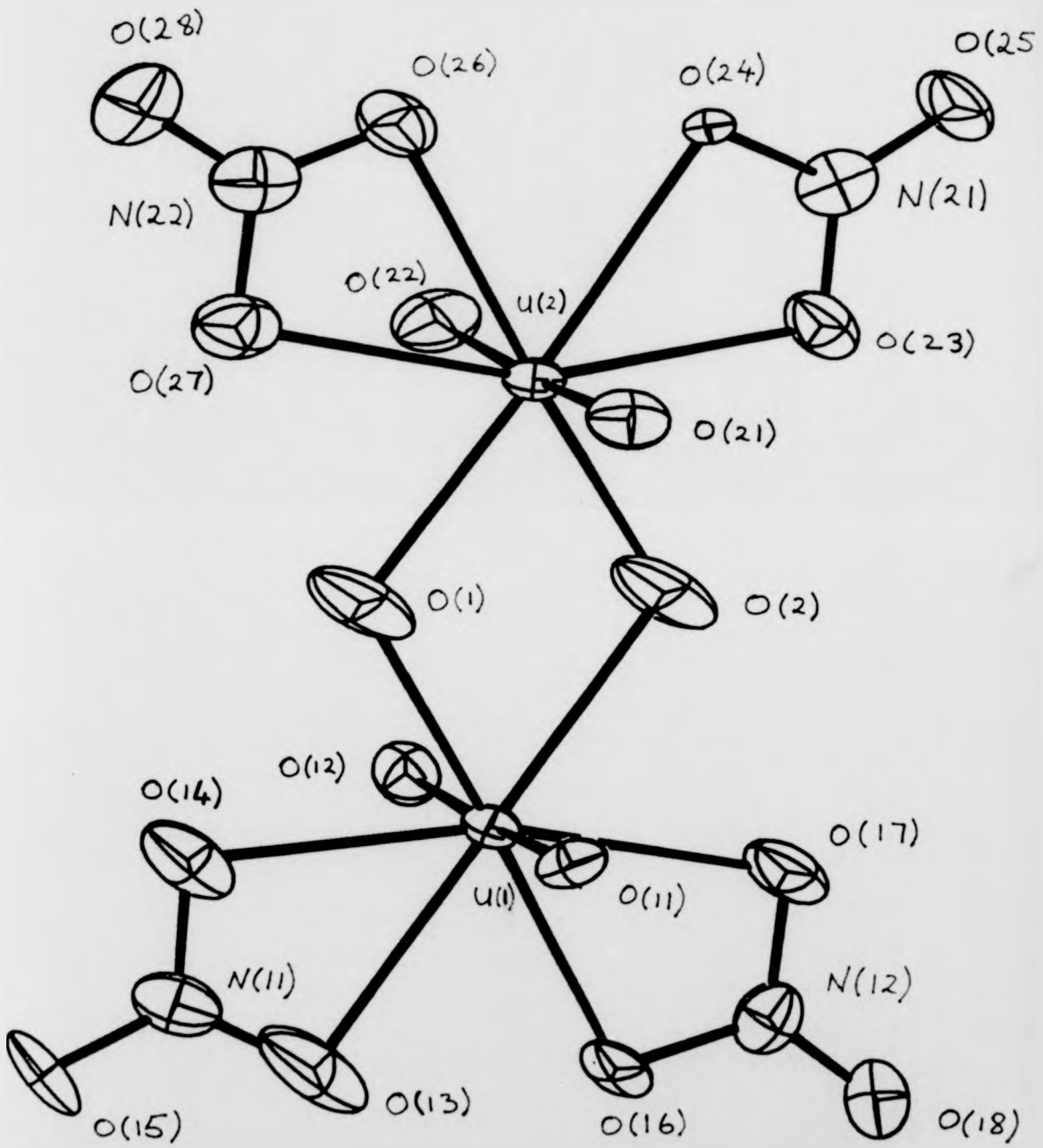

FIGURE 6.3. The $[(UO_2(NO_3)_2(OH)_2)_2]^{4-}$ [14] anion showing atomic numbering.

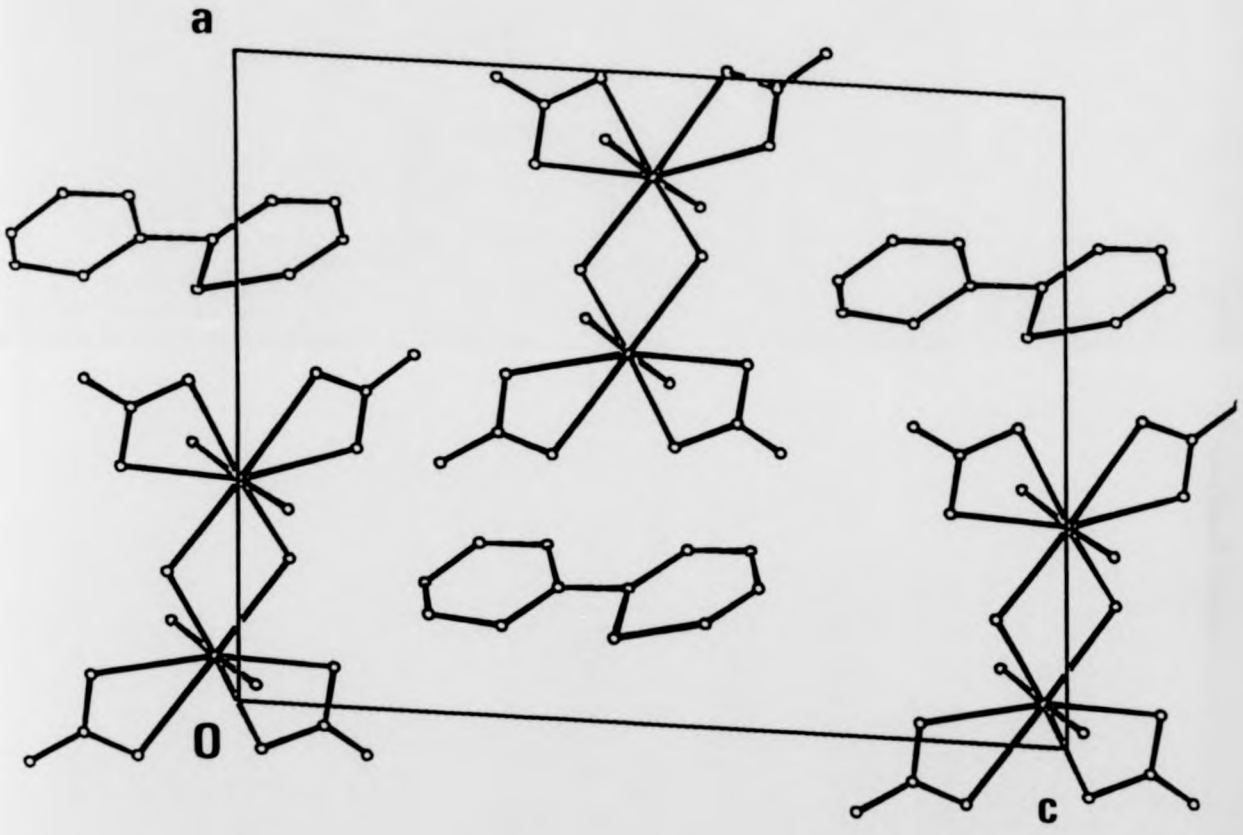

FIGURE 6.4. View of the unit cell of $[(UO_2(NO_3)_2OH)_2]^{2-}$ $[C_{10}H_{10}N_2]^{2+}$ [14] down the *b* axis.

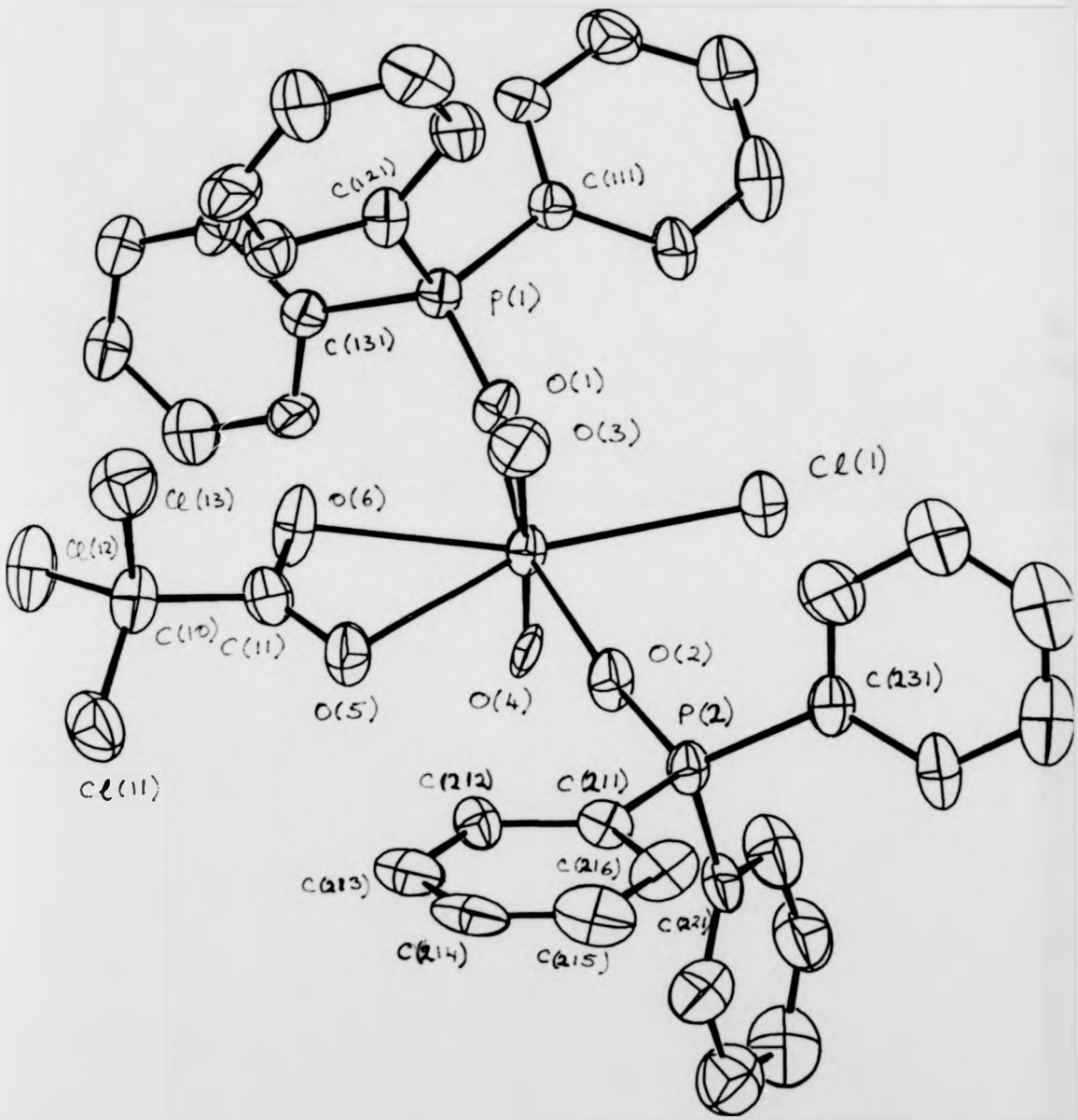

FIGURE 6.5. The $[UO_2(CCl_3COO)Cl(OPPh_3)_2]$ [15] molecule showing atomic numbering.

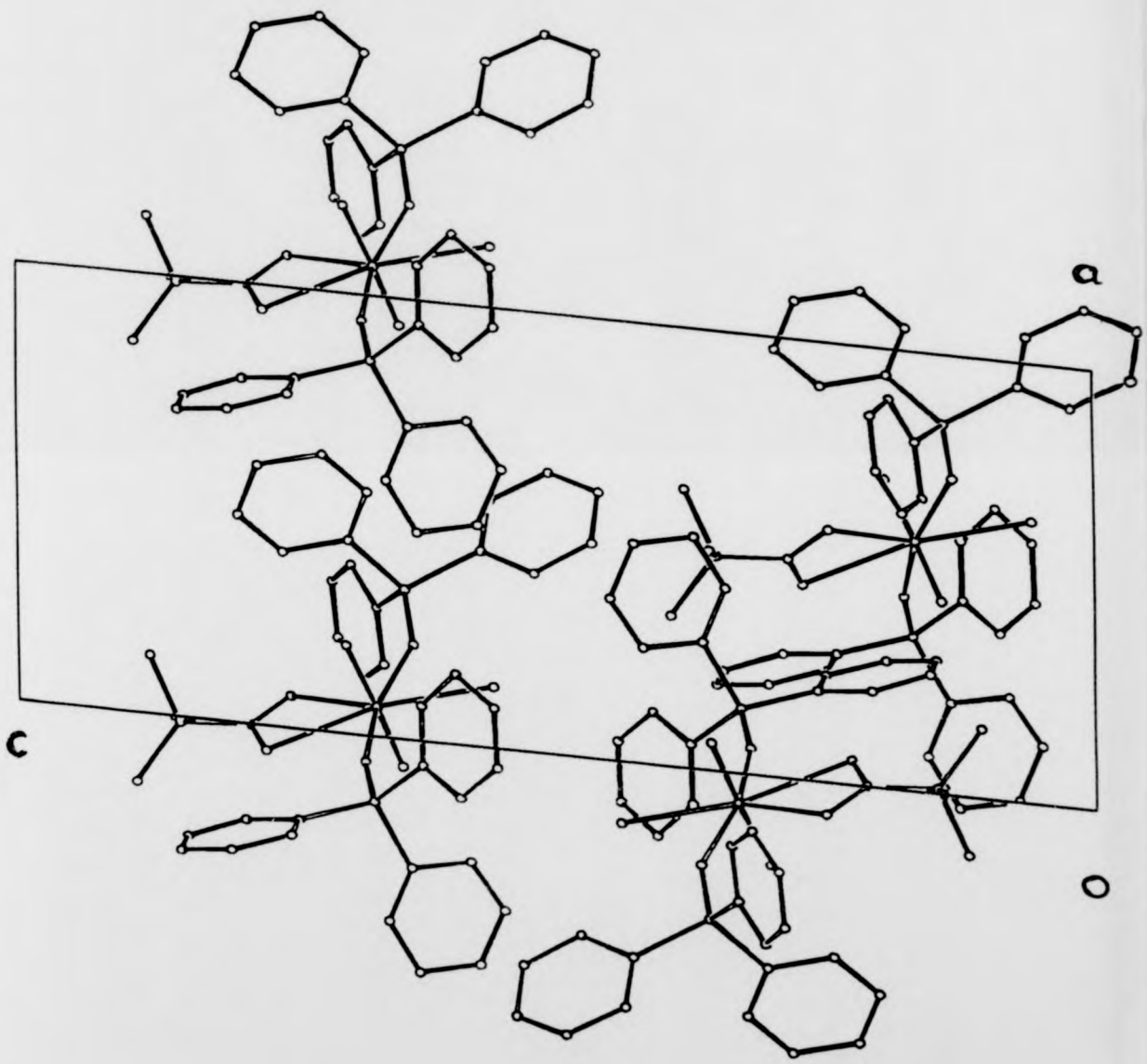

FIGURE 8.8. View of the unit cell of $[UO_2(CCl_3COO)Cl.(OPPh_3)_2$ [15] down the *b* axis.

TABLE 6.1

Atomic coordinates ($\times 10^4$) (with standard deviations in parentheses) for Bisnitrato dioxo tetrakis(glycinato)uranium(VI) [13]

a) Molecule 1

Atom	x	y	z
U(1)	0	0	0
O(11)	2591(8)	-668(4)	-141(4)
O(12)	1962(9)	1780(4)	-242(4)
O(13)	1902(10)	622(4)	1355(4)
C(11)	2499(12)	1506(7)	727(6)
C(13)	4001(14)	2210(6)	1147(6)
N(11)	4307(12)	3259(5)	373(5)
O(14)	369(7)	1144(4)	-1812(4)
O(15)	1697(9)	1807(4)	-3454(4)
C(12)	1976(11)	1370(5)	-2513(5)
C(14)	4359(12)	1126(6)	-2102(5)
N(12)	6084(10)	1304(5)	-2955(5)
N(10)	-901(13)	4139(6)	1108(5)
H(131)	5461	1857	1305
H(132)	3316	2305	1779
H(111)	5320	3600	659
H(112)	3000	3661	225
H(113)	4916	3164	-231
H(141)	4460	390	-1684
H(142)	4665	1557	-1670
H(121)	5730	1942	-3434
H(122)	6039	773	-3267
H(123)	7508	1327	-2711

Table 6.1 cont.

b) Molecule 2

Atom	x	y	z
U(2)	5000	5000	5000
O(101)	-833(12)	3246(5)	951(7)
O(102)	-2751(11)	4640(5)	1065(5)
O(103)	862(11)	4504(6)	1340(6)
O(21)	2513(8)	4324(4)	4849(4)
O(22)	7199(9)	4333(4)	3671(4)
O(23)	7126(8)	3207(4)	5255(4)
C(21)	7794(12)	3448(6)	4309(6)
C(23)	9409(13)	2730(6)	3927(6)
N(21)	9698(11)	1667(5)	4715(5)
O(24)	4722(8)	6110(4)	3173(4)
O(25)	3537(9)	6756(4)	1538(4)
C(22)	3186(12)	6334(5)	2484(5)
C(24)	794(11)	6105(6)	2876(6)
N(22)	-853(10)	6299(5)	2019(5)
N(20)	-4685(12)	-850(6)	-3877(5)
O(201)	-6443(11)	-545(6)	-3494(6)
O(202)	-2848(10)	-385(5)	-3895(5)
O(203)	-4740(11)	-1618(6)	-4245(7)
H(231)	10867	3060	3781
H(232)	8833	2635	3293
H(211)	8468	1237	4850
H(212)	9988	1874	5294
H(213)	10931	1302	4556
H(241)	375	6555	3308
H(242)	720	5368	3291
H(221)	-2338	6217	2235
H(222)	-473	5830	1652
H(223)	-648	6979	1599

TABLE 6.2

Bond lengths (Å) and bond angles (°) (with standard deviations in parentheses) for Bisnitrato dioxo tetrakis(glycinato)uranium(VI) [13] (Primed atoms are related to unprimed by an inversion centre)

a)Bond lengths	Molecule 1	Molecule 2
U-O(1)	1.765(5)	1.777(2)
U-O(2)	2.562(5)	2.502(6)
U-O(3)	2.489(6)	2.561(5)
U-O(4)	2.436(4)	2.438(4)
O(2)-C(1)	1.275(10)	1.263(8)
O(3)-C(1)	1.263(9)	1.256(9)
C(1)-C(3)	1.542(13)	1.498(11)
C(3)-N(1)	1.464(9)	1.481(8)
O(4)-C(2)	1.285(8)	1.269(8)
O(5)-C(2)	1.224(8)	1.228(8)
C(2)-C(4)	1.509(10)	1.493(9)
C(4)-N(2)	1.469(9)	1.474(9)
N(10)-O(101)	1.246(12)	1.245(10)
N(10)-O(102)	1.246(10)	1.251(10)
N(10)-O(103)	1.238(11)	1.243(12)

TABLE 6.2 cont.

b) Bond Angles	Molecule 1	Molecule 2
O(1)-U-O(1)'	180.0	180.0
O(1)-U-O(2)	92.7(4)	92.3(2)
O(1)-U-O(3)	87.1(2)	86.4(2)
O(1)-U-O(4)	90.4(2)	89.6(2)
O(2)-U-O(3)	51.9(2)	51.0(2)
	128.1(2)	129.0(2)
O(2)-U-O(4)	64.4(2)	64.3(2)
	115.6(2)	115.7(2)
O(3)-M-O(4)	116.0(2)	114.9(2)
	64.0(2)	65.1(2)
U-O(2)-C(1)	91.5(4)	95.7(5)
U-O(3)-C(1)	95.3(5)	93.1(7)
O(2)-C(1)-O(3)	121.2(8)	120.1(7)
O(2)-C(1)-C(3)	120.8(6)	118.6(7)
O(3)-C(1)-C(3)	117.8(7)	121.2(6)
C(1)-C(3)-N(1)	111.4(6)	112.2(6)
U-O(4)-C(2)	135.7(4)	135.7(4)
O(4)-C(2)-O(5)	124.4(6)	124.3(6)
O(4)-C(2)-C(4)	115.5(6)	116.6(6)
O(5)-C(2)-C(4)	119.6(6)	118.9(6)
C(2)-C(4)-N(2)	112.3(6)	113.0(6)
O(101)-N(10)-O(102)	119.9(8)	120.3(8)
O(101)-N(10)-O(103)	119.5(8)	120.3(8)
O(102)-N(10)-O(103)	120.5(8)	119.4(7)

TABLE 6.3

Hydrogen bonds; distances (Å) and angles (°) with standard deviations in parentheses

a) N(11)-H(113)...O(25)

N(11)-H(113)	0.91*
H(113)...O(25)	1.913(9)
N(11)...O(25)	2.810(9)
N(11)-H(113)-O(25)	168.2(8)

a) N(21)-H(212)...O(15)

N(21)-H(212)	0.91*
H(212)...O(15)	1.946(9)
N(21)...O(15)	2.788(9)
N(21)-H(212)-O(15)	153.1(7)

*Bond length fixed; H-atoms held in rigid tetrahedral geometry, with freedom for the NH_3 unit to move

TABLE 6.4

Atomic coordinates ($\times 10^4$) (with standard deviations in parentheses) for 4,4'-dipyridinium bis(dinitratohydroxy dioxouranate(VI)) [14]

Atom	x	y	z
U(1)	674.9(51)	1648.0(19)	-286.0(41)
U(2)	3418.2(51)	4319.5(19)	29.0(41)
O(1)	1959(23)	4124(44)	-826(22)
O(2)	2236(18)	1759(37)	605(15)
O(11)	256(17)	4249(47)	214(15)
O(12)	1182(18)	-963(46)	-799(15)
O(13)	260(22)	3241(56)	-1765(18)
O(14)	-933(21)	1350(47)	-1196(17)
O(15)	-1143(21)	2732(53)	-2543(17)
O(16)	-712(17)	-680(44)	290(15)
O(17)	597(18)	-514(55)	1138(17)
O(18)	-699(20)	-2405(54)	1541(16)
N(11)	-630(23)	2319(55)	-1856(20)
N(12)	-286(22)	-1274(55)	1014(19)
O(21)	3958(22)	1793(46)	-536(18)
O(22)	2981(19)	6854(43)	592(16)
O(23)	4009(20)	2297(49)	1425(17)
O(24)	5126(17)	4600(57)	939(16)
O(25)	5473(22)	2477(60)	2125(20)
O(26)	4884(19)	6703(53)	-576(17)
O(27)	3503(20)	6625(49)	-1419(18)
O(28)	4815(22)	8429(52)	-1839(19)
N(21)	4887(20)	3049(47)	1528(20)
N(22)	4426(24)	7296(57)	-1296(22)
N(3)	1996(22)	3321(52)	2258(16)
N(4)	2206(26)	9327(60)	6264(22)
C(101)	2639(33)	2536(75)	2927(24)
C(102)	2653(26)	3574(65)	3724(21)
C(103)	2031(27)	5599(64)	3847(26)
C(104)	1398(29)	6316(70)	3165(23)
C(105)	1462(33)	5142(82)	2321(29)
C(106)	2070(25)	6837(64)	4716(20)
C(107)	2697(28)	6065(64)	5407(20)
C(108)	2740(33)	7317(77)	6176(25)
C(109)	1612(34)	10149(83)	5594(25)
C(110)	1508(27)	9001(67)	4812(24)
H(1)	1718	4556	-1054
H(2)	1570	-1534	970
H(101)	3078	1247	2971
H(102)	3000	3059	4139
H(104)	437	9422	3187
H(105)	1764	4526	2151
H(107)	3071	4517	5384
H(108)	3767	6943	6482
H(109)	894	12370	5827
H(110)	733	9458	4416

TABLE 6.5

Bond lengths (Å) and bond angles (°) (with standard deviations in parentheses) for 4,4'-dipyridinium bis(dinitratohydroxy dioxouranate(VI)) [14]

a) Bond lengths

i) Anion

U(1)-O(11)	1.75(3)
U(1)-O(12)	1.81(3)
U(1)-O(13)	2.47(3)
U(1)-O(14)	2.48(3)
U(1)-O(16)	2.48(2)
U(1)-O(17)	2.51(3)
U(1)-O(1)	2.39(3)
U(1)-O(2)	2.41(2)
U(2)-O(21)	1.83(3)
U(2)-O(22)	1.78(2)
U(2)-O(23)	2.50(3)
U(2)-O(24)	2.59(2)
U(2)-O(26)	2.59(3)
U(2)-O(27)	2.59(3)
U(2)-O(1)	2.27(3)
U(2)-O(2)	2.35(2)
N(11)-O(13)	1.29(4)
N(11)-O(14)	1.25(4)
N(11)-O(15)	1.24(4)
N(12)-O(16)	1.26(4)
N(12)-O(17)	1.25(4)
N(12)-O(18)	1.19(4)
N(21)-O(23)	1.24(4)
N(21)-O(24)	1.31(4)
N(21)-O(25)	1.21(4)
N(22)-O(26)	1.27(4)
N(22)-O(27)	1.29(4)
N(22)-O(28)	1.20(4)

ii) Cation

N(3)-C(101)	1.36(5)
C(101)-C(102)	1.36(5)
C(102)-C(103)	1.42(5)
C(103)-C(104)	1.36(5)
C(103)-C(106)	1.50(5)
C(104)-C(105)	1.46(6)
N(3)-C(105)	1.25(5)
C(106)-C(107)	1.37(5)
C(107)-C(108)	1.37(5)
N(4)-C(108)	1.34(5)
N(4)-C(109)	1.34(5)
C(109)-C(110)	1.36(5)
C(110)-C(106)	1.43(5)

TABLE 6.5 cont.

b) Bond angles

i) Anion

O(11)-U(1)-O(12)	176.6(11)
O(11)-U(1)-O(13)	93.1(11)
O(11)-U(1)-O(14)	90.7(10)
O(11)-U(1)-O(16)	90.1(10)
O(11)-U(1)-O(17)	88.5(11)
O(11)-U(1)-O(1)	86.5(10)
O(11)-U(1)-O(2)	91.0(9)
O(12)-U(1)-O(13)	87.0(11)
O(12)-U(1)-O(14)	92.0(10)
O(12)-U(1)-O(16)	92.9(10)
O(12)-U(1)-O(17)	92.3(10)
O(12)-U(1)-O(1)	90.5(11)
O(12)-U(1)-O(2)	86.3(9)
O(13)-U(1)-O(14)	51.5(9)
O(13)-U(1)-O(16)	113.4(9)
O(13)-U(1)-O(17)	163.2(9)
O(13)-U(1)-O(1)	65.8(10)
O(13)-U(1)-O(2)	130.0(9)
O(14)-U(1)-O(16)	61.9(8)
O(14)-U(1)-O(17)	111.8(9)
O(14)-U(1)-O(1)	117.0(10)
O(14)-U(1)-O(2)	177.6(8)
O(16)-U(1)-O(17)	49.9(8)
O(16)-U(1)-O(1)	176.4(9)
O(16)-U(1)-O(2)	116.4(8)
O(17)-U(1)-O(1)	131.0(10)
O(17)-U(1)-O(2)	66.6(8)
O(1)-U(1)-O(2)	64.8(9)

U(1)-O(13)-N(11)	96(2)
U(1)-O(13)-N(11)	97(2)
O(13)-N(11)-O(14)	116(3)
O(13)-N(11)-O(15)	118(3)
O(14)-N(11)-O(15)	126(3)
U(1)-O(16)-N(12)	99(2)
U(1)-O(17)-N(12)	97(2)
O(16)-N(12)-O(17)	114(3)
O(16)-N(12)-O(18)	123(3)
O(17)-N(12)-O(18)	123(3)

TABLE 6.5 cont.

b) Bond angles cont

i) Anion cont

O(21)-U(2)-O(22)	176.0(13)
O(21)-U(2)-O(23)	87.5(11)
O(21)-U(2)-O(24)	86.7(11)
O(21)-U(2)-O(26)	83.5(11)
O(21)-U(2)-O(27)	85.6(11)
O(21)-U(2)-O(1)	92.1(11)
O(21)-U(2)-O(2)	90.8(10)
O(22)-U(2)-O(23)	91.6(10)
O(22)-U(2)-O(24)	89.7(10)
O(22)-U(2)-O(26)	93.1(10)
O(22)-U(2)-O(27)	93.8(10)
O(22)-U(2)-O(1)	91.4(11)
O(22)-U(2)-O(2)	92.4(10)
O(23)-U(2)-O(24)	49.7(9)
O(23)-U(2)-O(26)	110.0(9)
O(23)-U(2)-O(27)	159.2(9)
O(23)-U(2)-O(1)	132.8(10)
O(23)-U(2)-O(2)	65.1(8)
O(24)-U(2)-O(26)	60.5(8)
O(24)-U(2)-O(27)	110.2(9)
O(24)-U(2)-O(1)	177.3(11)
O(24)-U(2)-O(2)	118.8(9)
O(26)-U(2)-O(27)	49.7(8)
O(26)-U(2)-O(1)	116.9(10)
O(26)-U(2)-O(2)	172.7(8)
O(27)-U(2)-O(1)	167.2(10)
O(27)-U(2)-O(2)	134.6(8)
O(1)-U(2)-O(2)	67.7(10)

U(2)-O(23)-N(21)	101(2)
U(2)-O(23)-N(21)	95(2)
O(23)-N(21)-O(24)	114(3)
O(23)-N(21)-O(25)	124(3)
O(24)-N(21)-O(25)	122(3)
U(2)-O(26)-N(22)	97(2)
U(2)-O(27)-N(22)	97(2)
O(26)-N(22)-O(27)	117(3)
O(26)-N(22)-O(28)	123(3)
O(27)-N(22)-O(28)	121(3)

TABLE 6.5 cont.

b) Bond angles cont

ii) Cation

N(3)-C(101)-C(102)	121(4)
N(3)-C(105)-C(104)	120(4)
C(101)-C(102)-C(103)	119(3)
C(102)-C(103)-C(104)	118(3)
C(102)-C(103)-C(106)	120(3)
C(104)-C(103)-C(106)	122(3)
C(103)-C(104)-C(105)	119(4)
C(103)-C(106)-C(107)	122(3)
C(103)-C(106)-C(110)	119(3)
C(107)-C(106)-C(110)	118(3)
C(106)-C(107)-C(108)	120(3)
N(4)-C(108)-C(107)	122(4)
N(4)-C(109)-C(110)	123(4)

TABLE 6.6

Atomic coordinates ($\times 10^4$) (with standard deviations in parentheses) for mono(trichloracetato)monochlorodioxobis(triphenyl phosphine oxide) uranium(VI) [15]

Atom	x	y	z
U	682(1)	2399(0)	3329(0)
P1	3410(4)	1109(2)	3599(2)
P2	-1479(4)	4049(2)	3300(2)
Cl1	1403(5)	2961(2)	4412(2)
Cl11	-6327(6)	7007(3)	3803(2)
Cl12	-4993(7)	5702(2)	3580(2)
Cl13	-3426(6)	6929(3)	3935(2)
O1	2173(10)	1528(5)	3677(4)
O2	-597(12)	3418(5)	3219(4)
O3	2011(13)	2820(7)	3043(6)
O4	-621(13)	1982(8)	3574(5)
O5	-566(12)	2407(5)	2279(4)
O6	733(15)	1493(5)	2517(4)
C10	-4876(20)	6636(8)	3526(7)
C11	-20(17)	1863(7)	2138(7)
C111	2934(15)	232(7)	3334(6)
C112	1660(15)	4(8)	3397(6)
C113	1282(20)	-692(9)	3207(8)
C114	2165(19)	-1108(8)	2964(7)
C115	3435(18)	-889(8)	2912(7)
C116	3850(17)	-210(8)	3093(6)
C121	4450(15)	1051(7)	4305(6)
C122	5601(16)	634(9)	4381(7)
C123	6370(18)	596(10)	4930(8)
C124	6049(22)	991(9)	5397(8)
C125	4880(24)	1399(9)	5331(7)
C126	4057(18)	1460(8)	4787(6)
C131	4396(17)	1489(7)	3070(6)
C132	5525(18)	1886(7)	3253(7)
C133	6262(19)	2194(8)	2856(8)
C134	5876(21)	2091(9)	2221(7)
C135	4720(18)	1702(9)	2031(8)
C136	3986(17)	1384(8)	2452(7)

TABLE 6.6 cont.

Atom	x	y	z
C211	-2903(16)	3807(7)	3650(6)
C212	-2632(22)	3389(11)	4198(8)
C213	-3674(21)	3176(11)	4499(9)
C214	-4967(24)	3357(12)	4278(10)
C215	-5272(23)	3751(11)	3722(11)
C216	-4170(19)	3951(8)	3436(9)
C221	-558(17)	4702(7)	3762(6)
C222	801(20)	4734(9)	3749(8)
C223	1602(23)	5241(10)	4074(9)
C224	912(25)	5714(10)	4412(9)
C225	-451(25)	5694(9)	4437(8)
C226	-1206(21)	5170(8)	4110(7)
C231	-2060(146)	4425(7)	2585(6)
C232	-2175(16)	3982(8)	2086(6)
C233	-2694(16)	4252(10)	1536(7)
C234	-3025(16)	4949(10)	1476(8)
C235	-2906(20)	-5390(10)	1947(9)
C236	-2427(20)	5133(8)	2514(9)
C30	-698(35)	1745(11)	5001(9)
Cl31	107(8)	924(4)	5727(3)
Cl32	-669(11)	2127(4)	5727(3)

TABLE 6.6 cont.

Atom	x	y	z
C211	-2903(16)	3807(7)	3650(6)
C212	-2632(22)	3389(11)	4198(8)
C213	-3674(21)	3176(11)	4499(9)
C214	-4967(24)	3357(12)	4278(10)
C215	-5272(23)	3751(11)	3722(11)
C216	-4170(19)	3951(8)	3436(9)
C221	-558(17)	4702(7)	3762(6)
C222	801(20)	4734(9)	3749(8)
C223	1602(23)	5241(10)	4074(9)
C224	912(25)	5714(10)	4412(9)
C225	-451(25)	5694(9)	4437(8)
C226	-1206(21)	5170(8)	4110(7)
C231	-2060(146)	4425(7)	2585(6)
C232	-2175(16)	3982(8)	2086(6)
C233	-2694(16)	4252(10)	1536(7)
C234	-3025(16)	4949(10)	1476(8)
C235	-2906(20)	-5390(10)	1947(9)
C236	-2427(20)	5133(8)	2514(9)
C30	-698(35)	1745(11)	5001(9)
Cl31	107(8)	924(4)	5727(3)
Cl32	-669(11)	2127(4)	5727(3)

TABLE 6.7

Bond lengths (Å) and bond angles (°) (with standard deviations in parentheses) for Mono(trichloracetato)monochlorodioxobis (triphenyl phosphineoxide) uranium(VI) [15]

a)Bond lengths

i) Around uranium atom

U-O(1)	2.30(1)
U-O(2)	2.31(1)
U-O(3)	1.74(1)
U-O(4)	1.67(1)
U-O(5)	2.54(1)
U-O(6)	2.51(1)
U-Cl(1)	2.675(4)

ii) Trichloracetate group

C(11)-O(5)	1.22(2)
C(11)-O(6)	1.28(2)
C(11)-C(10)	1.54(2)
C(10)-Cl(11)	1.79(2)
C(10)-Cl(12)	1.78(2)
C(10)-Cl(13)	1.72(2)

iii) Phosphine oxide groups	(1)	(2)
O-P	1.50(1)	1.51(1)
P-C(11)	1.81(1)	1.77(2)
P-C(21)	1.80(1)	1.80(1)
P-C(31)	1.78(2)	1.79(1)
C(11)-C(12)	1.37(2)	1.46(2)
C(12)-C(13)	1.42(2)	1.37(3)
C(13)-C(14)	1.35(3)	1.38(3)
C(14)-C(15)	1.36(3)	1.45(3)
C(15)-C(16)	1.40(2)	1.40(3)
C(16)-C(11)	1.40(2)	1.33(2)
C(21)-C(22)	1.39(2)	1.37(3)
C(22)-C(23)	1.38(2)	1.40(3)
C(23)-C(24)	1.36(3)	1.41(3)
C(24)-C(25)	1.40(3)	1.37(3)
C(25)-C(26)	1.40(2)	1.40(2)
C(26)-C(21)	1.42(2)	1.39(2)
C(31)-C(32)	1.38(2)	1.39(2)
C(32)-C(33)	1.39(3)	1.38(2)
C(33)-C(34)	1.40(2)	1.36(3)
C(34)-C(35)	1.40(3)	1.34(3)
C(35)-C(36)	1.40(2)	1.39(3)
C(36)-C(31)	1.41(2)	1.39(2)

TABLE 6.7 cont.

b) Bond angles

i) Around uranium

O(3)-U-O(4)	177.5(6)
O(3)-U-O(1)	87.5(5)
O(3)-U-O(2)	91.0(5)
O(3)-U-O(5)	88.3(5)
O(3)-U-O(6)	87.9(5)
O(3)-U-Cl(1)	90.9(4)
O(4)-U-O(1)	93.0(5)
O(4)-U-O(2)	89.1(6)
O(4)-U-O(5)	89.4(5)
O(4)-U-O(6)	90.0(5)
O(4)-U-Cl(1)	91.6(4)
O(1)-U-O(2)	164.6(3)
O(1)-U-O(5)	123.4(3)
O(1)-U-O(6)	71.9(3)
O(1)-U-Cl(1)	83.1(2)
O(2)-U-O(5)	71.9(3)
O(2)-U-O(6)	123.4(4)
O(2)-U-Cl(1)	81.5(3)
O(5)-U-O(6)	51.5(4)
O(5)-U-Cl(1)	153.4(3)
O(6)-U-Cl(1)	155.0(3)

ii) Trichloracetate group

U-O(5)-C(11)	92.8(9)
U-O(6)-C(11)	92.9(9)
O(5)-C(11)-O(6)	122(1)
O(5)-C(11)-C(10)	120(1)
O(6)-C(11)-C(10)	117(1)
C(11)-C(10)-Cl(11)	105(1)
C(11)-C(10)-Cl(12)	110(1)
C(11)-C(10)-Cl(13)	113(1)
Cl(11)-C(10)-Cl(12)	108(1)
Cl(11)-C(10)-Cl(13)	111(1)
Cl(12)-C(10)-Cl(13)	110(1)

TABLE 6.7 cont.

b) Bond angles cont.

iii) Phosphine oxide groups	(1)	(2)
U-O-P	148.6(6)	166.3(6)
O-P-C(11)	109.5(6)	111.4(7)
O-P-C(21)	109.4(6)	110.1(7)
O-P-C(31)	113.3(6)	109.8(6)
P-C(11)-C(12)	118(1)	116(1)
P-C(11)-C(16)	121(1)	125(1)
C(11)-C(12)-C(13)	119(1)	120(2)
C(12)-C(13)-C(14)	120(2)	119(2)
C(13)-C(14)-C(15)	122(2)	122(2)
C(14)-C(15)-C(16)	120(2)	116(2)
C(15)-C(16)-C(11)	118(2)	124(2)
C(16)-C(11)-C(12)	121(1)	119(2)
P-C(21)-C(22)	122(1)	118(1)
P-C(21)-C(26)	117(1)	121(1)
C(21)-C(22)-C(23)	121(2)	122(2)
C(22)-C(23)-C(24)	120(2)	115(2)
C(23)-C(24)-C(25)	120(2)	124(2)
C(24)-C(25)-C(26)	122(2)	119(2)
C(25)-C(26)-C(21)	116(2)	119(2)
C(26)-C(21)-C(22)	121(1)	121(1)
P-C(31)-C(32)	121(1)	118(1)
P-C(31)-C(36)	118(1)	123(1)
C(31)-C(32)-C(33)	121(1)	119(1)
C(32)-C(33)-C(34)	120(2)	120(2)
C(33)-C(34)-C(35)	120(2)	122(2)
C(34)-C(35)-C(36)	120(2)	119(2)
C(35)-C(36)-C(31)	119(1)	120(2)
C(36)-C(31)-C(32)	120(1)	119(1)

References

1. H. Gusten, *Gmelin Handbuch URAN Suppl.*, A6, Ch.3, Springer-Verlag, Berlin, 1983.
2. M. Delcanale, R. Marchelli, A. Mangia, A. Dossena, and G. Casnati, *Angew. Chem. Suppl.*, pp. 794-802, 1983.
3. A. Bismondo, L. Rizzo, G. Tomat, D. Curto, P. Di Bernardo, and A. Cassol, *Inorg. Chim. Acta.*, vol. 74, p. 21, 1983.
4. V.V. Ramanujam, K. Rengaraj, and B. Sivasankar, *Bull. Chem. Soc. Jpn.*, vol. 52, p. 2713, 1979.
5. R.N. Shchelokov, I.M. Orlova, and G.V. Podneb, *Russ. J. Inorg. Chem.*, vol. 19, p. 744, 1974.
6. G.M. Sergeev and J.A. Korshunov, *Sov. Radiochem.*, vol. 15, p. 623, 1973.
7. J.A. Korshunov and G.M. Sergeev, *Sov. Radiochem.*, vol. 16, p. 771, 1974.
8. H.C. Freeman, M.R. Snow, I. Nitta, and K. Tomita, *Acta. Cryst.*, vol. 17, p. 1463, 1964.
9. T.G. Appleton and J.R. Hall, *J. Chem. Soc., Chem. Commun.*, p. 911, 1983.
10. N.W. Alcock, D.J. Flanders, T.J. Kemp, and M.A. Shand, *J. Chem. Soc., Dalton Trans.*, vol. In Press.
11. P.G. Jones, *Chem. Brit.*, vol. 17, p. 222, 1981.
12. N.W. Alcock, D.J. Flanders, and D. Brown, *J. Chem. Soc. Dalton Trans.*, In Press.
13. T.J.R. Weakley, *Inorg. Chim. Acta*, vol. 63, p. 161, 1982.
14. I.S. Ahuja and R. Singh, *Aust. J. Chem.*, vol. 26, p. 1871, 1973.
15. K.W. Bagnall, *Private Communication.*
16. N.W. Alcock, M.M. Roberts, and D.Brown, *J. Chem. Soc., Dalton Trans.*, p. 25, 1982.
17. G. Bombieri, E. Forsellini, J.P. Day, and W.I. Azeez, *J. Chem. Soc., Dalton Trans.*, p. 677, 1978.
18. G.M. Sheldrick, *SHELXTL User Manual,* Nicolet Instrument Co., 1981.
19. J.M. Stewart, "The X-RAY '76 system," TR-466, Computer Science Center, University of Maryland, U.S.A., 1976.

CHAPTER 7

EXPERIMENTAL SECTION

7.1. Techniques used in handling Neptunium-237

The neptunium 237 used was supplied as the dioxide, and was taken into solution by prolonged boiling with concentrated nitric acid being oxidised to NpO_2^+.[1] This Np(V) species is then oxidised to NpO_2^{2+} used for the formation of the compounds under examination. The oxidant, partially ozonised oxygen, is produced by the passage of oxygen through an electrical discharge. The gas mixture is passed through the Np(V) solution in diluted (4M) nitric acid, which is heated by a boiling water bath. The Np(V) → Np(VI) oxidation, which is accompanied by a colour change from dark-green to brown, and the oxidation of Np(IV) are thermodynamically favoured by the potential of the O_2/O_3 couple,[2] which is greater than those for Np(VI)/Np(V) and Np(VI)/Np(IV) (Ch.1.2):-

$$NpO_2^{2+} + e^- \rightarrow NpO_2^+ \; ; \; E^\circ = 1.236 \text{ V}$$

$$NpO_2^{2+} + 4H^+ + 2e^- \rightarrow Np^{4+} + 2H_2O; \; E^\circ = 0.938 \text{ V}$$

$$O_3 + 2H^+ + 2e^- \rightarrow O_2 + H_2O \; ; \; E^\circ = 2.07 \text{ V}$$

The solution containing NpO_2^{2+} ions can then be reacted with suitable ligands to give a product by crystallisation. If the solution contains any interfering ions, Np(VI) can be precipitated as $NpO_3(OH)_2$ by the careful addition of dilute aqueous ammonia and, after centrifugation and washing with water and acetone to remove the impurities, the hydroxide redissolved in the minimum quantity of dilute nitric acid.

In some cases the neptunium supplied contains a significant quantity of plutonium-238 which would be responsible for over 90% of the α-activity of the material. This element must be removed for safety reasons and as Pu(VI) will also come out of solution on the addition of ammonia the method of separation used is anion-exchange chromatography. The contaminated material is precipitated with ammonia and reduced with a saturated solution of ammonium iodide in concentrated hydrochloric acid to give Pu(III) and Np(VI). This solution is then put onto a column of AG 1-X4 resin, followed by a sufficient volume of 0.2M ammonium iodide in concentrated hydrochloric acid to elute through the blue Pu(III), which is not retained on anion exchangers at any acid concentration. Np(VI), conversely, has a high distribution coefficient in anion exchange resins at this acid concentration as Figure 7.1 shows.[3]

The distribution coefficient,[4] K_d of an ionic species on the resin is given by

$$K_d = \frac{m_e}{m_s} \times \frac{\textit{Volume of solution}}{\textit{Mass of resin}}$$

where m_s and m_e are the fractions of the ion on the resin and in solution respectively. Thus the Np(VI) remains adsorbed at the top of the column and can be eluted as a separate fraction by eluting with 2M hydrochloric acid. Such a separation typically reduces the α-activity due to plutonium-238 to 2-3%, corresponding to a very low level of plutonium contamination. The Np(IV) fraction can then be oxidised directly to Np(VI) as before and used for preparative work. The NpO_2^{2+} ions in solution reduce to NpO_2^+ over a period of time and the Np(VI) solution must be prepared freshly before each complex preparation.

All operations, including the usual crystal mounting techniques, on solid neptunium compounds were carried out in the nitrogen-flushed atmosphere of a depressurised glove box. Crystals were mounted on quartz fibres with "Araldite" and were then encapsulated with Lindermann glass capillaries. The mounted crystals were then transferred to a fume hood and monitored carefully to confirm the absence of any radioactive contamination. The capillaries were coated with a solution of 'Bostik' in acetone to ensure that any residual contamination was safely fixed to the glass and to strengthen the capillary.

The quantities of ^{237}Np handled in each preparation did not exceed 100 mg, obtained as a mixture of 5 and 6 oxidation states from an aqueous nitric acid stock solution, containing about 30 mg/cm^3 of the isotope. A more accurate estimate of the neptunium content may be obtained by radiometric analysis of an active source. The source is prepared by diluting 10 μl of the stock solution to 100 μl with water using micropipettes and transferring a 10 μl aliquot to a prepared tantalum disc. The disc is about 35 mm in diameter and is prepared by careful washing and the application of a thin coating of 'Zapon' lacquer around the edge. The active solution is spread to the perimeter bounded by the lacquer aided by the addition of two drops of a surfactant. The evenly-spread layer of neptunium solution is then evaporated gently under an infra-red lamp and then roasted in a bunsen flame. This produces a coating of tantalum oxide impregnated with about 30 μg of neptunium (i.e. fixed activity).

Using a Simpson counter, the α-counts on the source can be determined by averaging a series of 2 minute readings. Greater precision can be obtained by extending the counting period.

7.2. The Collection of X-ray Diffraction Data.

In the initial stages a suitable crystal must be selected, preferably with well defined edges and capable of extinguishing a transmitted beam of polarised light when oriented at the correct angles. After mounting on a quartz fibre the crystal is screwed onto a goniometer head and measured [5] ensuring that the orientation of each face relative to the angular ϕ-scale is known and can be kept constant during the data collection. The crystal is then

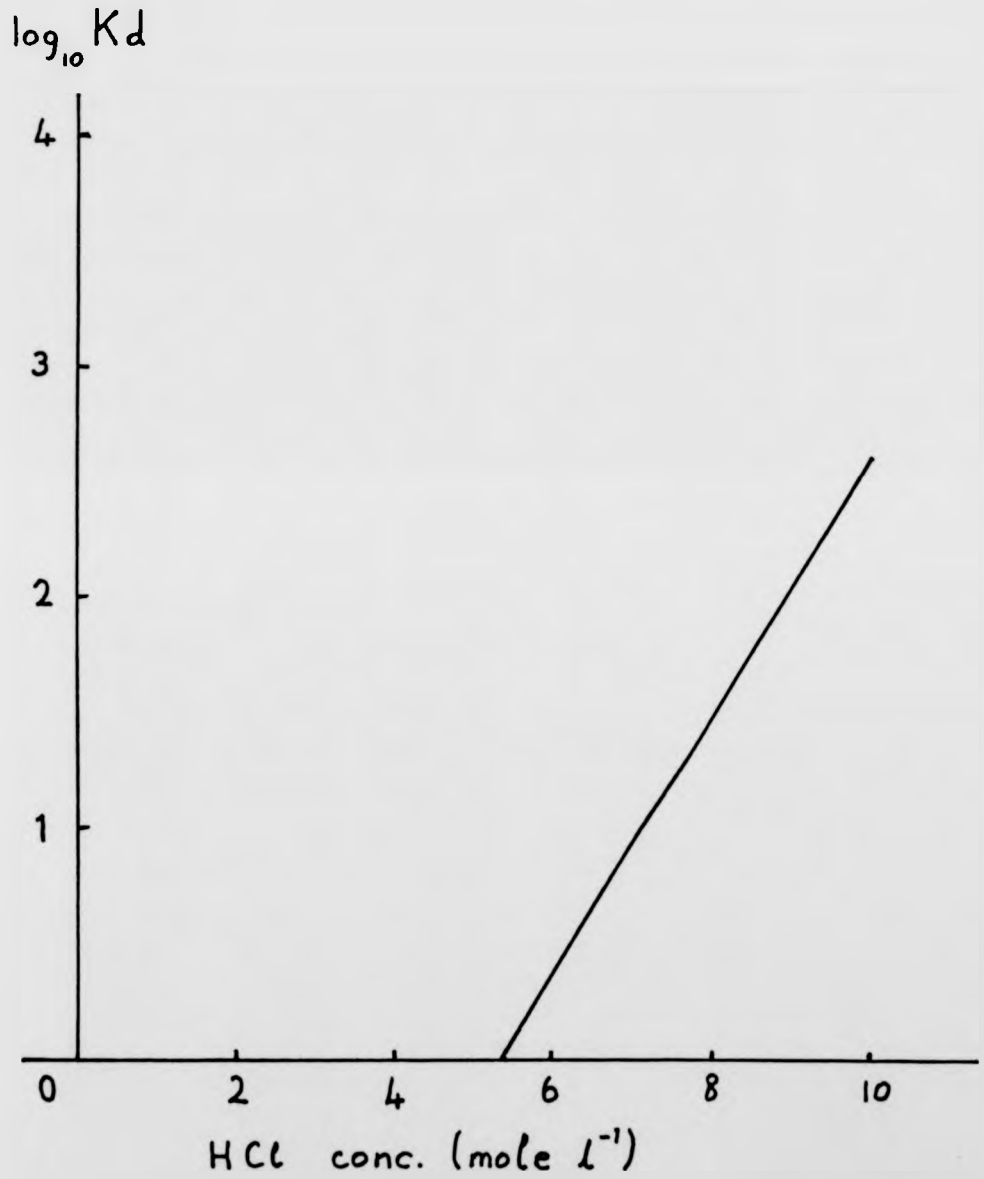

FIGURE 7.1. A plot of the distribution coefficient (Kd) of Np(VI) in hydrochloric acid on the anion exchange resin Amberlite IRA 400 (adapted from ref. 3)

transferred to the fully-automatic four circle Syntex $P2_1$ diffractometer used for the data collection (Figure 7.2), which is operated through a series of computer programs described in detail by Sparks. [6] The same author has also outlined the procedures to be carried out in centering and subsequent data collection. [7] The position of the crystal on the goniometer head G is adjusted through a series of translational movements until it is visually centred in the path of the X-ray beam, at the intersection of the ϕ and ψ axes (C in Figure 7.2). This is accomplished with the aid of an accurately aligned telescope with a cross-wire attached to the ψ circle.

A rotation photograph is now taken, recording the diffracted spots on a Polaroid film. The ψ and 2θ circles are set to 0° and the ϕ circle is rotated as the crystal is irradiated in the X-ray beam for 10-15 minutes. A pattern of diffracted spots, related by two orthogonal mirror planes, is recorded on the Polaroid film. The 2x- and 2y- coordinates of these are measured (Figure 7.3) and input to a program which sets ψ and 2θ for each reflection corresponding to the equations:-

$$\psi = \tan^{-1}\frac{y}{x}$$

$$2\theta = \cos^{-1}\frac{2d}{\sqrt{x^2+y^2+4d^2}}$$

where d is the distance from the crystal to the centre of the Polaroid film. With the 2θ and ψ circles set for the calculated position of a reflection the ϕ circle is rotated until the reflection enters the detector aperture. Once the position of the reflection is found , its position is refined by the determination of positions of half-height peak intensity. proceeding through a series of iterations until any variations lie within the tolerances 0.02°, 0.01° and 0.04° for 2θ, ω and ψ respectively. The position of the reflection will only be refined if its intensity is greater than a preset minimum value, which is normally set to 1000 c.p.s.

The program allows a maximum of 15 and recommends a minimum of 5 reflections to be selected and used in this centering procedure. The refined angular parameters of each reflection are stored and used in the auto-indexing program which computes 30 possible axial solutions for a unit cell and prints out their lengths (Å) and the cosines of the angles between them. The solutions of the shortest length in a hexagonal or orthogonal arrangement are selected to give a unit cell of a symmetry compatible with the atomic stereochemistry. In some cases the true unit cell may not be readily apparent in the solutions due to crystal twinning or the presence of satellite subcrystals. For this reason the maximum number of reflections are used and by trial and error, one or more reflections omitted until only those from one component are used in the unit cell determination.

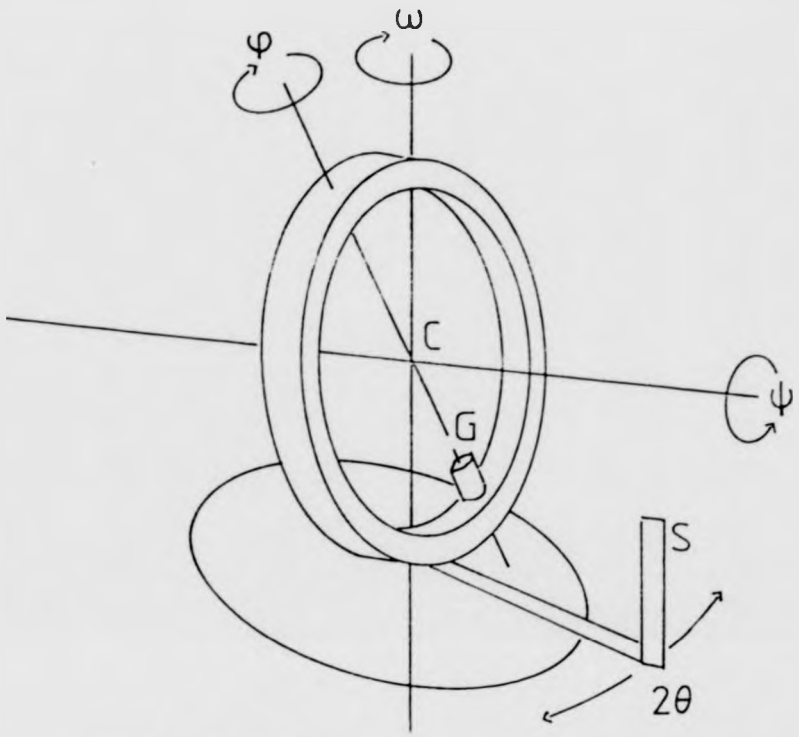

FIGURE 7.2. The four circles of the diffractometer

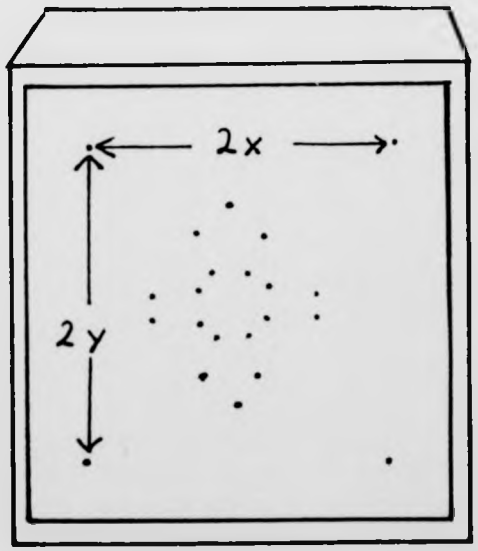

FIGURE 7.3. The pattern of spots on film from a rotation photograph.

The three selected axial solutions are then examined by Polaroid partial rotation photographs, which allow the true symmetry of the trial unit cell to be confirmed. An axis of symmetry is revealed by the axial photograph containing diffraction spots related by a mirror plane. This would correspond to the unique axis of a monoclinic cell, the c-axis of a hexagonal cell or any axis of a unit cell of higher symmetry. These photographs will also show any fainter interleaving layers of spots at fractions $\left\{\frac{1}{n}\right\}$ between the major layers indicating the order, n, by which the axis length needs to be multiplied. If a disordered array of diffraction spots is obtained, this indicates that the crystal is twinned and another crystal should be chosen and the procedure repeated.

More precise unit cell parameters with the hkl indices and refined angles of the reflections used in their calculation are derived from a least squares program. This program will also calculate the indices of any omitted reflections (above), and if these are integer values they can be included in the least squares calculation to give unit cell parameters of greater precision.

The computer controlling the diffractometer now has the information about the orientation of the unit cell axes stored and a data collection program can now be started using this information to set the circles for each reflection. Before this is done, however, it is necessary to plot a profile of one or more of the stronger reflections to determine the shape of the peak. If the peak is split, it indicates that the crystal is twinned and it is advisable to discard it. The peak is usually symmetrical, but its overall shape and symmetry will assist in the decision about the angular range of each reflection that has to be covered in the data collection.

Unit cell parameters of much greater precision are obtained by running the least squares program on a set of reflections of higher 2θ values, and improvements on this precision made with the most intense reflections available. The 15 high angle reflections are selected by running a rapid data collection program through a section of the 2θ range 20°-30°, depending on how strongly diffracting the crystal is. This preliminary data collection can also be used to determine if the unit cell is primitive or centred and if it is described in the correct Bravais lattice. If the lattice chosen is incorrect the use of a transformation matrix to produce the correct lattice at this point will save a great deal of computer time at a later date. The 15 high-angle reflections selected are input into the memory and the original centering program is used to refine their positions. The final least squares calculations will be based on these reflections and the standard deviations of the unit cell parameters are also calculated.

The full data collection is carried out based on the accurate unit cell, the procedure programmed to scan systematically and sequentially each reflection in reciprocal space bounded by the limiting sphere. The θ-2θ scan technique is used whereby the ω-circle, which controls the rotation of the reflecting crystallographic plane, moves at half the angular rate of the detector as the profile of the reflection is recorded. A preliminary scan of 2 seconds is used to determine a suitable scan rate for each reflection within the limits of 2.0-29.3 $^{\circ}$ min^{-1} depending on the intensity of this pre-scan. The background counts on either side of the reflection are also measured to give a true estimate of the integrated intensity through their profiles. Throughout the data collection, three or more strong check reflections are determined at regular intervals so that any decay of the crystal induced by exposure to X-rays can be monitored and the data rescaled if any decay should occur. The data obtained from each reflection is written onto a 9-track magnetic tape which is on-line during the running of the data collection program. The data on the tape is transferred to either the Burroughs B6800 or the Data General NOVA3 computer for structure solution.

The structure of the compound under study is solved by use of the heavy-atom method incorporated into a series of package programs under either the XRAY'76[8] or the SHELXTL[9] system. In structures where no one atom is significantly heavier than the others direct methods[10] are used, involving the calculation of a combination of phases for a sub-set of reflection data until a possible solution is reached. The use of this technique was not required in this work.

The precision of the data collected is increased in some cases by carrying out the data collection at low temperatures (typically -120°C to -100°C), and in others the use of low temperatures stabilises the compound under study and allows the data collection to be carried out. The low temperatures in the region of the crystal are achieved by using the Syntex LT-1 low temperature attachment on the diffractometer. This attachment plays a stream of cooled, dry nitrogen gas over the crystal, the gas being first cooled by a heat exchanger in a Dewar of liquid nitrogen and then heated to the required temperature.

7.3. The use of Oscillation and Weissenberg Photographic Methods.

These two photographic methods have been used in preliminary studies of the lattice parameters of crystals prior to their transfer to the diffractometer. The theoretical basis for these techniques, in particular the concept of the reciprocal lattice, can be found in ref. (11). A standard procedure can, however, be followed for most routine measurements of photographic films.

An oscillation photograph about a crystal axis can be obtained by oscillating a crystal (C) back and forth through 15° about an axis (A) which is perpendicular to the incident X-ray beam (Figure 7.4). The crystal should be well formed with distinct edges

and the edges parallel to the axis under examination aligned with the axis of rotation, as the external morphology of the crystal is determined by its internal symmetry. This alignment procedure is unnecessary on the diffractometer which can study a crystal in any orientation. The film, F, inside the cylindrical holder will record layer lines of diffraction spots which are graded with the Miller index corresponding to the axis under study (Figure 7.5). In the example the crystal is rotated about c, so the layer lines will be divided into the groups of reflections $hk0, hk1, hk2$, etc., and measurements of the spacing between the layers, y_n, can be used to calculate the axial length, z, from:

$$z = n\frac{\lambda}{\sin\left[\tan^{-1}\left(\frac{y_n}{R}\right)\right]}$$

where R is the radius of the camera holding the film, and y_n is the distance of the n^{th} layer from the zero layer. The film holder used has a diameter ($2R$) of 57.3 mm.

A tilt in the layer lines indicates that the crystal is slightly out of alignment, but once this has been corrected and the axis length calculated, the photograph can be examined for the presence of a symmetry axis. If such an axis is present it will be evident by the appearance of the set of diffraction spots related through a mirror plane along the zero layer, and this indicates the remaining two axes are perpendicular to the one measured in this photograph. In this case, measurement of the two remaining axes is quite straightforward and can be carried out by using the Weissenberg technique. This method involves excluding all the layer lines, except the one under examination, from the film by means of a cylindrical metal screen inside the camera the screen having a gap through which X-rays can enter and leave. While the crystal is being irradiated, the camera body is moved to and fro by 100 mm along the axis A. Every 1 mm of this motion is coupled to a 2° rotation of the crystal about A, so that a 200° range is covered. The exposure required for a good Weissenberg photograph is about 18 hours. For a determination of the unit cell parameters, only the zero layer is photographed but a full data collection to give a structural solution would require several layers to be photographed in this way.

The zero-layer Weissenberg photograph will show a distorted map of the $h0l$ reflections (Figure 7.6) if the crystal is monoclinic and rotated about the symmetry (b) axis. In addition the angle (β) between the axes a and c can be directly read off from the film, the reflections recorded are the $h00$ and $00l$ along the corresponding reciprocal lattice axes, a^* and c^* respectively with the angle β^* between, where:

$$\beta = 180 - \beta^*$$

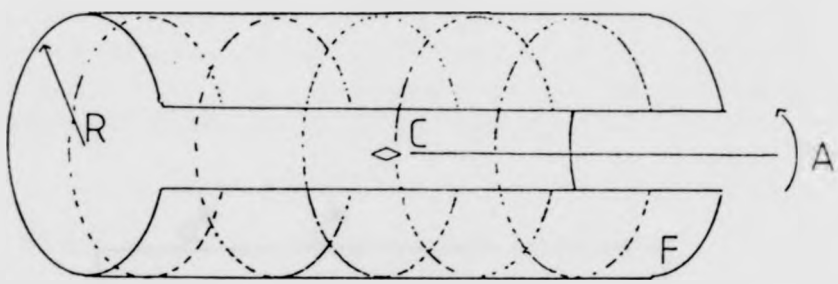

FIGURE 7.4.

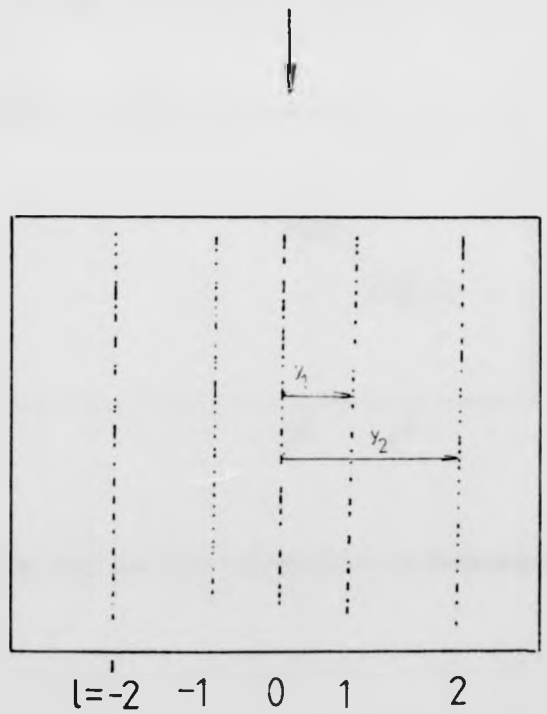

FIGURE 7.5. The pattern of spots recorded from an oscillation photgraph about a selected axis.

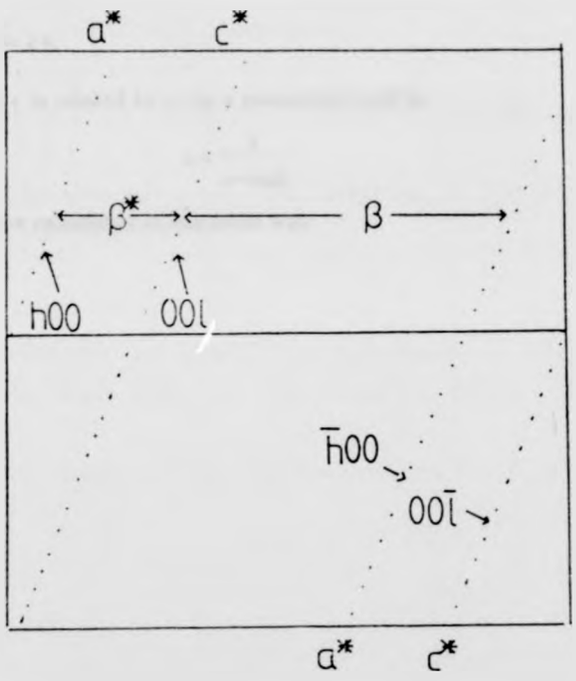

FIGURE 7.6. The axial reflections recorded from a Weissenberg photograph.

The remaining $h0l$ reflections lie between the reciprocal lattice axes.

The diameter of the camera body is such that the scale along the vertical axis of the film is 1 mm to every 1° of rotation. The axial reflections will therefore lie in rows inclined at angles of $\tan^{-1}2$ to the horizontal axis of the film. The vertical distance of the axial spots from the $\theta = 0°$ line is measured, and the value in mm corresponds to the θ value of the reflection in degrees. This is given as y_n, the distance of the n^{th} axial spot from the centre line. The reciprocal axis length c^*, for example, is then given by:

$$\xi_1 = 2\sin y_1$$

where $\xi_1 = \frac{\xi_n}{n}$, and $\xi_1 = c^*$.

The direct axis length, c is related to c^* in a monoclinic cell by

$$c = \frac{\lambda}{c^* \sin\beta}$$

The axis length a can be calculated in the same way.

References

1. "The Actinides," in *Comprehensive Inorganic Chemistry, Vol. 5*, ed. A.F. Trottman-Dickenson, Pergamon, New York, 1973.
2. F.A. Cotton and G. Wilkinson, in *Advanced Inorganic Chemistry (4th Edtn.)*, p. 492, Intersciences, 1980.
3. C. Keller, in *The Chemistry of the Transuranium Elements*, pp. 310-311,462-463, Verlag Chemie, 1971.
4. E. Lederer and M. Lederer, in *Chromatography: A review of principles and applications*, p. Ch. 11, Elsevier Publishing Company, 1957.
5. N.W. Alcock, *Acta Cryst.*, vol. A26, p. 437, 1970.
6. R.A. Sparks, *Abstracts of the American Crystallographic Association*, p. 20, Ottawa, Canada, 1970.
7. R.A. Sparks, in *Crystallographic Computing Techniques*, ed. F.R. Ahmed, pp. 452-467, Munksgaard, Copenhagen, 1976.
8. J.M. Stewart, "The X-RAY '76 system," TR-466, Computer Science Center, University of Maryland, U.S.A., 1976.
9. G.M. Sheldrick, *SHELXTL User Manual,* Nicolet Instrument Co., 1981.
10. M.M. Woolfson, in *Direct Methods in Crystallography*, Oxford University Press, 1961.
11. G.H. Stout and L.H. Jensen, in *X-ray Structure Determination*, MacMillan, London, 1968.

CHAPTER 8

Conclusions and Proposals for Further Investigations

8.1 Conclusions

The observation which may most readily be made from the work presented here is a determination of the actinide contraction from uranium to neptunium. The changes in the M-O bond lengths of the actinyl(VI) ions in Compounds 1-4 (Chapter 2) are summarised in Table 8.1 and a mean value for the contraction determined as 0.037Å. This value for the contraction corresponds closely to the value of 0.034Å found in previous work,[1] although both values are larger than the difference between the metallic radii of uranium and neptunium (0.02Å).[2] The greater contraction of the M-O bond length found on replacing U by Np in $MO_2(C_5H_7O_2)_2C_5H_5N$ (Compounds 7 and 8, Chapter 4) from 1.83(1) to 1.78(2)Å appears to be due to both steric effects and the actinide contraction and so has been excluded from the calculation.

TABLE 8.1

Contraction (Å) of the M-O(MO_2^{2+}) bond on substitution of neptunium for uranium.

Complex	Metal		
	U	Np	Δ
$MO_2(NO_3)_2C_{10}H_8N_2$	1.763(13)	1.728(7)	0.035
$MO_2(CH_3COO)_2C_{10}H_8N_2$	1.774(8)	1.730(10)	0.044
	1.765(8)	1.720(10)	0.035
[$MO_2(C_5H_7O_2)_2C_{10}H_8N_2$	1.83(1)	1.78(2)	0.05]

Mean Δ = 0.037Å

The U-O (UO_2^{2+}) bond lengths and equatorial coordination numbers of the compounds studied are given in Table 8.2 and confirm the findings[3] that the equatorial coordination has no significant effect on the uranyl(VI) U-O bond length. Equally the expected

difference in U-ligand bond lengths with different donor atoms does occur and the general trend for U-N(ligand) bonds to be longer than U-O(ligand) bonds can be observed from the data in Table 8.3. The mean difference in bond lengths of 0.116Å is significantly greater than the difference between the van der Waals radius of oxygen (1.52Å) and of nitrogen (1.55Å)[4] and between the covalent bond lengths found in CH_3OH (C-O : 1.43(3)Å)[5] and CH_3NH_2 (C-N : 1.48(1)Å).[6] This difference is also observed in the neptunyl(VI) compounds which contain both O- and N-donor atoms in the ligands (Compounds 2,4 and 8) where the mean difference is 0.245Å. This increased difference is due to the greater length of the Np-N bond in compound 4 (see Chapter 2).

Only one U(VI)-Cl distance has been determined (in compound 15) and the bond length of 2.675Å reflects the greater bulk of the chlorine atom (van der Waals radius: 1.75Å [4]) and the consequent difficulty in packing such an atom around the central metal atom. The increase in van der Waals radius of chlorine compared to that of the other donor atoms corresponds more closely to the increase in U-L bond length than to the C-Cl covalent bond length of 1.800(14)Å observed in CH_3Cl.[7] The metal-chlorine bond also shows a significant change on replacement of uranium with neptunium as the Np-Cl bond lengths in $NpCl_2O_2$.2tppo are 2.622 and 2.645Å.[8] The Np-Cl bond length in compound 12 of 2.685Å is greater than would be expected but since the value is an average of two Np(VI)-Cl bonds and one Np(V)-Cl bond it is not strictly comparable.

TABLE 8.2

U-O(UO_2^{2+}) bond lengths (Å) and equatorial coordination numbers.

Compound	E.C.N.	U-O bond length
1	6	1.763(13)
3	6	1.774(8)
		1.765(8)
5	6	1.735(10)
7	5	1.83(1)
9	5	1.752(6)
		1.733(6)
10	6	1.75(1)
13	6	1.765(5)
		1.777(2)
14	6	1.75(3)
		1.81(3)
		1.83(3)
		1.78(2)
15	5	1.74(1)
		1.67(1)

Mean for E.C.N. = 5 : 1.759(9)

Mean for E.C.N. = 6 : 1.761(14)

TABLE 8.3

Metal-equatorial ligand bond lengths (Å) and the relevant donor atom.

a) Uranyl compounds	O	N
1	2.494(13) 2.481(12)	2.578(13)
3	2.459(9) 2.429(9)	2.642(9)
	2.475(9) 2.438(9)	2.631(10)
5	2.500(17) 2.490(12)	2.557(22)
7	2.34(1) 2.44(1)	2.47(1)
9	2.385(6) 2.349(5)	-
	2.338(6) 2.383(6)	
	2.489(8)	
10	2.31(1) 2.53(1)	-
	2.53(1)	
13	2.562(5) 2.502(6)	-
	2.489(6) 2.561(5)	
	2.436(4) 2.438(4)	
14	2.47(3) 2.50(3)	-
	2.48(3) 2.59(2)	
	2.48(2) 2.59(3)	
	2.51(3) 2.59(3)	
	2.39(3) 2.27(2)	
	2.41(2) 2.35(2)	
15	2.30(1) 2.31(1)	-
	2.54(1) 2.51(1)	
Mean	2.457(14)	2.573(14)
Δ	0.116	

b) Neptunyl compounds	O	N
2	2.484(8) 2.472(8)	2.564(9)
4	2.460(9) 2.455(9)	2.842(13)
	2.476(9) 2.430(9)	2.835(13)
8	2.33(2) 2.37(2)	2.56(3)
Mean	2.428(12)	2.673(14)
Δ	0.245	

8.2. Proposals for Further Investigations.

It would be of considerable interest to extend the investigations of the 2,2'-dipyridyl complexes described in Chapter 2 by replacing the central metal atom with plutonium. The balance of steric forces, particularly in the acetate complex, between the actinide contraction and the extension of the M-N(ligand) bond may however preclude the formation of crystals in the same space groups. Further attempts to produce neptunyl(VI) complexes with 1,10-phenanthroline and the elucidation of the structure of the uranyl(VI) acetate complex with 1,10-phenanthroline (complex 6 - Chapter 3) would also be of value in extending the work covered in Chapters 2 and 3.

Another more general area for further crystallographic investigation would be complexes containing other nitrogen donor ligands.

References

1. M.M. Roberts, *"Structural Studies of Uranyl and Neptunyl Complexes", Thesis for Ph.D. Degree,* University of Warwick, 1981.
2. W. Muller, *A.C.S. Symp. Series 131: Lanthanide and Actinide Chemistry and Spectroscopy, Chapter 9.*, 1980.
3. R.G. Denning, "Properties of the UO_2^{n+} (n=1,2) Ions," in *Gmelin Handbuch URAN Suppl. Vol A6*, pp. 31-79, 1983.
4. A. Bondi, *J. Phys. CHem.*, vol. 68, p. 441, 1964.
5. K.J. Tauer and W.N. Lipscomb, *Acta. Cryst.*, vol. 5, p. 660, 1952.
6. M. Atoji and W.M. Lipscomb, *Acta. Cryst.*, vol. 6, p. 770, 1053.
7. R.D. Burbank, *J. Am. Chem. Soc.*, vol. 75, p. 1211, 1953.
8. N.W. Alcock, M.M. Roberts, and D. Brown, *J. Chem. Soc. Dalton Trans.*, p. 25, 1982.

APPENDIX A

An Outline of the Crystallographic Theory on which the Structure Solving Techniques are based.

The fundamental characteristic of the crystalline state is a very high degree of internal order, i.e. the internal structure of a crystal is periodic in three dimensions. This precise internal order is demonstrated when a crystal is used as a three-dimensional diffraction grating for X-radiation (as X-rays have wavelengths comparable to interatomic distances). The pattern can be shown to arise from reinforcing reflections which occur, as shown in Figure A.1, when the angle, θ, is such that the path difference (2x) between the coincident rays is λ, the X-ray wavelength or a multiple of λ. This condition satisfies the Bragg equation:

$$2d\sin\theta = n\lambda \qquad (1)$$

where d is the interplanar spacing defined by the atoms in the planes and n is an integer. The family of planes which give rise to reflections in this way are described by the Miller indices (hkl). Figure A.2 shows how each plane intersects the a,b and c axes of the unit cell at fractions a/h, b/k and c/l respectively.

Diffraction of X-rays by a crystal produces a pattern of spots which contains information about the relative positions and types of atoms in the unit cell and allows the crystallographer to determine a unit cell for the compound being studied. The possible unit cells belong to seven crystal systems, some of which may contain lattice point centering. Combination of the seven crystal systems with the possible centering produces a total of 14 Bravais lattices which are detailed in Figure A.1. The various forms of lattice centering found are illustrated in Figure A.3. The lattice may exist in P (primitive), R (rhombohedral), I (body centered), C (centered on one face) or F (centered on all faces) forms, and the correct choice can be deduced from the general systematic absences in the reflection data:

P	No absence
I	$h+k+l \neq 2n$
C	$h+k \neq 2n$
F	$h+k \neq 2n$, $k+l \neq 2n$
	$h+l \neq 2n$
R	$-h+k+l \neq 2n$

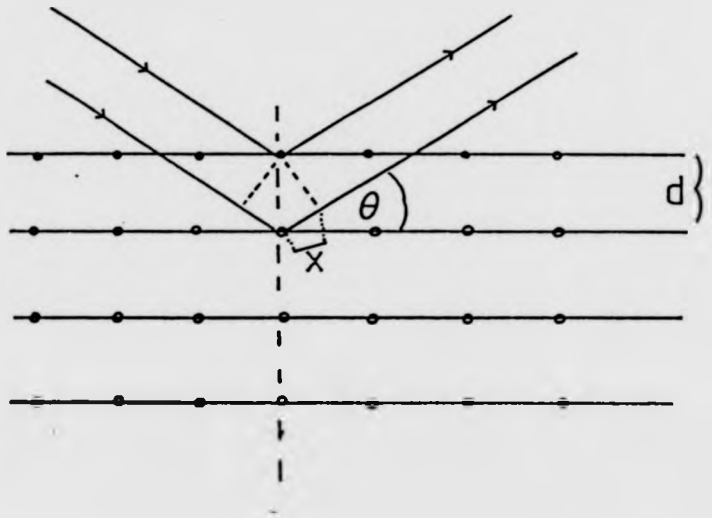

A.1. The diffraction of X-rays from crystal planes.

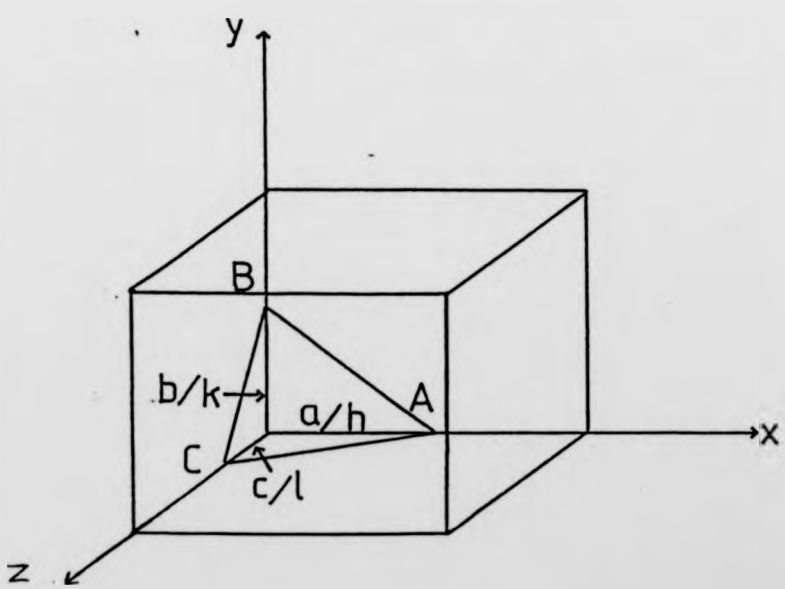

A.2. The derivation of Miller indices (hkl) for any planes of reflection (ABC) within the unit cell.

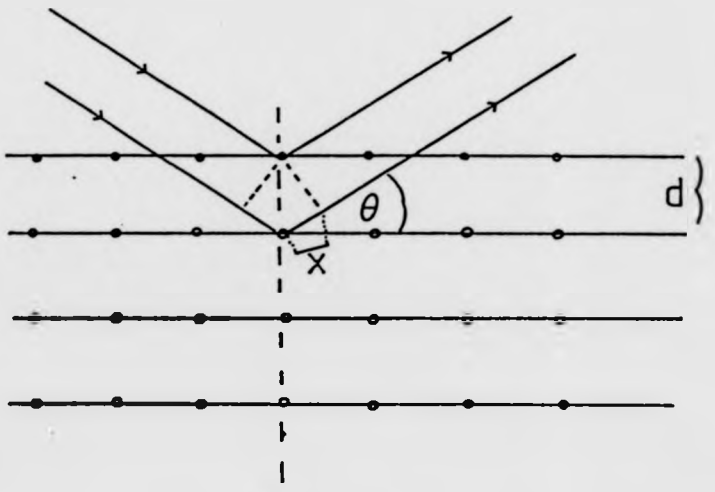

A.1. The diffraction of X-rays from crystal planes.

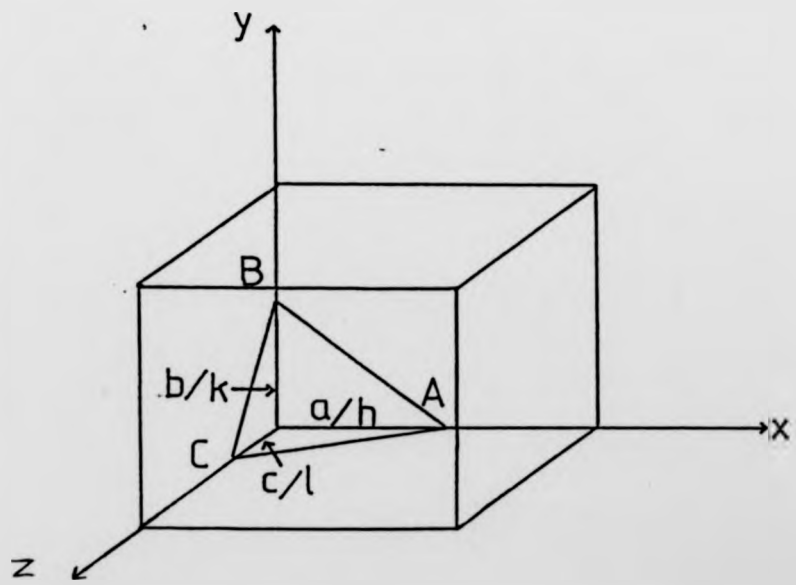

A.2. The derivation of Miller indices (hkl) for any planes of reflection (ABC) within the unit cell.

System	Number of lattices in system	Lattice symbols	Nature of unit-cell axes and angles[1]	Lengths and angles to be specified	Symmetry of lattice[2]
Triclinic	1	P	$a\neq b\neq c$ $\alpha\neq\beta\neq\gamma$	a, b, c α, β, γ	$\bar{1}$
Monoclinic[3]	2	1st setting P, B	$a\neq b\neq c$ $\alpha=\beta=90°\neq\gamma$	a, b, c γ	$2/m$
		2nd setting P, C	$a\neq b\neq c$ $\alpha=\gamma=90°\neq\beta$	a, b, c β	
Orthorhombic	4	P C[4] I F	$a\neq b\neq c$ $\alpha=\beta=\gamma=90°$	a, b, c	mmm
Tetragonal	2	P[5] I	$a=b\neq c$ $\alpha=\beta=\gamma=90°$	a, c	$4/mmm$
Cubic	3	P I F	$a=b=c$ $\alpha=\beta=\gamma=90°$	a	$m\bar{3}m$
Trigonal	1	R[6]	$a=b=c$ $\alpha=\beta=\gamma$ $<120°, \neq 90°$	a α	$\bar{3}m$
Hexagonal	1	P[7]	$a=b\neq c$ $\alpha=\beta=90°$ $\gamma=120°$	a, c	$6/mmm$

TABLE A.1. The 14 Bravais lattices and conventional unit cells.

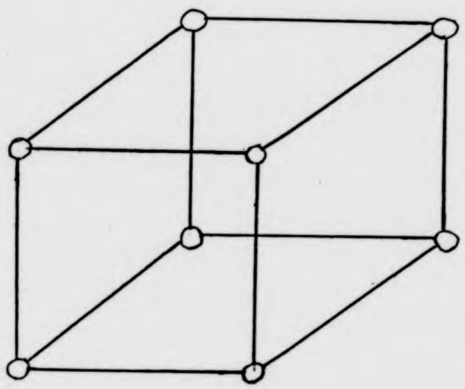

P

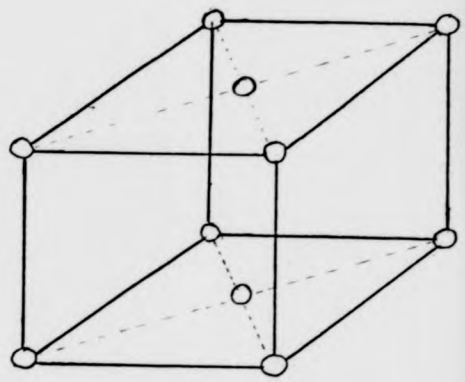

C

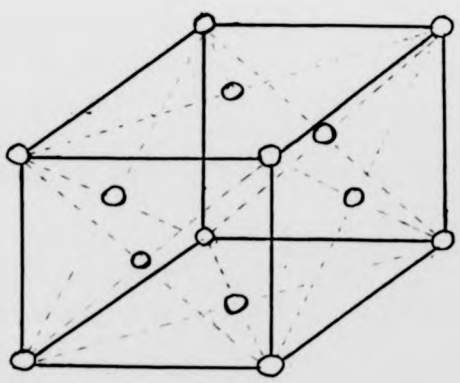

F

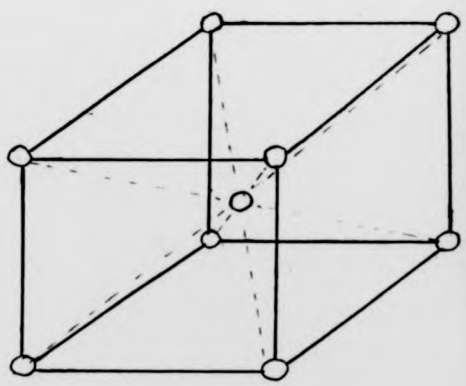

I

A.3. The possible types of lattice centering.

The lattice centered on a single face may often be found in either the A- or B- centered forms, it then becomes necessary to reorientate the axes to the conventional C- centered form.

Further information about the symmetry of the crystal under study may also be derived from the intensity pattern and in addition to the Bravais lattice the probable space group can be identified. The 230 space groups [1] represent the distinct ways of arranging objects on one of the fourteen Bravais lattices by the use of certain symmetry operations. The symmetry operations may be divided into two types, the first involving point symmetry and the second involving space symmetry or translation. Operations of the first type, namely rotation axes, rotation-inversion axes and mirror planes, do not affect the systematic absences, whereas the presence of operations of the second type, namely screw axes and glide planes, may be deduced from the systematic absences.

A screw axis describes the distributions of a set of atoms (the asymmetric unit) rotated relative to one another through (360/n)° about an axis and a fractional shift (m/n) along the unit cell axis to which the screw axis is parallel. The axis is given the n_1 notation, and a two fold screw axis having translation by ½ a unit cell dimension and a rotation through 180° is denoted by 2_1. If such an axis were parallel to the b direction the systematic absence would be $0k0 : k \neq 2n$. A glide plane results from the combination of translation with the mirror operation, and is parallel to a lattice vector. A c-glide plane has a translation of ½ along c and reflection normal to the b direction. This glide plane is recognised by the systematic absence $h0l : l \neq 2n$. These latter systematic absences and their related symmetry operations are summarised in Table A.2.

Once all the reflection data have been collected and stored on disk (Chapter 7), the integrated intensities (I_{hkl}) are converted to their corresponding structure factors (F_{hkl}). This is accomplished using either the program SYNDAT [2] or the data reduction program in SHELXTL [3] The two parameters are related by the equation:

$$\left|F_{hkl}\right| = \left|\frac{KI_{hkl}}{Lp}\right|^{-\frac{1}{2}} \qquad (2)$$

where K is a scale factor, and L and p are the Lorentz and polarisation factors given by:

$$L = \frac{1}{\sin}\theta \qquad (3)$$

$$p = \frac{1+\cos^2 2\theta}{2} \qquad (4)$$

The derivation of these equations can be found in ref (4)

Type of reflection	Condition for possible reflection[1]	Glide plane ( ) or { } or screw axis [ ] or ⟨ ⟩			Systems of axes involved	
		Orientation	Component	Symbol[1]		
$hk0$	$h=2n$	(001)	$a/2$	a	Monoclinic (1st setting), tetragonal	Orthorhombic
	$k=2n$		$b/2$	b		
	$h+k=2n$		$a/2+b/2$	n		
	$h+k=4n$ $(h,k=2n)$		$a/4\pm b/4$	d		
$0kl$	$k=2n$	{100}	$b/2$	b	Orthorhombic, tetragonal, cubic	
	$l=2n$		$c/2$	c		
	$k+l=2n$		$b/2+c/2$	n		
	$k+l=4n$ $(k,l=2n)$		$b/4\pm c/4$	d		
$h0l$	$l=2n$	(010)	$c/2$	c	Monoclinic (2nd setting)	Orthorhombic
	$h=2n$		$a/2$	a		
	$l+h=2n$		$c/2+a/2$	n		
	$l+h=4n$ $(l,h=2n)$		$c/4\pm a/4$	d		
$hh2\bar{h}l$	$l=2n$	{1$\bar{1}$00}	$c/2$	c	Hexagonal	
$h\bar{h}0l$	$l=2n$	{11$\bar{2}$0}	$c/2$	c		
hhl	$(2h+)l=2n$	{1$\bar{1}$0}	$(a/2+b/2+)c/2$	$(n)\ c$	Rhombohedral[2]	Tetragonal, cubic[3]
	$2h+l=4n$		$a/4+b/4+c/4$	d		
$h00$	$h=2n$	⟨100⟩	$a/2$	2_1	Orthorhombic, tetragonal	Cubic
				4_2		
	$h=4n$		$a/4$	$4_1, 4_3$		
$0k0$	$k=2n$	[010]	$b/2$	2_1	Monoclinic (2nd setting), orthorhombic	
$00l$	$l=2n$	[001]	$c/2$	2_1	Monoclinic (1st setting), orthorhombic	
				4_2	Tetragonal	
	$l=4n$		$c/4$	$4_1, 4_3$		
$000l$	$l=2n$	z-axis	$c/2$	6_3	Hexagonal	
	$l=3n$		$c/3$	$3_1, 3_2, 6_2, 6_4$		
	$l=6n$		$a/6$	$6_1, 6_5$		

TABLE A.2. Determination of translation elements of symmetry from special reflections.

The structure factor, F_{hkl}, may be defined as the superposition of j waves scattered in the direction of the reflection hkl by the j atoms in the unit cell and considered as a Fourier synthesis of this series of waves. Each wave will have an amplitude proportional to the scattering factor (f) of the atom[1] to which it is related and a phase angle which will depend on the position of the atom in the unit cell.

These programs output a file containing a list of h,k,l,F and $\sigma(F)$ values for each reflection. Any variation in the values obtained for a set of check reflections (typically three repeated every 200 reflections) is used to calculate a correction for the reflections to be used in the structure determination. This correction is applied at this point. Reflections with faulty backgrounds are identified by

$$B_l - B_r > 3\sqrt{B_l + B_r}$$

(where B_l and B_r are the left and right backgrounds for each reflection) but not omitted from the reflection file.

At this point in the processing the option exists to exclude the low intensity reflections with $I/\sigma(I)<3.0$ from the output file, deeming the reflections with $I/\sigma(I)\geq 3.0$ to be observed. The exclusion of the low intensity reflections will usually result in a lower R-factor for the refined structure and will save significantly on computation times.

After this initial processing, an absorption correction should always be applied unless the material under consideration has a very low linear absorption coefficient. This absorption correction is performed using the program ABSCOR[5] which calculates the thickness, T, of the crystal through which the radiation has to pass at every orientation. The incident radiation of intensity I_o is therefore attenuated by an amount which can be calculated from the equation:

$$I = I_o e^{-\mu T} \tag{5}$$

where I is the measured intensity and μ is the linear absorption coefficient given by the equation:

$$\mu = \sum(\sigma_i n_i) \times Z/U \tag{6}$$

where σ_i is the linear absorption coefficient of atom i for the X-ray wavelength being used and n_i is the number of such atoms in the molecule. A precise correction for absorption is of particular importance for crystal having extreme values of T, e.g. plate- or needle-shaped crystals, or for compounds containing a high proportion of heavy atoms.

Although the intensities of the reflections produced by the scattering effect of the atoms present in the crystal have been measured, it is not possible to measure the associated phase differences which depend on the relative positions of the atom in the unit cell. The phase, α, associated with each observed structure factor modulus, $|F_o|$, is given by:

$$F_o = |F_o| \cos\alpha + i|F_o| \sin\alpha \tag{7}$$

and the best estimate of the phases can be obtained by calculating a set of structure factors, F_c, based on an approximate model of the actual structure to be determined and a calculation of an approximation of the true electron density from the observed structure factor amplitudes, $|F_o|$, with the calculated phases. The expression describing the distribution of electron density, ρ_{xyz}, in the unit cell is:

$$\rho_{xyz} = \frac{1}{V} \sum_{h=-\infty}^{h=\infty} \sum_{k=-\infty}^{k=\infty} \sum_{l=-\infty}^{l=\infty} F_{hkl} \left| \cos 2\pi(hx+ky+lz) - i \sin 2\pi(hx+ky+lz) \right| \tag{8}$$

where F_{hkl} contains the phase information and can represent either F_o or F_c and V is the unit cell volume.

Compounds containing one or a small number of heavy atoms in the asymmetric unit constitute a special case since the heavy atom will dominate the scattering of the X-rays and the majority of the phase differences are due to this heavy atom. Under these circumstances an approximate solution can be found by using the Patterson function. The Patterson function is a Fourier synthesis using only the indices and the $|F|^2$-value of each diffracted beam and requiring no knowledge of the phases:

$$P_{(UVW)} = \frac{1}{V} \sum_{h=-\infty}^{h=\infty} \sum_{k=-\infty}^{k=\infty} \sum_{l=-\infty}^{l=\infty} |F_{hkl}|^2 \cos 2\pi(hx+ky+lz) \tag{9}$$

The Patterson function is evaluated for each point U,V,W of a three dimensional grid which has the size and shape of the unit cell. The peaks in the map correspond to the vectors between any two pairs of atoms in the structure at, say, x_1,y_1,z_1 and x_2,y_2,z_2 where $U=x_2-x_1$, $V=y_2-y_1$ and $W=z_2-z_1$. If there are only a few heavy atoms present in the structure (eg. U or Np as in the compounds presented here) then the highest peaks will correspond to the vectors between the heavy atoms. The approximate position of the heavy atoms can then be found and used to calculate F_c values.

The lighter atoms can then be located by using a difference Fourier synthesis based on ΔF values for each reflection, where

$$\Delta F = |F_o| - |F_c| \tag{10}$$

This will produce a map with peaks corresponding to the remaining atom positions and these can be used to obtain a more precise estimation of the phases associated with the F_c values which will approach the true values associated with F_o. Once the approximate positions of all the atoms has been determined improvements can be made by utilising least squares refinement methods to minimise a function D given by:

$$D = \sum_{r=1}^{m} W_r \left(|F_o| - |F_c|\right)^2 \tag{11}$$

where W_r is the weighting function applied to reflection r. The reliability of the structure during the process of refinement is indicated by the agreement between the values of F_o and F_c for each reflection. This is measured by the reliability factor R, where

$$R = \frac{\Sigma\left|\left(|F_o| - |F_c|\right)\right|}{\Sigma\left(|F_o|\right)} \tag{12}$$

and the convergence of F_c and F_o produces a value of about 0.04 for most small structures.

Each atom in the structure has an associated temperature factor so that the atomic scattering factor for an atom at rest, f, is repaced by

$$f\ e^{-B_{iso}\left[(\sin^2\theta)/\lambda^2\right]} \tag{13}$$

where B_{iso} represents the isotropic temperature factor. The variation of f with $\sin\theta/\lambda$ is shown in Figure A.4 for a variety of values of B which is usually between 2.0 and 5.0Å^2. B is related to the mean-square amplitude ($\bar{U}^2$) of atomic vibration by

$$B = 8\pi^2\bar{U}^2 \tag{14}$$

Thus an increase in temperature will produce an increase in thermal motion of the atoms producing a more diffuse electron cloud at each atomic position. This is shown by a rise in B and the X-ray diffraction intensity falls off with increasing $\sin\theta/\lambda$ (Figure 4). Conversely a decrease in temperature will reduce the thermal motion of the atoms and will allow the data collected at higher values of 2θ to contribute to better resolution in the final structure. This is one of the reasons that data collections are carried out at low temperatures if other practical circumstances allow it.

The environments of atoms in most crystals are not isotropic, however, and a more precise description of the thermal motion assumes that the motion is ellipsoidal. This produces six "anisotropic temperature factors" which are incorporated into the function used to modify f (*c.f.* equation 13):

$$e^{-(b_{11}h^2 + b_{22}k^2 + b_{33}l^2 + b_{12}hk + b_{23}kl + b_{31}hl)} \tag{15}$$

where the factors b_{11},b_{22} and b_{33} describe the axis lengths of the thermal ellipsoid and b_{12},b_{23} and b_{31} describe the orientation of those axes with respect to the crystallographic axes. This introduces a further six parameters for each atom in the structure given anisotropic temperature factors and a corresponding increase in the computing time required

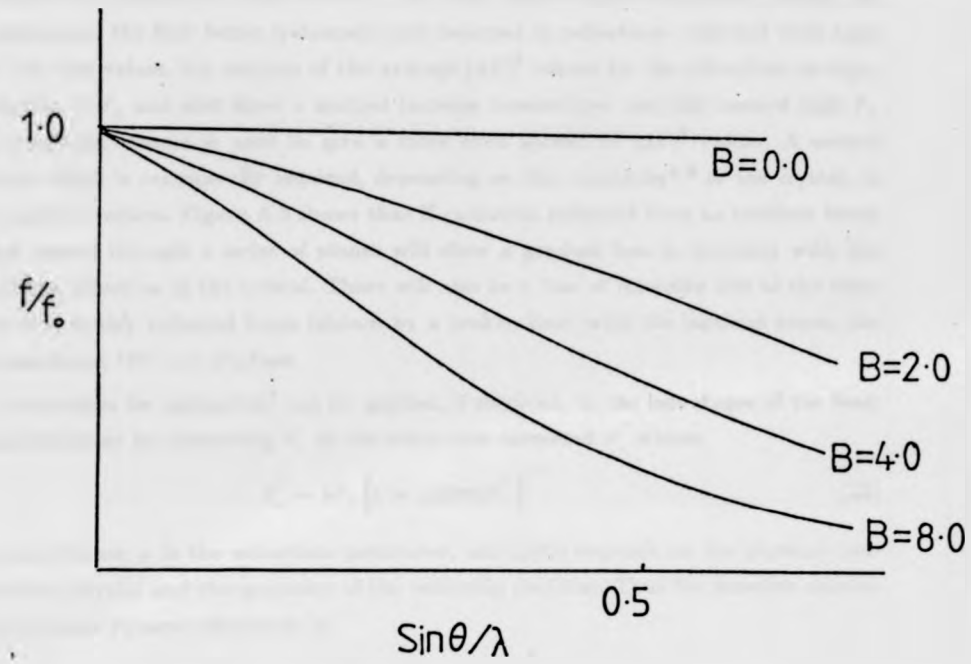

A.4. The variation of the atomic scattering factor (f) with $\sin\theta/\lambda$.

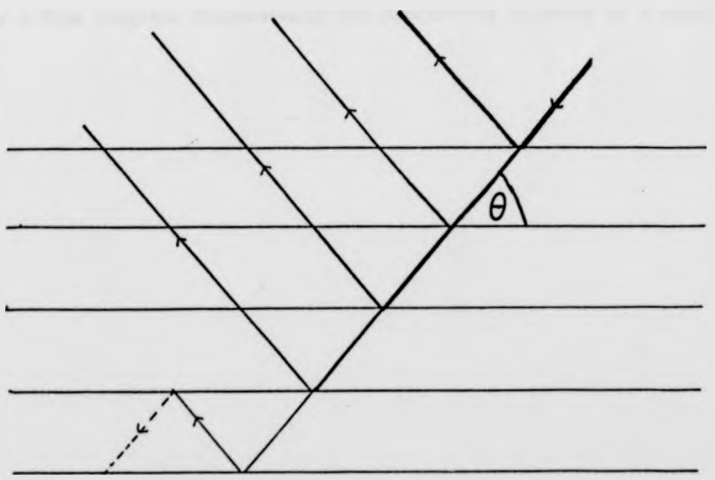

A.5. The effect of extinction.

for a least squares refinement, but this will assist in achieving a low R-factor.

There are a number of other errors in the data which require correction during the final refinement, the first being systematic and incurred in reflections collected with high F_o and low sinθ values. An analysis of the average $(\Delta F)^2$ values for the reflections at regular intervals of F_o and sinθ show a marked increase toward low sinθ and toward high F_o and a weighting scheme is used to give a more even spread of $(\Delta F)^2$ values. A second correction which is occasionally required, depending on the mosaicity[4,6] of the crystal, is an isotropic correction. Figure A.5 shows that X-radiation reflected from an incident beam that has passed through a series of planes will show a gradual loss in intensity with the depth of the reflection in the crystal. There will also be a loss of intensity due to the coincidence of a doubly reflected beam (shown by a broken line) with the incident beam, the two beams being 180° out of phase.

A correction for extinction[7] can be applied, if required, in the last stages of the least squares refinement by converting F_c to the extinction corrected F_c^* where:

$$F_c^* = kF_c \left[1 + g\beta(2\theta)F_c^2\right]^{-\frac{1}{4}} \qquad (16)$$

k is a scale factor, g is the extinction parameter, and $\beta(2\theta)$ depends on the physical constants of the crystal and the geometry of the reflecting position. Thus the function minimised by the least squares refinement is:

$$D = \sum_{r=1}^{m} W_r \left(|F_o| - |F_c^*|\right)^2 \qquad (17)$$

(*cf.* equation 11).

Figure A.6 is a flow diagram summarising the procedures involved in a structure determination.

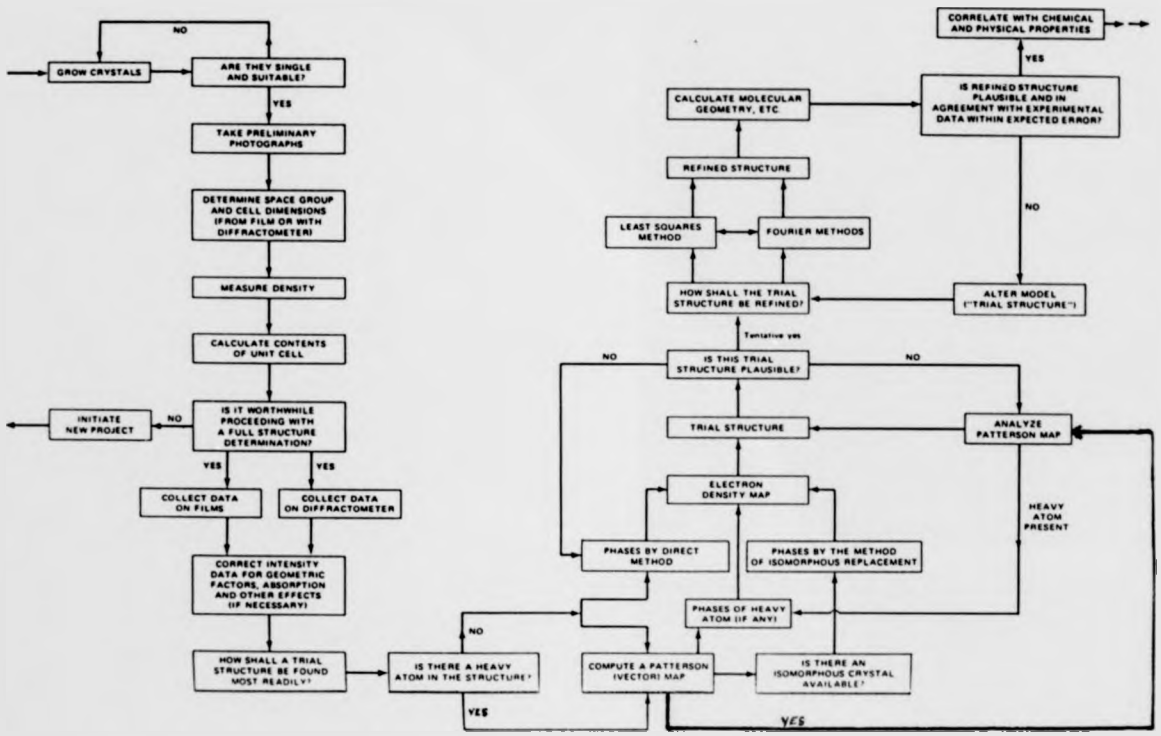

A.6. Structure determination flow diagram.

References

1. *International Tables for X-ray Crystallography,* D. Reidel Publishing Company, Dordrecht : Holland / Boston : U.S.A., 1983.
2. N.W. Alcock, *SYNDAT - a data reduction program for a Syntex* $P2_1$ diffractometer, 1974.
3. G.M. Sheldrick, *SHELXTL User Manual,* Nicolet Instrument Co., 1981.
4. G.H. Stout and L.H. Jensen, in *X-Ray Structure Determination*, MacMillan, London, 1968.
5. N. W. Alcock, "The Analytical Method for Absorption Correction," in *Crystalographic Computing*, ed. F. R. Ahmed, p. 271, Munksgaard, Copenhagen, 1970.
6. J.D. Dunitz, *X-ray Analysis and the Structure of Organic Molecules*, Cornell University, London, 1979.
7. A.C. Larson, *Acta. Cryst.*, vol. 23, p. 664, 1967.

APPENDIX B

Final Structure Factor Tables

The structure factor tables for compounds 1,2,3,4,7 and 13 have already been deposited with the editor of *J. Chem. Soc. Dalton Trans.* as these structures have been published or accepted for publication in that journal. The tables for the remaining structures will also be deposited when the structures are published and so have been omitted from this thesis. These table are available on request.